Nano Research

Open Access

Review Article

Electrochemical approaches for integrated CO_2 capture, concentration, and utilization: Mechanisms, synergies, and challenges

Minqing Zhan, Guanchu Lu ✉, Xihan Chen, Chaoyu Wang, Yinglin Zheng, Qun Li, Jiabin Wu ✉, and Huaiguang Li ✉

Guangdong Basic Research Center of Excellence for Aggregate Science, School of Science and Engineering, The Chinese University of Hong Kong, Shenzhen 518172, China

Cite this article: *Nano Research*, **2026**, *19*, 94908371. https://doi.org/10.26599/NR.2026.94908371

ABSTRACT: Electrochemical carbon capture and utilization (eCCU) has emerged as a transformative technology to mitigate carbon emissions while enabling a circular carbon economy. This review systematically examines integrated electrochemical CO_2 capture and concentration (eCCC), with particular focus on pH-swing systems, coupled with electrochemical CO_2 reduction reaction (CO_2RR) or utilization. The synergy between these processes is critically analyzed: eCCC efficiently captures diluted CO_2 steam from flue gases and releases it in pure form, providing an ideal feedstock for subsequent electrocatalytic conversion to value-added products including carbon monoxide, formate, ethylene, and ethanol. This electron-driven approach offers substantial advantages over conventional thermal methods, including reduced energy penalties, operational flexibility, and compatibility with renewable energy sources. However, significant challenges persist in catalyst stability, system integration, energy efficiency optimization, and economic viability on scale. This review provides a comprehensive analysis of these barriers and presents a forward-looking perspective on research priorities and development pathways to accelerate the implementation of practical electrochemical carbon capture and utilization technologies for industrial decarbonization and sustainable chemical production.

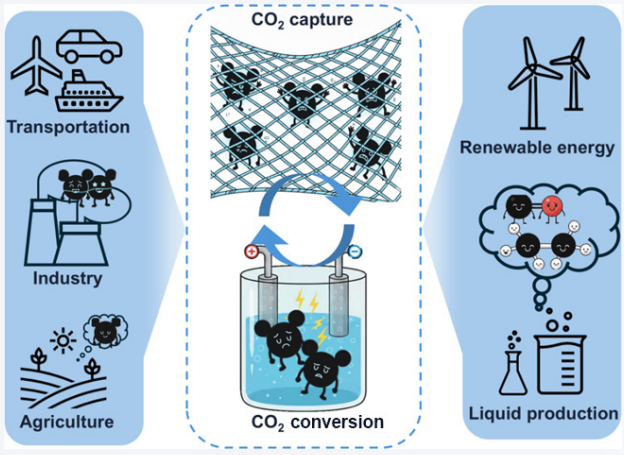

KEYWORDS: electrochemical carbon capture, direct air capture, electrochemical reduction of carbon dioxide, carbon capture, utilization, and storage (CCUS)

1 Introduction

The escalating concentration of atmospheric carbon dioxide (CO_2), now exceeding 420 ppm, stands as a principal driver of anthropogenic climate change, precipitating a global imperative for decarbonization [1–5]. Although the transition to renewable energy sources is paramount, the consensus from the Intergovernmental Panel on Climate Change (IPCC) underscores that achieving ambitious climate targets, particularly limiting warming to 1.5 °C, is virtually impossible without the large-scale deployment of carbon capture, utilization, and storage (CCUS) technologies [6–8]. Traditional chemisorption-based capture methods, predominantly employing aqueous amines (e.g., monoethanolamine (MEA)), have demonstrated commercial-scale efficacy. However, their widespread adoption is critically hampered by prohibitively high energy penalties, often consuming 15%–30% of a power plant's output, primarily associated with the thermal regeneration of the sorbent at temperatures exceeding 100 °C. This process engenders not only substantial operational costs but also significant emissions of degradation products, presenting environmental and operational liabilities [9–12].

In response to these challenges, electrochemical carbon capture and concentration (eCCC) has emerged as a disruptive paradigm, offering a pathway to circumvent the thermal energy demands of

Received: November 12, 2025; **Revised:** December 11, 2025
Accepted: December 23, 2025

✉Address correspondence to Guanchu Lu, luguanchu@cuhk.edu.cn; Jiabin Wu, wujiabin@cuhk.edu.cn; Huaiguang Li, lihuaiguang@cuhk.edu.cn

conventional systems. By leveraging renewable electricity as the primary energy input, eCCC systems can potentially achieve lower carbon footprint and greater integration with intermittent renewable sources, such as solar and wind [13]. Among various electrochemical CO_2 capture (ECC) strategies, electrochemical pH-swing systems have garnered significant and growing interest. These systems exploit a fundamental principle: The solubility of CO_2 in water is profoundly pH-dependent [14, 15]. CO_2 hydrates to form carbonic acid (H_2CO_3) in acidic and neutral conditions but is released as gas; conversely, in alkaline conditions, CO_2 is absorbed and converted into bicarbonate (HCO_3^-) and carbonate (CO_3^{2-}) ions [16, 17]. Electrochemical methods provide an elegant means to modulate this pH swing *in-situ* and on demand, without the need for external heat addition.

The core mechanism involves the electrogenic generation of acids and bases at paired electrodes (or within membrane-separated cells) to drive a cyclic process. Typically, at the cathode, water reduction generates hydroxide ions (OH^-) and hydrogen gas (H_2), creating a localized high-pH environment that captures CO_2 into dissolved inorganic carbon (DIC) species. Simultaneously, at the anode, water oxidation generates protons (H^+) and oxygen gas (O_2), creating an acidic environment that forces the dissociation of carbonic acid and the release of pure CO_2 gas [18, 19]. The elegance of this design lies in its conceptual simplicity and the avoidance of thermal cycles.

Beyond capture, the electrochemical carbon capture and utilization (eCCU) has rapidly gained traction as a complementary strategy that not only mitigates emissions but also valorizes CO_2 into fuels and chemicals of industrial relevance, such as carbon monoxide (CO), formate, methane, methanol, and C_{2+} products [20]. These electrochemical reduction processes, typically driven at the cathode of CO_2 electrolytes, harness renewable electricity to directly transform CO_2 into value-added outputs while coupling with oxygen evolution [21, 22]. The integration of capture and conversion presents a compelling opportunity: bypassing the costly intermediate step of CO_2 compression and purification [23]. Instead, captured CO_2 (from concentrated streams or directly from air) can be electrochemically converted *in-situ*, thus creating an integrated capture–conversion platform that improves overall energy efficiency and economic viability [24].

Despite these synergies, realizing such integration remains scientifically and technologically challenging. eCCC systems must be designed not only for efficient capture but also to provide CO_2 feedstocks in forms compatible with downstream electroreduction [23, 25]. Conversely, eCCU requires catalysts with high activity, selectivity, and stability under conditions that may involve fluctuating CO_2 concentrations, impurities, or supporting electrolytes introduced by capture processes [22]. Furthermore, the techno-economic competitiveness of integrated eCCU systems hinges on reducing overpotentials, mitigating membrane and catalyst degradation, and ensuring scalability of reactor architectures [10, 26, 27].

In recent years, the interest in the field of integrated CO_2 capture and conversion has increased. Several review papers have been published to assess the progress in it. For instance, Zito et al. (2023) provided an overview of electrochemical CO_2 capture and concentration [28], Pei et al. (2023) stated the possibility of combination of carbon capture and utilization via electrochemistry [29], Wei et al. (2023) focused on the CO_2 capture with electrochemical upgrading [30], and Kim et al. (2023) focused on the electrochemical reduction of capture CO_2, providing the future direction [23]. However, a comprehensive analysis of fully integrated electrochemical strategies is still lacking. Existing works often fail to systematically address the classification, underlying mechanisms, and performance metrics of such systems. As shown in Fig. 1(b), the number of publications in this area has risen rapidly from 2015 to 2025, highlighting its emerging importance. Nevertheless, several reviews have discussed CO_2 capture, utilization, and storage in general [3, 18]. Interestingly, a granular analysis of the publication trend in Fig. 1(b) reveals a distinct evolution in research priorities over the last decade. Before 2018, the field was predominantly characterized by material discovery, focusing on identifying stable redox-active carriers (e.g., quinones and bipyridines) and elucidating fundamental proton-coupled

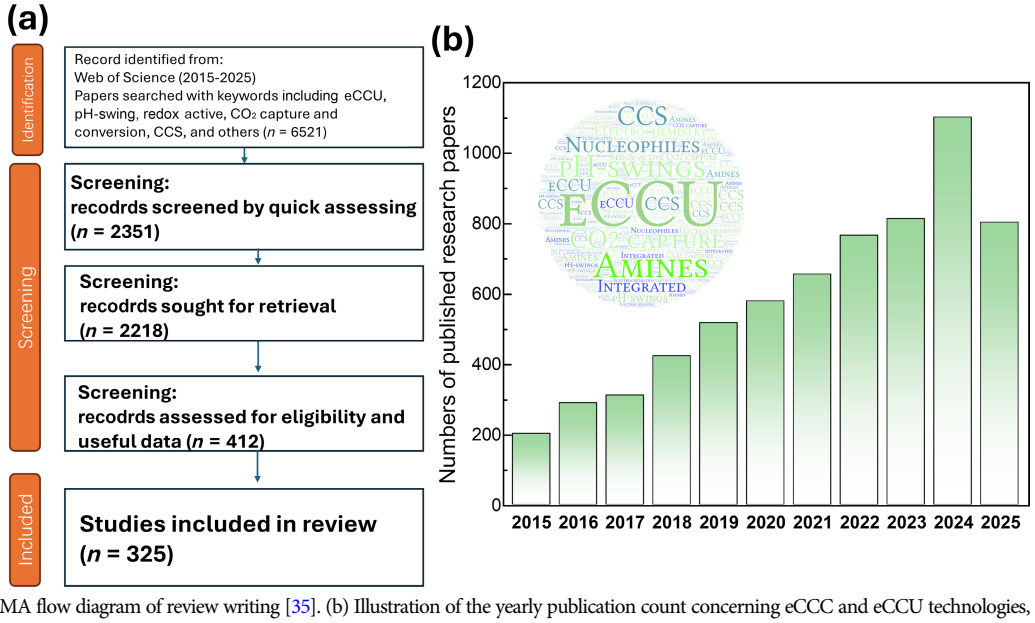

Figure 1 (a) PRISMA flow diagram of review writing [35]. (b) Illustration of the yearly publication count concerning eCCC and eCCU technologies, covering the period from 2015 to August 2025. These data were obtained through a search on Web of Science using keywords such as "eCCU", "electrochemical carbon capture", "electrochemical carbon capture and utilization", and "integrated electrochemical carbon capture and utilization".

electron transfer (PCET) kinetics [18, 31]. However, a paradigm shift is observable post-2020, when the "research hotspot" has broadened significantly toward system integration. The surge in publications from 2022 to 2025 is largely attributed to the rise of fully integrated eCCU systems and the development of dual-function amine-mediated pathways that couples capture directly with electrolysis [32]. This exponential growth trajectory stands in stark contrast to the trends observed in mature carbon capture technologies, such as thermochemical amine scrubbing or pressure swing adsorption (PSA) [8, 33]. Conversely, although mature thermochemical and adsorption technologies have reached a stage of technological saturation, characterized by a focus on incremental optimization and retrofitting, electrochemical approaches are demonstrating a trajectory of disruptive and exponential growth. This divergence is fundamentally driven by the global energy transition: As renewable electricity becomes the lowest-cost energy vector, eCCC is increasingly favored over phonon-driven (thermal) processes, positioning eCCU as a unique and dominant frontier for next-generation decarbonization [27, 34]. Moreover, Fig. 1(b) demonstrates a preferred reporting items for systematic reviews and meta-analyses (PRISMA) flow diagram which depicts the selection process for literature included in this review [35].

Dedicated analyses focusing on electrochemical approaches remain limited, particularly in terms of elucidating their mechanistic foundations, potential synergies, and the critical challenges that must be addressed for large-scale deployment [36–38]. To address these gaps, this review provides a comprehensive analysis of fully integrated electrochemical strategies through three distinct lenses: First, we propose a systematic classification framework (Types I–III) to categorize the degree of integration, identifying pathways to transition from decoupled steps to single-reactor architectures [39]. Second, we offer a deep mechanistic analysis of the physicochemical incompatibilities, such as thermodynamic potential mismatches and impurity intolerance, that currently hinder the coupling of capture media (e.g., redox carriers and amines) with electrocatalytic interfaces. Third, we conduct a rigorous techno-economic assessment (TEA), utilizing metrics such as specific primary energy consumption for CO_2 avoided (SPECCA) to benchmark emerging electrochemical methods against mature thermochemical processes, culminating in a quantitative roadmap for industrial commercialization [1, 9].

This review offers a comprehensive overview of electrochemical technologies for integrated CO_2 capture, concentration, and utilization. Despite increasing interest in these approaches, there is a lack of reviews combining technical and economic assessments. We first explore the mechanistic foundations and material innovations driving electrochemical CO_2 capture systems. We then highlight recent advancements in CO_2 electro-reduction and strategies for directly coupling capture with conversion to improve efficiency. The review also covers economic analyses of eCCC and eCCU processes, offering insights into their feasibility and cost-effectiveness. Finally, we discuss the synergies between capture and conversion, address the persistent challenges for large-scale application, and identify future directions crucial for overcoming these barriers. We try to provide a roadmap for advancing electrochemical CO_2 capture technologies and guiding their future development for climate mitigation.

2 Electrochemical CO_2 capture system

The concept of electrochemical CO_2 capture can be traced back to early work on molten carbonate fuel cells (MCFCs), which was repurposed in the late 1960s as CO_2 concentrators. In 1969, Huebscher and Babinsky reported a dual-stack system incorporating an air blower and cooling units, achieving a CO_2 purity of up to 97%–98% [40]. Since then, carbon capture technologies have been deployed across two major domains: large stationary sources, such as flue gas from power generation, metallurgy, and cement production [41]; and more distributed sources, including transport exhaust, residential emissions, and agriculture [42]. Conventional post-combustion capture using amine-based solvents has been widely adopted for concentrated point sources, whereas direct air capture with inorganic hydroxides has been explored for more dilute and mobile streams. Despite their effectiveness, both organic and inorganic sorbents exhibit strong CO_2 binding, resulting in large negative adsorption enthalpies that necessitate high-temperature regeneration, thereby imposing substantial energy penalties.

Electrochemical approaches have emerged as a promising alternative, offering isothermal operation with improved reversibility, higher energy efficiency, and inherently safer operating conditions. Broadly, as can be seen from Fig. 2, electrochemically

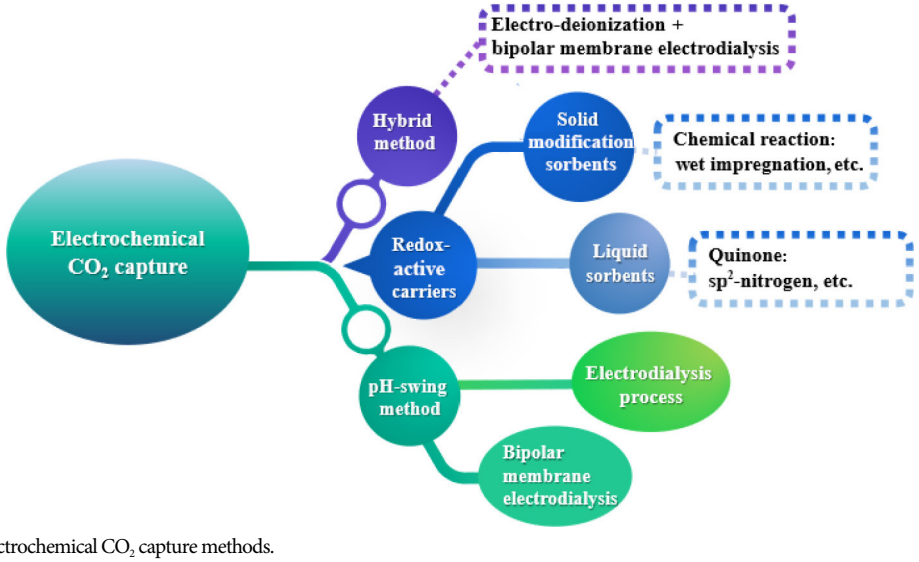

Figure 2 Summary of electrochemical CO_2 capture methods.

mediated CO_2 capture can be categorized into four different types, including pH-swing systems, redox-carrier systems, molten carbonate, and hybrid methods [14, 43]. Among them pH-swing systems and redox-carrier systems are most researched [44, 45]. In the pH-swing approach, reversible electrochemical reactions generate local acidic or alkaline environments, enabling cyclic absorption and release of CO_2 [18]. In the redox-carrier approach, a redox-active molecule with at least two stable oxidation states, commonly quinones, bipyridines, disulfides, or transition-metal complexes, undergoes reduction to form a nucleophilic species (R^{n-}) that binds CO_2 to yield carbonate adducts. Subsequent electrochemical oxidation regenerates the original form (R), releasing concentrated CO_2 ($R + ne^- + nCO_2 \leftrightarrow R(nCO_2)^{n-}$) [46–48]. Quinones are of particular interest due to their highly reversible redox couples and the strong affinity of their reduced oxyanion species toward CO_2. Together, these two electrochemical paradigms exemplify how capture and concentration can be achieved through reversible electron and mass transfer processes, circumventing the energy-intensive thermal regeneration inherent to conventional sorbent-based systems. We also summarized different electrochemical CO_2 capture technologies in Table 1, which concluded various techno-economics metrics for further comparison.

Table 1 The summary of electrochemical CO_2 capture technologies

Metrics		Adsorption conditions	CO_2 capture rate	Capture energy consumption	Detachment condition	Energy consumption	Ref.
PH-swing system	Seawater battery-carbonation	Ambient air	50 ppm-CO_2/h	—	—	—	[49]
	BMED (KOH)	—	—	—	Air, load ratio of 0.9	8.8 GJ/ton CO_2	[50]
	High-pressure BPMED	—	—	—	6 atm	333 kJ/mol CO_2	[51]
	Flow cell (CPS)	Ambient air	—	126 kJ/ mol	—	—	[52]
	PCET (PAAQ)	Mixed N_2/CO_2, 0.012 bar	0.0161 mL/h CO_2	197 kJ/mol	Mixed N_2/CO_2, 0.012 bar	197 kJ/mol	[53]
	PCET (EDA)	Simulate flue gas (0.15 bar CO_2)	—	21.0 kJ/mol	—	—	[54]
	PCET (CO_2-carbonate system)	Air (400 ppm CO_2)	—	16 to 75 kJ/mol (ideal cycle)	—	—	[18, 19]
	H_2-recycling electrochemical system (sulphate addition)	Air (0.3 atm)	—	247 kJ/mol	—	—	[55]
	DSPZ	Mixed N_2/CO_2, 0.465 bar CO_2	—	48.9 kJ/mol	~ 0 bar CO_2	60 kJ/mol	[18, 19]
	Anion exchange resins	Dry air (RH = 33%)	—	—	Ambient/room	374 kJ/mol	[56]
	$K_3Fe(CN)_6/K_4Fe(CN)_6$ and 1,8-ESP	30% CO_2 concentration	—	49 to 63 kJ/mol CO_2	Electrochemical acidification	—	[57]
	AEM-based	—	—	—	Current density (20 A/m^2)	63 kJ/mol	[58]
	Zwitterionic BzSP exhibits	Lower than 10% CO_2	—	102 kJ/mol CO_2	CO_2:N_2 mixture (10:90)	136 kJ/mol CO_2	[59]
Redox-active capture molecules	BDT-Q	13% CO_2 and 3.5% O_2	—	108 kJ/mol	—	—	[46]
	NR/NRH_2	Non-pretreated air (ca. 1000 mL/min)	9.167 mL/h	65 kJ/mol	—	—	[46]
	CVE	Air (200 sccm)	0.049 mmol/h	3.8 GJ/ton	—	—	[60]
	Isoindigo and their derivatives	10% CO_2 and 3% O_2 mix, balanced by N_2	—	143.7 kJ/mol CO_2	under pure CO_2	224 kJ/mol CO_2	[61]
	Amine-QH_2-H_2O	—	—	—	Untreated	0.7 GJ/ton	[62]
	Brønsted acids and amine	10% CO_2 and 21% O_2	—	—	10% CO_2 with 2% O_2	62.3 kJ/mol CO_2	[63]
	Quinone-functionalised carbons	CO_2	—	Consumption of 254 kJ/mol per cycle	CO_2	Consumption of 254 kJ/mol per cycle	[64]
	4-fluorophenyl thiolate/4-fluorophenyl disulfide redox couple	20% CO_2 in N_2	—	–27.62 kJ/mol CO_2	20% CO_2 in N_2	153 kJ/mol CO_2	[65]
Electrochemically mediated regeneration	Amine	15% CO_2	—	—	15% CO_2	40–80 kJ$_e$/mol CO_2	[66]
	Na_2Q	12.5 vol.% CO_2	—	—	12.5 vol.% CO_2	—	[67]
	Cu–EDA–CO_2–H_2O	Industrial smoke	—	—	Industrial smoke	97 kJ/mol CO_2 (generation rate is 2.05×10^{-7} kg/s)	[68]

2.1 pH-swing system

In pH-swing system, CO_2 was captured by cyclically modulating proton concentration in aqueous media, exploiting the equilibria of $CO_2/HCO_3^-/CO_3^{2-}$. As can be seen in Figs. 3(a) and 3(b), during capture (high pH), cathodic water reduction generates OH^-, driving CO_2 chemisorption into bicarbonate/carbonate ions. Proton flux is commonly managed using electrodialysis or bipolar membrane electrodialysis (BPMED), which operate at low voltages to avoid thermal penalties while enabling spatially separated capture and release.

In comparison to conventional CO_2 capture methods, the electrochemical pH-swing process exhibits much lower energy consumption and easier integration with renewable energy systems [69]. ED has been applied to aqueous CO_2 capture and release in configurations ranging from ocean capture to $KHCO_3$ concentration from K_2CO_3 sorbents, thereby improving the regeneration efficiency. BPMED offers an alternative by splitting water under an applied electric field, generating OH^- and H^+ that migrate in opposite directions across the bipolar membrane, thus sustaining a pH gradient for CO_2 capture and release. During regeneration (low pH), anodic water oxidation produces H^+, protonating these species and releasing CO_2 [18, 19]. This process could be described by Eqs. (1)–(4) [13]

$$CO_2(g) + H_2O \leftrightarrow CO_2(aq) + H_2O \quad (1)$$

$$CO_2(aq) + H_2O \leftrightarrow H_2CO_3 \quad (2)$$

$$H_2CO_3 + H_2O \leftrightarrow HCO_3^- + H_3O^+ \quad (3)$$

$$HCO_3^- + H_2O \leftrightarrow CO_3^{2-} + H_3O^+ \quad (4)$$

2.1.1 *Electrodialysis process*

The electrolysis-driven concept was first demonstrated by Stucki et al., who coupled KOH-based CO_2 absorption with electrolytic solvent regeneration, releasing pure CO_2 and H_2 (Eq. (5)) [70]. With optimized cell and membrane configurations, the process can produce a stoichiometric gas mixture ($3H_2$ + CO_2) suitable for methanol synthesis [71], and this is also the first concept of integration of electrochemical CO_2 capture and utilization. Building on this foundation, Rau, Park, and others expanded the ED process using (bi)carbonate products [72–74]. For example, when natural carbonate minerals such as $CaCO_3$ are dissolved at the anode by locally generated acid, the released ions react with CO_2 at the cathode to form soluble calcium bicarbonate ($Ca(HCO_3)_2$), which can be stably stored in the ocean or underground (Eq. (6)). This pathway co-produces hydrogen, and for every ton of H_2 generated, up to 22 tons of CO_2 can be captured, enabling carbon-negative hydrogen if operational emissions are minimized. The chemical reactions are listed as follows

$$4H_2O + 2K_2CO_3 \rightarrow 4KOH + 2CO_2 + 2H_2 + O_2 \quad (5)$$

$$2CaCO_3 + 2CO_2 + 4H_2O \rightarrow 2Ca^{2+} + 4HCO_3^- + 2H_2 + O_2 \quad (6)$$

An alternative ED configuration employs saltwater electrolysis. Here, NaCl electrolysis generates NaOH at the cathode, which reacts with CO_2 to form solid carbonates such as $CaCO_3$, thereby eliminating the need for a desorption step. However, this approach must address the challenge of managing toxic chlorine gas produced at the anode, which requires scrubbing or repurposing as a feedstock. Despite its potential, ED is most effective in high-concentration CO_2 streams (e.g., flue gas) rather than direct air capture (DAC). To address energy and efficiency limitations, several groups have proposed modifications. Yamada's team replaced thermal regeneration with vacuum desorption, cutting energy use to as low as 0.81 GJ/tCO_2 [75]. Darton's group compared electrolysis and electrodialysis for DAC [76], accounting for membrane K^+ selectivity and industrial-scale air contactors, and found theoretical energy limits of 162 kJ/mol for electrolysis and 154 kJ/mol for electrodialysis. Carlson's group proposed a resin wafer-electrode deionization (RW-EDI) system that captures CO_2 in alkaline chambers and releases it in acidic chambers via electrochemical pH swings, achieving 80% capture from simulated flue gas (15% CO_2/85% N_2) with > 98% purity [77].

Moreover, ED can circumvent energy-intensive gas evolution reactions (oxygen evolution reaction/hydrogen evolution reaction (OER/HER) or Cl_2 evolution) by employing reversible redox mediators. This strategy eliminates the thermodynamic penalties and kinetic overpotentials associated with gaseous product formation, substantially reducing operating voltages [78, 79]. Two dominant approaches have emerged:

(1) Gas recirculation systems

Recirculating H_2(g) produced at the cathode to the anode stimulates the hydrogen oxidation reaction (HOR) to replace OER (Eqs. (7) and (8)) [80, 81]

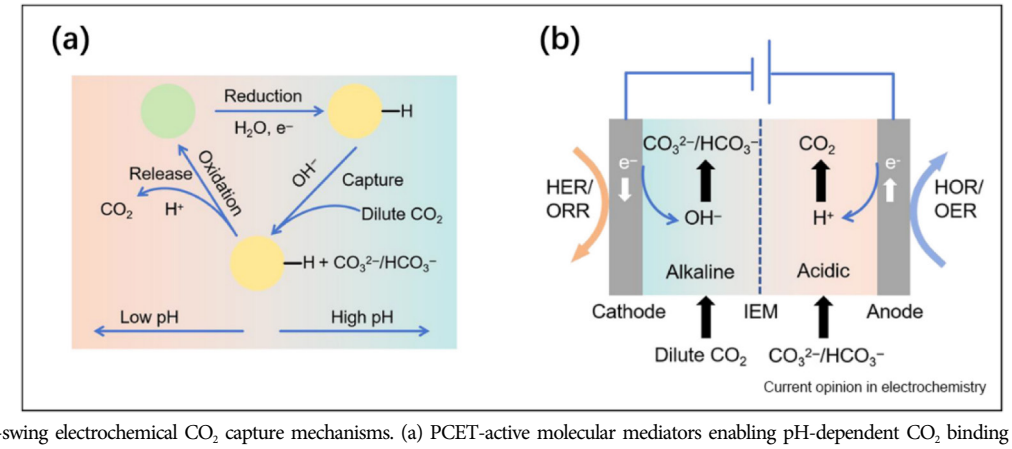

Figure 3 Two pH-swing electrochemical CO_2 capture mechanisms. (a) PCET-active molecular mediators enabling pH-dependent CO_2 binding and release. (b) Ion-exchange-membrane-regulated CO_2 absorption and regeneration. Reproduced with permission from Ref. [48], © Elsevier. B.V. 2025.

$$\text{Anode}: 2H_2 \rightarrow 4H^+ + 4e^- \quad (7)$$

$$\text{Cathode}: 2H_2O + 2e^- \rightarrow 2OH^- + 2H_2 \quad (8)$$

This closed-loop operation achieves proton/hydroxide generation at voltages as low as 1.3 V (ΔpH = 14) by exploiting the near-equilibrium potential of HOR/HER (Table 1).

(2) Oxygen-mediated cathode reactions

Alternatively, replacing HER with oxygen reduction reaction (ORR) at the cathode avoids H_2 production entirely (Eqs. (9) and (10)) [82]

$$\text{Anode}: 2H_2O \rightarrow 4H^+ + O_2 + 4e^- \quad (9)$$

$$\text{Cathode}: O_2 + 2H_2O + 4e^- \rightarrow 4OH^- \quad (10)$$

This creates an O_2 redox cycle where anodically generated oxygen is consumed at the cathode, maintaining a net zero gas flux. Cell voltages typically range from 1.3 to 2.2 V, contingent on O_2 supply efficiency (Table 2).

However, even employing H_2 recirculation or ORR-mediated strategy in ED process, there are inherently couple CO_2 capture with gas production (H_2, O_2, or Cl_2), increasing energy and purification costs. More promisingly, by employing BPMED [22], which decouples CO_2 capture from gas production and offers a pathway to reduce energy demand.

2.1.2 *Bipolar membrane electrodialysis*

BPMED integrates an anion-exchange layer (AEL) and a cation-exchange layer (CEL) at a functional interface. Under an applied electric field exceeding the junction potential, bipolar membranes (BPMs) catalytically dissociate water into protons (H^+) and hydroxide ions (OH^-) at this interfacial region (Figs. 4(a) and 4(b)) [83]. This reaction establishes a controlled pH gradient (ΔpH) across the membrane, forming the foundation for electrochemical pH-swing processes. This enables CO_2 capture and solvent regeneration in a single electrochemical process. As early as 2011, Eisaman et al. conducted one of the first experimental demonstrations of regenerating CO_2 from aqueous potassium carbonate/bicarbonate solutions using BPMED [84]. Their results showed that, in a commercial-scale system (ignoring electrode contributions), the minimum energy consumption at the low-current limit of $KHCO_3$ was about 100 kJ/mol CO_2. Since DAC typically requires ~ 200 kJ/mol CO_2 for absorption into hydroxide solutions and ~ 300 kJ/mol CO_2 when the regeneration is included, BPMED represented a significant step toward lowering energy demand (Fig. 4(c)). Building on this, Sabatino et al. demonstrated DAC by wet scrubbing with aqueous KOH [85], followed by solvent regeneration and CO_2 recovery via BPMED, achieving capture costs as low as 236 kJ/mol CO_2.

However, the economic barrier remains high due to the cost and limited durability of bipolar and ion-exchange membranes, which affect both capital and operating expenses. Economic analysis showed total costs ranging from $1757 to $860 per ton of CO_2 (depending on energy demand and productivity) [85]. With future improvements in membrane conductivity, stability, and cost, total expenses could potentially fall below $250 per ton of CO_2, making BPMED competitive with thermochemical regeneration methods that rely on natural gas [86]. Another life cycle assessment (LCA) research conducted by Houssam et al., they designed a BPMED process coupled with CO_2 transportation and utilization devices (Fig. 5(a)), the electricity supply also heavily influenced BPMED process, it can achieve net-negative emissions in regions (UK, Spain, Denmark, and France) with low-carbon electricity (< 0.3 kWh/kg CO_{2eq}) but requires dedicated renewable plants in areas with carbon-intensive grids [87].

Beyond CO_2 capture, the versatility of BPMED enables integration with other separation processes. For example, Wang et al. proposed a newly BPMED system that simultaneously treats aniline wastewater and captures CO_2 [88], its treated wastewater and capture CO_2 under different current, while Jiang et al. introduced BPMED for CO_2 capture coupled with amino acid

Table 2 Voltage comparison and recent advancements

System type	Voltage range (ΔpH = 14)	Energy savings mechanism
Conventional OER/HER	> 2.2 V	Baseline (gas evolution penalty)
H_2 recirculation	1.3–1.8 V	Elimination of OER overpotential
ORR-mediated	1.3–2.2 V	Avoidance of H_2 evolution

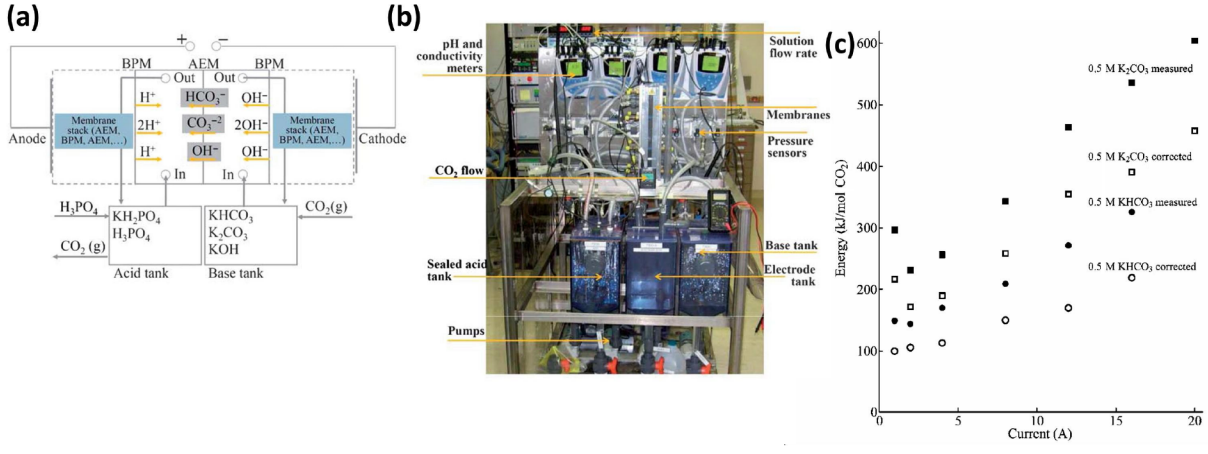

Figure 4 (a) Schematic of the experimental setup. (b) Photo of the experimental setup. (c) Energy vs. current for K_2CO_3 (squares) and $KHCO_3$ (circles). Reproduced with permission from Ref. [84], © The Royal Society Chemistry 2011.

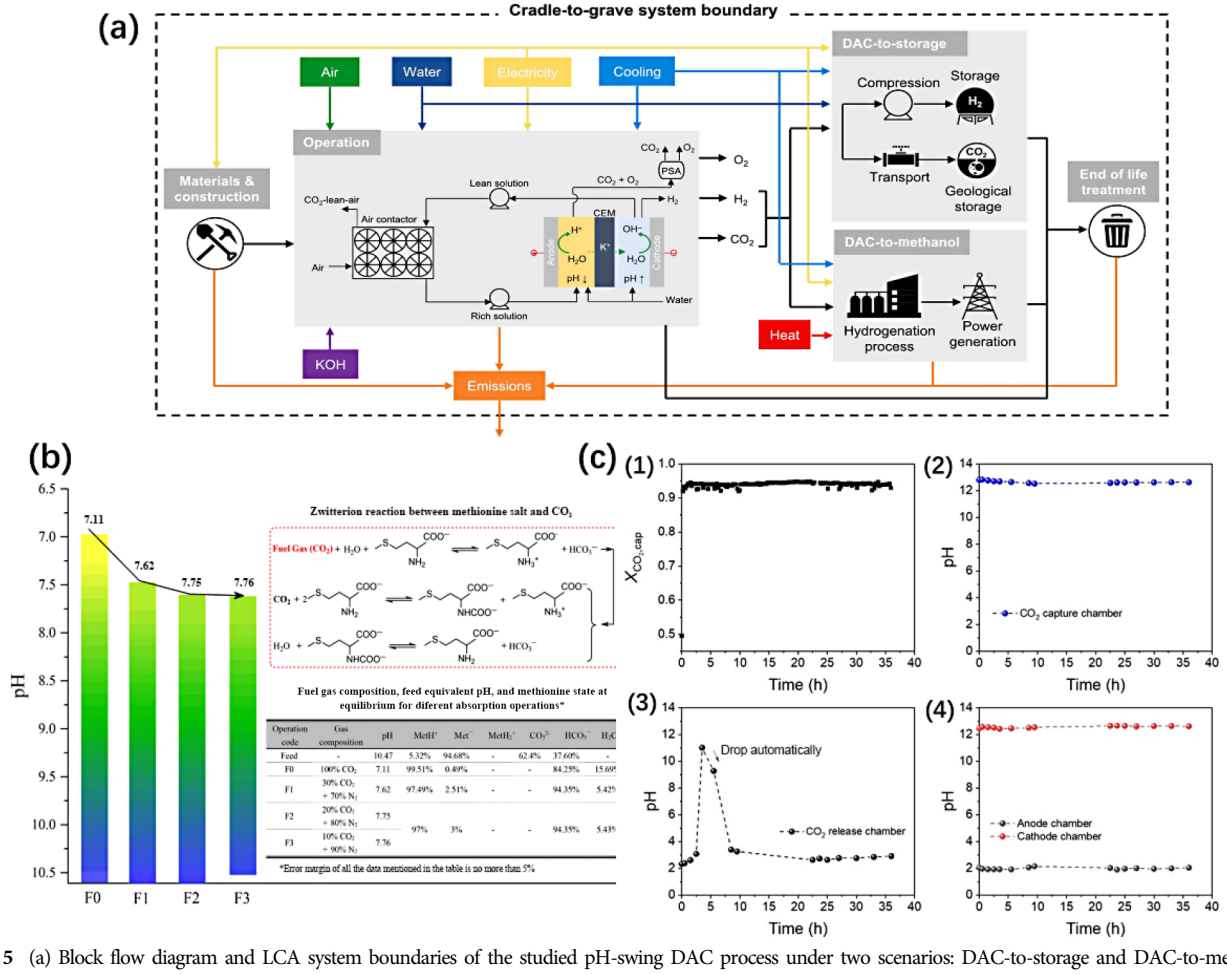

Figure 5 (a) Block flow diagram and LCA system boundaries of the studied pH-swing DAC process under two scenarios: DAC-to-storage and DAC-to-methanol. Reproduced with permission from Ref. [87], © Elsevier Ltd. 2025. (b) The pH variation and composition change in the methionine salt intermediate as a function of time during CO_2 absorption for fuel gases F_0 to F_3. Reproduced with permission from Ref. [22], © Elsevier B.V. 2017. (c) Results of the continuous DAC experiment showing (1) the fraction of CO_2 captured from air ($X_{CO_2,cap}$), and the time dependence of the pH values in (2) the CO_2 capture chamber, (3) the CO_2 release chamber, and (4) the anode chamber and the cathode chamber of the H-cell during the 40-mA galvanostatic electrolysis at 25 °C. Reproduced with permission from Ref. [89], © Wiley-VCH GmbH 2024.

separation [22], achieving up to 99.6% methionine extraction at an energy cost of 7.0 kWh per kg CO_2. Even the flue gas feed stream (10% CO_2) could achieve 97% amino acid production (Fig. 5(b)), presenting the potential of BPMED process in CO_2 capture area. Such multi-functional applications illustrate the broader utility of BPMED but also highlight the trade-off between performance and cost. Except the CO_2 in gas phase, the ocean absorbs 40% of all CO_2 emissions. Rachel et al. used hydrogen and a redox salt to shift the water's pH to extract CO_2 while also generating and consuming power. It is energy-competitive with other CO_2 removal methods, especially if pumping costs are low. By using variable electricity pricing, operational costs can be significantly reduced, saving up to $65 per ton of CO_2. At a large-scale plant, this could mean $6.5 million in annual savings. For further reducing the membrane cost of BPMED process, Jiayin et al. designed a three-room H-cell, with the two chambers separated by porous filter papers. In this process, diluting CO_2 from flue gas or air is absorbed by OH^- in the gas contactor and converted into carbonate (CO_3^{2-}) or bicarbonate (HCO_3^-) species in solution [89]. The resulting carbonate/bicarbonate solution is then circulated to the CO_2 release chamber, where it reacts with H^+ to liberate concentrated CO_2. In 35 h of continued DAC experiments, the process kept stable CO_2 capacity and high purity CO_2 released smoothly in CO_2 release chamber (Fig. 5(c)). Their research provides a strategy to reduce the cost of the pH-swing process and prove its efficiency.

Moreover, BPMED is advancing as a versatile platform that seamlessly integrates CO_2 capture with its direct utilization, creating valuable products [90–92]. A prime example is the work by Bi et al., in which BPMED simultaneously treats saline wastewater and captures CO_2 to produce high-purity sodium carbonate (Na_2CO_3) [93]. The process begins with using BPMED to split the wastewater's sodium chloride into sodium hydroxide (NaOH) and acid. The resulting NaOH solution then actively absorbs CO_2, converting it directly into Na_2CO_3 into a single, integrated system. BPMED's application extends beyond carbonate production. It can also extract dissolved CO_2 directly from seawater [94], enabling the creation of renewable and carbon-neutral fuels. Furthermore, innovative processes combine BPMED with crystallization to capture CO_2 while extracting valuable minerals like magnesium from brine or seawater [95].

In a related but distinct electrochemical approach, a BPM cell can be configured for electrochemical CO_2 reduction reaction (CO_2RR). Here, CO_2 is fed to the cathode and electrochemically converted into carbon monoxide (CO) [96], competing with

hydrogen production. A key feature of this system is the BPM itself, which efficiently manages ion transport. Bicarbonate and carbonate ions formed at the cathode migrate to the membrane's interface, where they react with protons from the anode, regenerating CO_2 and water and thus facilitating continuous operation. These diverse strategies underscore the significant potential of electrochemical membrane systems for efficient and synergistic carbon capture and conversion [41, 97].

In summary, BPMED offers a promising electrochemical pathway for CO_2 capture and regeneration, with the potential for co-benefits in multi-pollutant treatment. The primary challenge lies in reducing the membrane cost and the energy demand-critical steps toward scaling BPMED as a viable alternative for carbon capture

2.1.3 *Hybrid system*

EDI combines ion exchange membrane technology with ion exchange resins. Datta et al. developed a technology that utilizes a RW-EDI device for *in-situ* electrochemical pH control, capturing CO_2 from flue gas in an alkaline chamber, and then releasing (recovering) captured CO_2 (purifying) in the acidic chamber of the same device. Although Datta's research has demonstrated feasibility, there is currently limited research on EDI + BPMED in the field of carbon dioxide capture, and there are no clear energy calculation and cost analysis cases. This technology is still more commonly used in semiconductor production and laboratory analysis of ultrapure water [98].

2.1.4 *Summary of pH-swing system*

The pH-swing CO_2 capture system represents an emerging class of electrochemically mediated separation technologies designed to overcome the intrinsic thermodynamic and efficiency limitations of traditional amine scrubbing [18, 87, 90]. By splitting water into H^+ and OH^- ions using electrolysis method or bipolar membranes, the process captures CO_2 in alkaline media and releases it under acidic conditions, eliminating the need for heat-driven desorption. This electricity-powered approach reduces regeneration energy from 3 to 4 GJ/t CO_2 in amine scrubbing to below 1.5 GJ/t CO_2, enabling operation with renewable power sources [3]. The modular and low-temperature design minimizes solvent degradation, emissions, and corrosion, while allowing compact and scalable cell architectures. Challenges remain in reducing membrane cost, improving electrode durability, and achieving efficient large-scale operation. Integrating pH-swing systems with renewable grids and DAC units could deliver a sustainable and low-carbon pathway for distributed CO_2 separation and utilization, bridging electrochemical innovation with global decarbonization strategies [18, 99].

2.2 Redox-active capture molecules

Redox-active capture molecules utilize electrochemically driven redox reactions to generate nucleophilic species capable of binding CO_2 at its electrophilic carbon center, forming stable adducts for reversible capture [100]. This concept dates to 1989, when Mizen and Wrighton demonstrated that electrochemically reduced 9,10-phenanthrenequinone (PAQ) could react with CO_2 to form carbonate adducts, as shown in Fig. 6(a), establishing one of the earliest systems for reversible and redox-mediated CO_2 capture [101]. Also, the mechanism of redox-active carriers reacting with CO_2 is shown in Fig. 6(b) [102]. With the progression of scientific research, various redox-active capture adsorbents have emerged, as shown in Fig. 6(c) [103], specifically amine, quinone, disulfide, and other types of adsorbents, which have yielded a wealth of research findings. Recent work also proved that redox-active molecules could also be applied into DAC process, as shown in Fig. 6(d). In the following text, a concise overview of the classification of redox-active adsorbents will be provided [104].

To function as a redox-active CO_2 carrier, a molecule must contain both a CO_2-binding site and a redox-active site. CO_2 binding typically involves the electrophilic carbon of CO_2 interacting with an electron-rich nucleophile, such as a metal center forming a metal carboxylate, an alkoxide forming a carbonate, or an amide forming a carbamate [103, 105]. The redox-active site must induce a significant redistribution of electron density at the CO_2-

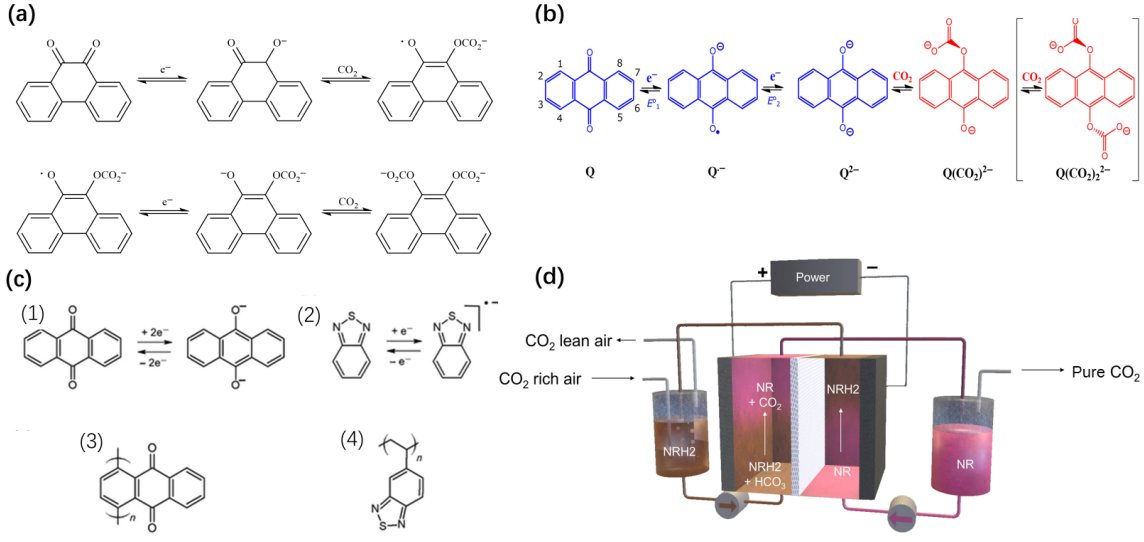

Figure 6 (a) Absorption/desorption process of PAQ with CO_2. Reproduced with permission from Ref. [101], © The Electrochemical Society 1989. (b) The stepwise electrochemical CO_2 reaction scheme employed in DFT calculations includes two electron transfer steps followed by one chemical step. The electrochemical CO_2 capture scheme includes one further chemical step. Reproduced with permission from Ref. [102], © Bui, A. T. et al. 2022. (c) Schematic illustrations of redox-active organic monomers, (1) anthraquinone (AQ) and (2) 2,1,3-benzothiadiazole (BTZ), and redox-active organic polymers, (3) poly-anthraquinone (PAQ) and (4) poly-benzothiadiazole (PBTZ). Reproduced with permission from Ref. [103], © American Chemistry Society 2023. (d) Electrochemical device employing quinone polymers for DAC of CO_2. Reproduced with permission from Ref. [104], © Seo, H. et al. 2023.

binding site to enhance or reduce its nucleophilicity, thereby controlling binding and release. The proximity of the redox site to the CO_2-binding site is critical: When separated by more than a single atom, electronic communication diminishes, and the difference in binding affinity between redox states becomes negligible [46, 102]. The following sections examine correlations between CO_2 binding affinity and reduction potential for quinones (Section 2.2.1) and transition-metal complexes (Section 2.2.2), followed by design strategies for stable, high-performance redox carriers (Section 2.2.3).

2.2.1 *Quinones*

Among organic molecules and transition-metal complexes that meet the criteria for redox-active CO_2 carriers, quinones are the most extensively studied due to their well-characterized redox and protonation behavior, commercial availability, and high CO_2 affinity at moderate potentials. Consequently, quinones have become primary focus in eCCC [31]. Their capture mechanism involves electrochemical reduction to generate nucleophilic dianions (Q^{2-}), which react with CO_2 to form stable carbonate adducts. Oxidation of the adduct releases CO_2 and regenerates the quinone, enabling a fully reversible capture cycle [106].

Usually, quinone molecules are fully conjugated diketone organic compounds, and the number of benzene rings, type of functional groups, position, and quantity of functional groups can significantly affect the electrochemical behavior and binding affinity with CO_2 in different types of quinone molecules [107, 108]. In the early research on using quinones for electrochemical carbon capture, non-aqueous media such as organic solvents and ionic liquids were often used to avoid the influence of hydrogen ions [109]. Barlow et al. used ethanol to increase the anodic transfer of the reduction potential of quinone oxidation–reduction carrier 2,3,5,6-tetrachlorobenzoquinone (TCQ), thereby endowing quinone with O_2 stability and solving the oxygen-sensitive problem often faced by quinone based CO_2 capture systems [110]; Tam et al. studied the applicability of three reduced naphthoquinones with different methyl substitutions on the quinone ring as electrocatalysts for CO_2 capture and conversion under anaerobic conditions in non-proton organic solvent acetonitrile [111]; Gurkan et al. explored the potential application of electrocarboxylation of quinones in ionic liquids for the separation of CO_2 from gas mixtures [112]; Scovazzo et al. demonstrated the electrochemical separation of CO_2 from gas mixtures with < 1% concentration using 2,6-di-tert-butyl-1,4-benzoquinone as a carrier in ionic liquids (IL) and organic solvent electrolyte media [40]. Research demonstrates that the CO_2-binding affinity of quinones can be tuned by attaching electron-withdrawing or electron-donating functional groups at the ortho position. Anna et al. used density functional theory (DFT) calculations to quantify this effect, showing that the strategic functionalization can favor electrochemical reduction over side-reactions with O_2 without significantly hindering CO_2 capture [102]. They also found that the steric bulk and position of these groups are relative to the quinone oxygen impact CO_2 reactivity. Building on this framework, Xing et al. engineered isoindigo-based quinones that break the traditional trade-off between redox potential and CO_2 binding strength. These novel carriers, with their facile synthesis, high tunability, and biocompatibility, represent a significant advance toward more efficient and reliable redox carriers for electrochemical carbon capture [61].

The widespread adoption of quinone-based sorbents for electrochemical CO_2 capture is primarily hindered by two challenges: their inherent susceptibility to oxygen and the difficulty of operating them in robust, aqueous electrolytes [113, 114]. When deployed in streams containing oxygen (e.g., flue gas or air), reduced quinone species can be oxidized, generating superoxide radicals (O_2^-) [110]. These radicals initiate destructive side reactions that degrade the sorbent and electrolyte, compromising the system longevity. Significant research efforts are focused on overcoming these limitations. To address the oxygen instability, Jeffrey et al. demonstrated a simple yet effective strategy of adding 2 M ethanol to a commercial quinone sorbent (TCQ/dimethyl formamide (DMF)), which achieved an efficiency of 26% in concentrating a 10% CO_2 stream. However, this system still relied on organic solvents. Similar works are conducted by Hatton's group, who developed a series of oxygen-stable quinone-structure molecules, and discovered that heterocyclic quinone compounds showed the oxygen-stable properties [46]. Based on this, benzodithiophene quinone (BDT-Q) was synthesized, and the continuous flow cell results showed the simulated flue gas (3.5% O_2/13% CO_2) capture capacity and the electron utilization achieved to 1.6 and 0.8 per molecule. Surprisingly, the electrochemical work of BDT-Q could reach 108 kJ/mol, showing the potential of low desorption energy cost.

For aqueous systems, two main strategies have emerged. The first involves designing water-soluble quinone molecules, such as the sulfonated and glycol-functionalized anthraquinones synthesized by Yan et al. Although this demonstrated CO_2 capture capability [112], their long-term oxygen tolerance requires further improvement through molecular design.

The second promising strategy utilizes high-concentration "water-in-salt" electrolytes. Liu et al. showed that a concentrated LiTFSI aqueous electrolyte effectively mitigates the incompatibility between water and quinone chemistry. This approach offers multiple advantages: It enhances the reactivity between CO_2 and the quinone, suppresses competitive side reactions, reduces water evaporation, and minimizes the dissolution of electroactive compounds from electrodes. Cyclic voltammetry (CV) showed in Fig. 7(b) that measurements confirm the enhanced performance in these concentrated media, making them highly attractive for practical and quinone-mediated carbon capture applications [112].

In addition, Diederichsen et al. demonstrated a solvent-free and continuous-flow system for electrochemically mediated carbon capture using a modified naphthalene quinone derivative (LQ) in an ethylene glycol dimethyl ether (DEGME) electrolyte [114]. The process, illustrated in Fig. 7(a), is based on two key redox reactions (11) to (12) shown below; the reduction of LQ in the presence of CO_2 to form a carbonate complex, and the oxidation of a ferrocene derivative (Fc_1N_{112}-TFSI) as a counter reaction.

$$LQ + 2e^- + 2CO_2 \rightarrow LQ(CO_2)_2^{2-} \quad (11)$$

$$Fc_1N_{112}\text{-TFSI} \rightarrow FcN_{112}\text{-TFSI}^+ + e^- \quad (12)$$

The system consists of a tank containing 7 mL of Fc_1N_{112}-TFSI and NaTFSI (DEGME with a concentration of 0.7 M), a second tank containing 7 mL of LQ electrolyte (LQ:NaTFSI:DEGME molar ratio of 1:1:4), and a commercial flow cell (Fig. 7(b)) [115]. During the capture step, the LQ in the flow pool decreases and is continuously supplied to the LQ tank, resulting in a decrease in the concentration of discharged CO_2. Once the battery is turned off and the system is in a stationary state, the concentration of emitted CO_2

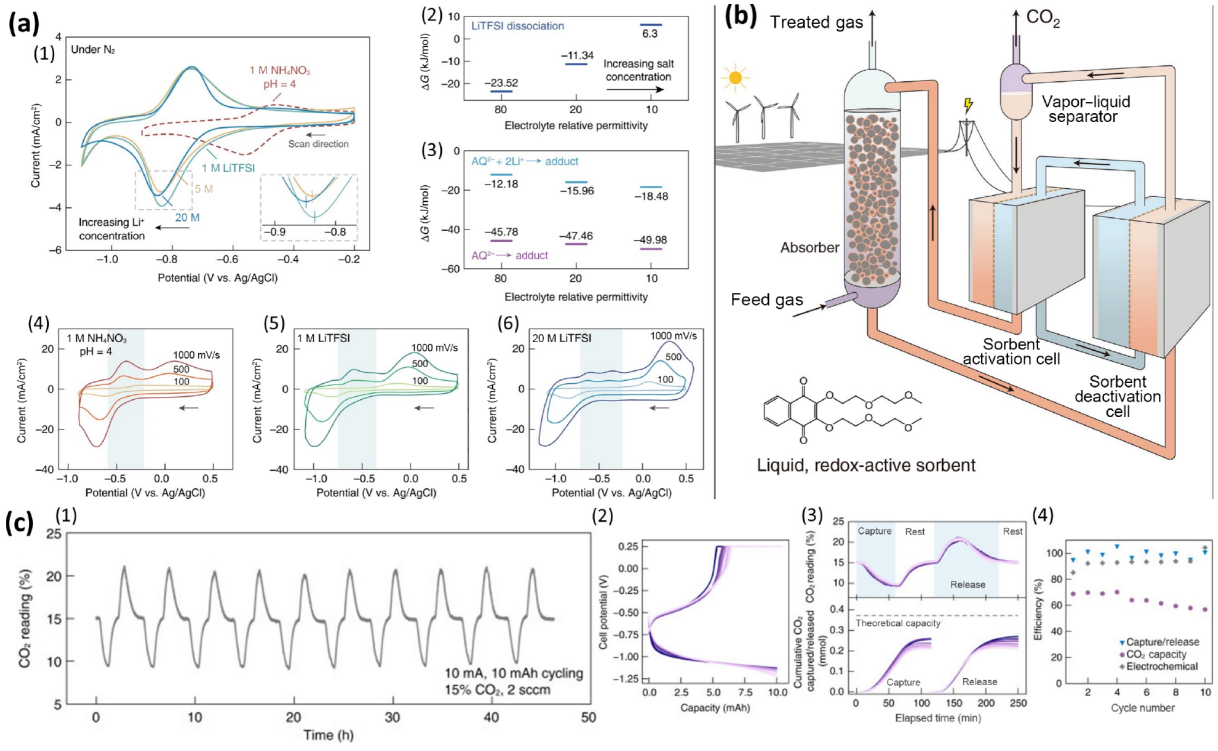

Figure 7 (a) (1) CV curves of PAQ-CNT in 1 M NH_4NO_3 and 20 M LiTFSI under N_2. (2) The free energy change for LiTFSI dissociation at different electrolyte permittivities. (3) The free energy change for quinone-CO_2 adduct formation at different electrolyte permittivities, starting from both AQ^{2-} and AQ^{2-} complexed with Li^+. CV curves of PAQ-CNT at different scan rates in (4) 1 M NH_4NO_3, (5) 1 M LiTFSI, and (6) 20 M LiTFSI under CO_2. The shaded area corresponds to the oxidation of quinone dianions that are unreacted with CO_2. Reproduced with permission from Ref. [113], © Liu, Y. Y. et al. 2020. (b) Illustration of the continuous-flow capture system. (c) (1) CO_2 reading at the exit of the LQ tank over repeated capture and release cycles for 48 h of operation. (2) Voltage–capacity curves for the 10 repeated cycles, with lighter colors representing later cycles. (3) The CO_2 reading for each individual capture–release cycle with the cumulative amount of CO_2 captured and released in each cycle shown below, relative to the theoretical capacity. (4) The efficiency of the electrochemical charge and discharge (gray crosses), efficiency of the CO_2 capture capacity relative to the theoretical value (purple circles), and the efficiency of the CO_2 capture and release relative to each other (blue triangles) for the 10 cycles. Reproduced with permission from Ref. [115], © Elsevier Inc. 2021.

slowly increases. In the continuous flow test, the research group tested the electrochemical performance of the battery (Fig. 7(c)(1)). By integrating the capture and release curves of each cycle through superposition curves, the accumulated CO_2 captured and released was calculated (Figs. 7(c)(2) and 7(c)(3)) [116]. Based on the above data, the group obtained the electrochemical efficiency (defined as the electrochemical charging capacity relative to the discharge capacity), CO_2 capacity utilization efficiency (defined as the amount of CO_2 captured relative to the theoretical value), and capture amount (Fig. 7(c)(4)) of the system, and found that the total quinone CO_2 capacity utilization rate of the given cycle hovered around 70% in the first few cycles. The experimental results show that for LQ electrolytes, the turning flow system is completely feasible. LQ adsorbent provides extremely high solubility of the capturing agent, but its drawback is that it requires some diluents to achieve reasonable conductivity and salt concentration [116].

Although the method of solvent dissolution of quinones has been widely used, it also has drawbacks: instability of organic solvents, low solubility of quinones, and cost and energy issues. Another commonly used solution is to fix quinone substances in an electrode-like structure to avoid the problems in the presence of liquid solvents, and it is always called self-supported electrode.

Take Wang et al.'s research as an example, as shown in Fig. 8(a). This group grafted hydroquinone and quinone functional groups onto a graded porous carbon framework through Friedel Kleinfrd reaction to selectively capture and remove CO_2 in flue gas and natural gas, and the adsorption isotherm results indicate that OAC can be easily regenerated without any other thermal input, and the highest CO_2 capacity measured at 273 K and 298 K is 5.41 and 3.46 mmol/g [116]. Wielend et al. reported a method using anthraquinone as a thin film electrode to achieve reversible electrochemical capture and release of CO_2, and in terms of the performance, the material exhibits 5.9 mmol CO_2/g AQ. Although the material dissolves after repeated cycles under N_2 conditions, it can maintain relative stability when forming a carbonate-like structure under CO [117]. Hartley et al. developed quinone-functionalized porous carbon materials for electrochemically driven CO_2 capture. This group synthesized anthraquinone-grafted carbon using mesoporous carbon CMK-3 with a pore size > 4 nm as the carrier, by loading diazo radical initiators and 2-aminoanthraquinone (2-AAQ) on it. The test results showed that the CO_2 adsorption capacity of the adsorbent could reach 0.4 mmol/g [64]. Figure 8(b) shows that it can capture and release CO_2 stability under different potentials. Another promising material was developed by Youhong et al., who created a novel porous polymeric electrode incorporating poly-(vinylanthraquinone) (PVAQ) [118]. As shown in Fig. 8(c), the sorbents showed a stable CO_2 capture–release ability with oxygen existence, and even in high humidity (75%), it runs for more than 160 h. For the long-time stability, the CO_2 capture ability kept for more than 100 cycles with flue gas (Fig. 8(d)). This electrode achieved a notable CO_2 capture capacity of approximately 30–80 kg/(m^3·day) and demonstrated

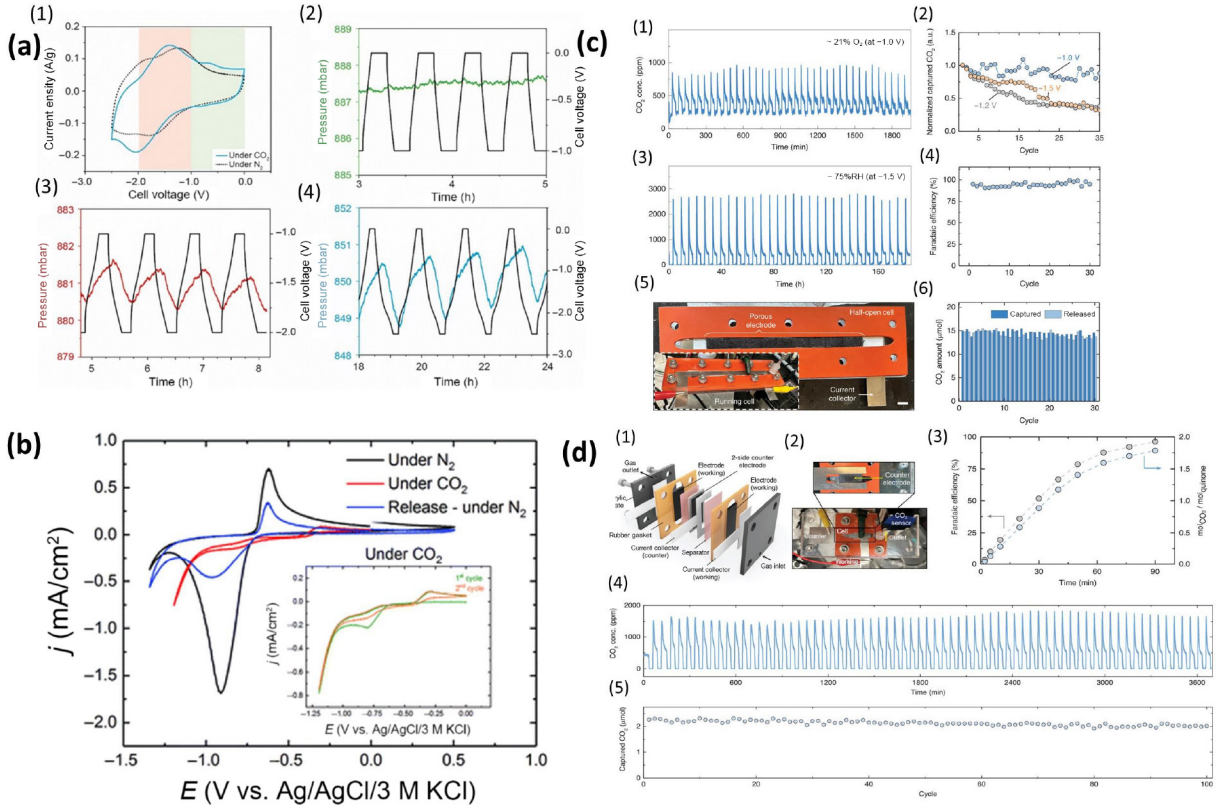

Figure 8 (a) (1) CV curves under N_2 (black dashed line) and CO_2 (blue line) at 1 mV/s. (2)–(4) Showing pressure and voltage data of f-CMK-3 under CO_2 with different cell voltage windows. Experiments ran a constant current at 0.1 A/g, and then the voltage was held for 10 min. (2) 0 to −1 V, pressure: green line. (3) −1 to −2 V, pressure: red line. (4) 0 to −2.5 V, pressure: blue line. Reproduced with permission from Ref. [64], © The Royal Society of Chemistry 2023. (b) CV curves of AQ/Cr–Au/glass in 0.1 M Na_2SO_4. The insert shows the comparison of the first and the second cycle of CV under CO_2 Reproduced with permission from Ref. [117], © The Royal Society of Chemistry 2018. (c) (1) CO_2 capture–release signals in air. (2) Normalized captured CO_2 amount for porous polymeric electrodes (PPEs) operating in air at applied voltages of −1.0, −1.2, and −1.5 V. (3) CO_2 capture–release signals under humid conditions (~ 75%RH), operated at −1.5 V. (4) Calculated Faradaic efficiency for each cycle. (5) Photo of PPE (7 mm × 120 mm) and the running flow-through cell. (6) The corresponding amount of captured and released CO_2 for each cycle is under 75%RH. (d) (1) Schematic showing the parallel configuration of the cell. (2) Photos of the assembled cell. (3) Faradaic efficiency and quinone utilization efficiency at a capture potential of −1.5 V with varying capture duration. (4) Long-term cycling stability. (5) Capture capacity of a parallelly stacked cell over 100 cycles. Experiments were conducted at room temperature with a 400 ppm CO_2 source in N_2 at 5 sccm. Reproduced with permission from Ref. [118], © Guo, Y. H. et al. 2024.

excellent cyclability. In summary, these combinations of high performance quinones and durability solid porous sorbents mark a significant step toward practical and energy-efficient carbon capture systems [119, 120].

Ultimately, advancing quinone-based carbon capture requires a multi-disciplinary strategy that merges molecular design with materials and electrochemical engineering. Success hinges on overcoming the intertwined challenges of oxygen stability and aqueous compatibility to develop viable systems. Achieving this will position quinones as a foundation for scalable and low-energy carbon capture technologies [121].

2.2.2 *Di-chalcogenide compounds and thiol salt*

Organic sulfur compounds are often used as nucleophilic and electrophilic reagents, a characteristic that has been demonstrated through multiple experiments. Considering the electrophilicity of CO_2, the characteristics of organic sulfur compounds can be used for CO_2 capture [121].

As early as 1989, Meilin researched the electrochemical properties of organic disulfide/thiolate redox couples, and these compounds have been utilized in redox-flow batteries area to enhance the batteries recycle performance. The research on the use of sulfides for CO_2 capture can be traced back to the achievements of Buttry's research group. Buttry et al. achieved electrochemical capture of CO_2 by utilizing the reduction of organic disulfide precursors to generate nucleophilic thiol salts, namely the capture agent thiol benzyl ester (RS^-), which is effective for CO_2 [122]. They tested the capture and regeneration processes of CO_2. The tested results clearly indicate that when there is a reduction current in the working electrode chamber, the CO_2 in the blowing airflow is completely consumed, generating thiol benzyl ester, which then reacts with CO_2. The release of CO_2 in the desorption experiment is due to the oxidation of thiocarbonate, and each equivalent of oxidation charge releases 1 equivalent of CO_2 [122]. The experiment used ionic liquid (IL) medium and DMF as solvent.

Based on Buttry's research, other research groups conducted research on the potential of other disulfides in CO_2 capture. Bushnell et al. compared the ability of benzyl diselenide and benzyl telluride to reversibly bind to CO_2 with benzyl disulfide and also studied the effect of solvent polarity on the thermodynamics of CO_2 capture [123]. The results proposed by this group indicate that the potential of studying BnTe-TeBn and BnSe-SeBn in carbon capture and storage (CCS) is worth considering. Kheirabadi et al. studied the catalytic activity of four different organic disulfide compounds ($C_{11}H_{12}NO_3Se$-$SeC_{11}H_{12}NO_3$, $C_9H_{10}NO_2Te$-$TeC_9H_{10}NO_2$, $C_{12}H_{12}NTe$-$TeC_{12}H_{12}N$, and $C_{12}H_{12}NSe$-$SeC_{12}H_{12}N$) at different

temperatures and substituents on the capture and release of CO_2 [124]. The obtained results offer that the organic di-selenide compounds as $C_{12}H_{12}NSe$-$SeC_{12}H_{12}N$ and $C_{11}H_{12}NO_3Se$-$SeC_{11}H_{12}NO_3$ could be the best candidate for use in CCS technologies.

Although sulfur-containing compounds have demonstrated potential as redox-active CO_2 sorbents, their practical performance remains largely unvalidated, with a notable scarcity of flow-cell experiments under realistic capture conditions. Recent work by Li et al. identified thiolate/disulfide redox couples as highly promising sorbents for scalable electrochemical CO_2 capture. By conjugating the π-system of a benzene ring with the electron pairs of sulfur atoms, they developed a system using a 4-fluorophenyl thiolate/disulfide couple [65]. In a flow-cell test with simulated flue gas (20% CO_2), this system demonstrated exceptional performance, achieving an initial CO_2 capacity utilization of ~ 100% and an average release/capture efficiency of ~ 90%. These results robustly validate the significant potential of thiolate-based chemistry for practical and large-scale carbon capture applications.

In summary, this field is considered to have the potential to address carbon capture issues and requires further exploration [125, 126].

2.2.3 *Bipyridines and sp² nitrogen base*

Bipyridine is a group of organic compounds with the chemical formula $(C_5H_4N)_2$, consisting of two pyridine $(C_5H_4N)_2$ rings. Bipyridine is the most popular research object in many fields of redox reactions. When it is reduced, bipyridine becomes nucleophili [127], which makes it have the potential as a carrier for oxidation–reduction CO_2 capture.

As early as 1994, Ohkubo's research group conducted a study on the interaction between CO_2 and the electrochemically reduced N-propyl-4,4'-bipyridine cation [128]. This group found that under specific conditions, electrolysis can produce a single electron-reducing substance of N-propyl-4,4'-bipyridine cation, which is a neutral free radical but can react with CO_2 [128, 129]. Buttry et al. conducted experimental, simulation, and computational studies on the interaction process between N-methyl-4,4'-bipyridine reduction and CO_2, and their research suggests that reducing $Mebipy^+$ in the presence of CO_2 forms the Mebipy–CO_2 compounds. The reaction processes are as follows (Eqs. (13)–(18)) [129]

$$Mebipy^+ + e^- \leftrightarrow Mebipy \quad (13)$$

$$2Mebipy \leftrightarrow Mebipy^+ + Mebipy^- \quad (14)$$

$$Mebipy^- + CO_2 \leftrightarrow Mebipy{-}CO_2^- \quad (15)$$

$$Mebipy{-}CO_2^- \leftrightarrow Mebipy{-}CO_2 + e^- \quad (16)$$

$$Mebipy{-}CO_2 \leftrightarrow Medipy + CO_2 \quad (17)$$

$$Mebipy \leftrightarrow Mebipy^+ + e^- \quad (18)$$

$Mebipy^+$ is reduced by an electron to form neutral Mebipy. In the presence of CO_2, Mebipy· undergoes dismutation to form $Mebipy^+$ and $Mebipy^-$. The latter reacts with CO_2 to form Mobipy–CO_2^-, leading to the disappearance of more cathodic redox events. Then, the CO_2 adduct can be electrochemically oxidized by two electrons, returning to the parent $Mebipy^+$ cation. For these monoalkylated pyridinium species, due to disproportionation events, stoichiometry requires two electrons to capture a CO_2 molecule [130]. Based on this, Ranjan et al. discussed the reaction progress between 4,4′-bipyridine and CO_2 without thermal activation [130].

The reaction between $Bpy^{\cdot-}$ and CO_2 may be a nucleophilic addition of pyridine nitrogen to the carbonyl carbon of CO_2, forming a bipyridyl N-carboxylate adduct. The oxidation of this adduct can occur on the bipyridyl carbon to obtain zwitterions, or on the carboxylate radical to obtain double radicals and release CO_2, as shown in Fig. 9(a) above [130]. Figure 9(b) shows that the single electron reduction of 4,4-bipyridine under nitrogen atmosphere is reversible, indicating that the bipyridine radical anion ($Bpy^{\cdot-}$) is stable on the millisecond time scale. When the solution is saturated with CO_2, it can be observed that the cathodic peak shifts to a lower potential, which is due to the rapid reaction of $Bpy^{\cdot-}$ with CO_2 to form adducts. Figures 9(c) and 9(d) respectively show the changes in substances and energy during the capture of CO_2. According to the calculations of Ranjan's research group, the entire CO_2 capture reaction in both solvents is exothermic [131].

Subsequent research established bipyridines and related structures as a distinct class of redox-tunable CO_2 sorbents based on sp^2-hybridized nitrogen. Unlike the spontaneous capture by sp^3 nitrogen in traditional amines, these Lewis bases only bind CO_2 after being electrochemically reduced, rendering the capture process electrically controllable [132, 133]. Based on this mechanism, researchers such as Liu and Hatton et al. developed a library of such compounds, including 4,4-bipyridine (BPy), quinoxaline (QX), phenazine (PhN), various azo derivatives (azobenzene (AzB) and azopyridine (AzPy)), and others [46, 47, 61, 104, 134–136]. Cyclic voltammetry confirms the CO_2 capture capability of this entire series. Among these molecules, Li et al. tested the CO_2 capture ability of AzPy/dimethyl sulfoxide (DMSO) sorbent, which showed continuous flue gas capture ability and stable operation for more than 20 cycles [61]. Further investigation into the reaction thermodynamics via DFT revealed a critical advantage: The interaction between CO_2 and these redox-tunable Lewis bases is weaker than the reaction enthalpy of traditional amine-based capture. This weaker binding, particularly noted in phenazine and azo compounds, translates to a significantly lower energy requirement for sorbent regeneration, making them exceptionally promising for designing energy-efficient electrochemical carbon capture processes [136]. Based on this, AzB was specifically investigated for its oxygen stability. Liu et al. demonstrated that mixing AzB with ethanol created a synergistic and oxygen-stable CO_2 capture system [105]. Their results confirmed that both components could electrochemically capture CO_2 even in the presence of O_2, significantly extending the practical applicability of sp^2 nitrogen sorbents to more realistic and oxygen-containing flue gas conditions. Based on this, Seo et al. expanded the CO_2 capture from flue gas to air. One stable pyridinyl radical's compounds named 1-aminopyridinyl (1-APyl) have been discovered. The 1-APyl radical solution exhibits a constant capacity for capture of CO_2 from inlet streams of concentration from 1% to 100% with 1.25 electron utilization [137]. It also demonstrated for 5 cycles with no significant loss in performance with oxygen presence.

In contrast to quinone or sulfur-based systems, sp^2 nitrogen compounds like piperidine and bipyridine offer a distinct practical advantage: They do not require complex synthesis, thereby enhancing their commercial viability [132, 138]. More importantly, they introduce a transformative opportunity for direct air capture

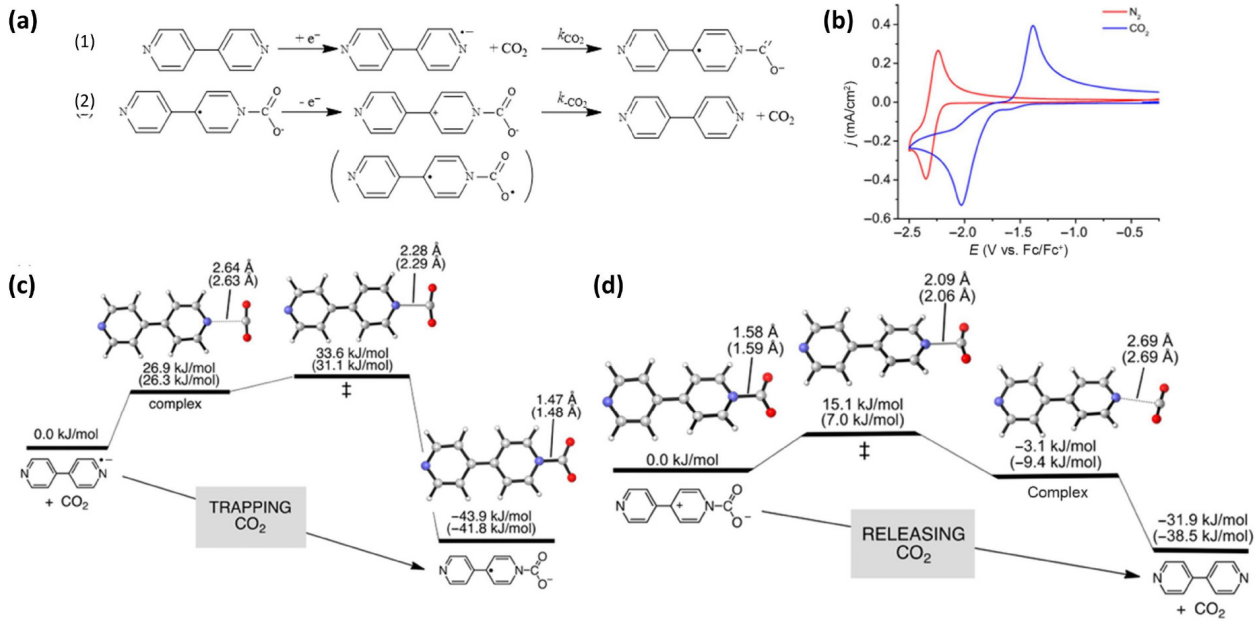

Figure 9 (a) (1) One-electron reduction of 4,4′-bipyridine to give a radical anion that reacts with CO_2 to form a bipyridinyl radical N-carboxylate adduct. (2) One-electron oxidation of the adduct to give a short-livedintermediate that fragments to liberate the starting 4,4′-bipyridine and CO_2. (b) Cyclic voltammetry curves of 10 mM 4,4′-bipyridine in N-butyl-N-methyl pyrrolidinium bis(trifluoromethyl sulfonyl) imide ionic liquid solvent at room temperature, purged with nitrogen (red), and purged with CO_2 (blue). (c) Computed free energies and structures for stationary points along the reaction coordinate for the reaction of the bipyridine radical anion with CO_2 in acetonitrile. (d) Computed free energies and structures for stationary points along the reaction coordinate for decarboxylation of the oxidized CO_2 addition product. Reprinted with permission from Ref. [130], © American Chemical Society 2015.

and large-scale separation by replacing the energy-intensive thermal regeneration of amine solutions with efficient electrochemical cycling. This positions them as a promising pathway toward scalable and less energy-intensive carbon capture technologies [139].

2.2.4 Other redox-active organics

2.2.4.1 Phenazine

Due to oxygen sensitivity issues, no previous system based on phenothiazine and phenothiazine was able to capture CO_2 from ambient air. It was reported that Hatton and Seo used neutral red (NR), a commercial organic dye molecule, as an oxygen insensitive organic redox active compound to increase its solubility in aqueous systems in the presence of niacinamide (NA) as a water-soluble promoter (Fig. 10(a)) [104].

As shown in Figs. 10(b) and 10(d), experimental results confirm the NRH_2 system's robust performance for CO_2 capture, demonstrating a fast absorption rate across a wide range of CO_2 concentrations (1%–15%) and achieving its highest capacity at 15% CO_2. Figure 10(c) reveals the CO_2 capture mechanism of NR-based solution, and the schematic is shown in Fig. 10(e). In summary, the system combines this high performance with critical practical advantages: robustness, stability, reversibility, and a clear potential for scalability.

Further advancing this field, Heping et al. developed a phenazine derivative (DHPS) that exhibits exceptional energy-saving potential [140]. DHPS demonstrated significant dynamic performance and cycling stability in a flow cell. This system successfully captured CO_2 from a 15% CO_2/N_2 stream at the cathode and released high-purity CO_2 at the anode. The process achieved a high current efficiency of 95.8% and an exceptionally low estimated energy consumption of 0.49 GJ per ton of CO_2 at 10 mA/cm^2. Another work conducted by Pang's group, (phenazine-1,8-diyl)bis(ethane-1-sulfonate) (1,8-ESP) was conducted [140, 141]. It demonstrated the continuous CO_2 capture with over 1200 cycles. The capture capacity reached 1.4 mol_{CO2}/L sorbents with an energetic cost of 55 kJ/mol_{CO2} at 10 mA/cm^2.

For future commercialization, research should focus on enhancing system scalability through the structural optimization and the development of more efficient substances. Furthermore, given the sensitivity of such PCET carriers to gases like O_2 and SO_x, integrating gas-selective membranes and pre-treatment steps for desulfurization and denitrification will be critical for developing robust and real-world applications [135, 142].

2.2.4.2 Quinacridone

Sarciftci et al. proposed a creative idea to directly electrochemically capture and release CO_2 using industrial organic pigments [121, 143]. Quinacridone is a brightly colored red powdery substance with the molecular formula of $C_{20}H_{12}N_2O_2$, often used for coloring industrial products [144]. Sariciftci et al. found that introducing CO_2 gas into a solution can lead to a reaction with the reduced QNC pigment, forming the QNC carbonate anion and using tetrabutylammonium (TBA) as a counter ion. This team used this characteristic to design an electrochemical cell, in which an electrochemical reduction electrode composed of a quinacridone film (about 100 nm thick) on an ITO carrier forms quinacridone carbonate, and the captured CO_2 can be released through electrochemical oxidation [120].

This group also compared the desorption effects of electrochemical and thermal methods. For heat release, the amount of CO_2 is determined to be 9.60×10^{-8} mol. Correspondingly, the release amount under electrochemical conditions is 1.94×10^{-7} mol, indicating that electrochemical release is more effective than heat release.

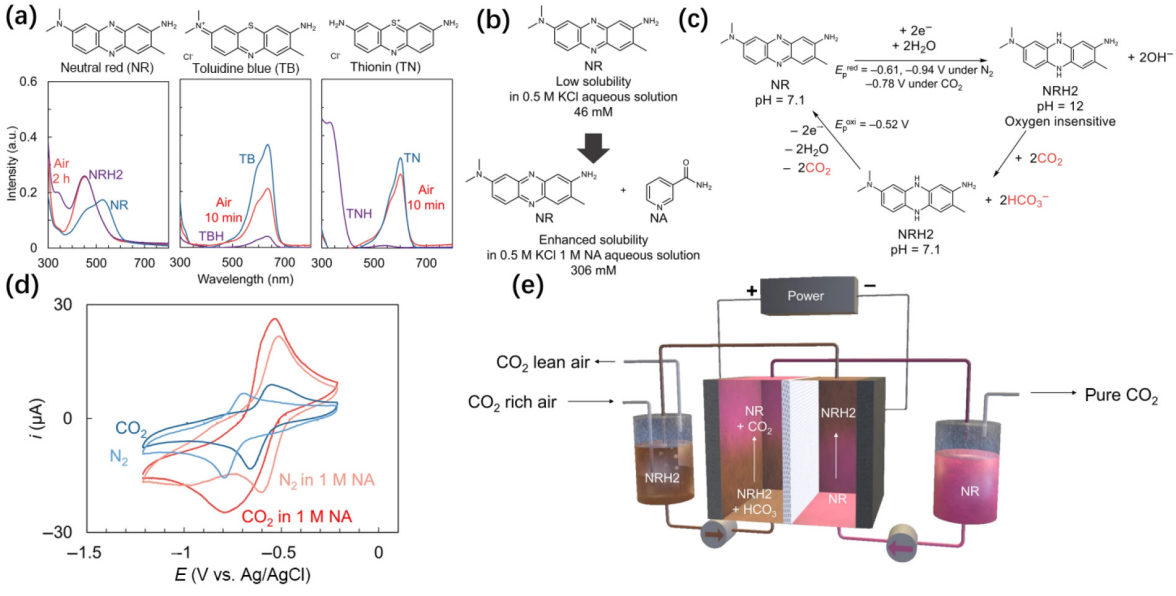

Figure 10 Electrochemical carbon captures using a redox pair of NR/NRH_2 in an aqueous solution. (a) Ultraviolet–visible (UV–vis) spectra for NR, toluidine blue (TB), and thionin (TN) in an aqueous solution during tests for air sensitivity. (b) NR solubility enhancement in water with the inclusion of 1 M nicotinamide (NA) as a hydrotropic agent. (c) Scheme of the reversible electrochemical CO_2 capture and release using the NR/NRH_2 redox system in water. (d) The CV of 5 mM NR under nitrogen (pastel blue curve, pH 6) and CO_2 (blue curve, pH = 7) in water with 0.1 M lithium perchlorate. (e) Overview of the continuous flow electrochemical cells for CO_2 capture and release experiments. Reproduced with permission from Ref. [104], © Seo, H. and Hatton, T. A. 2023.

2.2.4.3 Biological compounds

In a significant expansion of molecules for electrochemical carbon capture (eCCC), Heping et al. proposed the biomolecule riboflavin 5′-monophosphate (FMN) as a PCET mediator [145]. This approach enhances CO_2 capture while avoiding the competing hydrogen and oxygen evolution reactions and the need for precious metal catalysts [1].

The mechanism involves the electrochemical conversion of FMN to $FMNH_2$ at the cathode, which generates hydroxide ions (OH^-) to absorb CO_2 from a dilute gas stream. The CO_2-laden $FMNH_2$ solution is then circulated to the anode, where it is re-oxidized to FMN, releasing protons (H^+) and causing the subsequent release of pure CO_2. This system demonstrated a remarkably low energy consumption of 9.8 kJ/mol of CO_2, substantially outperforming conventional quinone-based sorbents. Furthermore, the lab-scale testing over 21 cycles confirmed excellent stability, with a minimal capacity fade rate of only 0.39% per cycle [145].

2.2.4.4 Inorganic redox carriers

As early as 1933, Dubois et al. attempted to use metallocene and octahedral ruthenium(II) complexes as carbon dioxide carriers and evaluated their synthesis and energy efficiency [109]. This group evaluated metals with different numbers of binding sites using cyclic voltammetry and the controlled potential Coulomb method. By observing the redox potential, it was found that the communication between the ruthenium atom (redox site) and the nitrogen atom (carbon dioxide binding site) of the imidazole ligand was insufficient, which indirectly reflected that the binding constant K of carbon dioxide would not be changed. In the cyclic voltammetry experiment, this team found that electronic communication between sites was sufficient for carbon dioxide pumping, and the distance between the redox metal center and the CO_2 binding site significantly affected the compound's ability to capture and release CO_2.

Unfortunately, as of now, research on transition metals applied in the field of carbon dioxide capture is still insufficient. At present, research in this field is more focused on theoretical foundations, with limited data on cost and practical applications [146].

2.3 Electrochemically mediated regeneration

Regeneration can be carried out through desorption or chemical reactions. Chemical, microbiological, catalytic, ultrasonic, microwave, thermal, photolysis, and electrochemical regeneration processes have been evaluated. Electrochemical regeneration (ECR) is an attractive method due to its simplicity, minimal chemical consumption, low investment, potential for environmental operation, and *in-situ* regeneration [33]. The method can be classified simply based on the regeneration object, and the most extensively studied one is electrochemical-mediated amine regeneration. The detailed introduction is as follows [147].

2.3.1 Electrochemically mediated amine regeneration (EMAR)

Amine capture of CO_2 can be achieved through the formation of amino formate/protonated amine pairs and/or bicarbonate [148], depending on the characteristics of the amine [149]. As a material that has received widespread attention in conventional carbon capture, it is also considered to have great potential in the field of electrochemical capture.

At present, the commonly used method for adsorbent regeneration in industrial production is thermal regeneration, but this method requires continuous high temperature washing, which brings a lot of energy loss problems. The application of electrochemistry in the amine capture of carbon dioxide is often in the amine regeneration step; it's been called EMAR. The electrical power required by EMAR is equivalent to the energy loss of state-of-the-art hot washing processes and is considered to have considerable prospects [150, 151].

In the current EMAR technology, ethylenediamine (EDA)-

copper, the electrochemical-mediated CO_2 capture method, is considered a promising technology that can replace traditional amine-based CO_2 capture (Fig. 11(a)). Hatton et al. tested the continuous EMAR process of a mixture of primary EDA and aminoethyl ethanolamine (AEEA) for over 100 h (Fig. 11(b)), and the results indicate that the desorbed gas is 100% carbon dioxide, indicating the feasibility of this scheme. In another research, Hatton's team also evaluated the efficiency of EMAR technology, and the model predicted that an efficiency of 69% could be achieved at higher temperatures and pressures, while laboratory scale systems produced 1.6 mL/min CO_2 when operating at 0.4 volts and a Faradaic efficiency (FE) of 42% [152]. To address the issues of strong corrosiveness and poor copper cycling performance in EDA-Cu technology, Zhang et al. further investigated the capture performance of EDA-based mixed solvents. The group selected traditional primary amine, secondary amine, and tertiary amine (MEA, DEA, and TEA) to blend with EDA. The experimental results showed that the mixed solvent can improve the reaction process in the EMAR system and has lower corrosiveness (Fig. 11(c)). At the same time, the mixed solution will reduce energy demand (Fig. 11(d)) and improve copper cycling performance (Fig. 11(e)) [153]. The research of this group provides a possible direction for further exploration of EMAR technology, which is to improve it by starting with mixed solvents.

It should be noted that the EMAR technology mentioned earlier is currently more commonly used to capture post-combustion carbon dioxide, rather than directly capturing air carbon dioxide. We also look forward to the future application of this technology in direct air capture.

2.3.2 *Electrochemical regeneration of spent alkaline*

Alkaline adsorbents have the advantages of good adsorption performance and high efficiency and are therefore widely used. However, the high energy consumption problem in the traditional regeneration process of alkaline adsorbents (such as thermal regeneration) hinders the further development of alkaline adsorbents and limits their application scenarios [154]. The use of electrochemistry for regeneration has advantages such as low energy consumption and simple control and is considered an effective path to solve the problem of desorption.

Shu et al. utilized an H_2 cycle electrochemical cell, which generates a pH gradient to desorb CO_2 at low pH, while the alkaline capture solution (NaOH) is regenerated at high pH, achieving simultaneous solvent regeneration and CO_2 desorption in a continuous system [155]. The experimental results of the group indicate that the minimum energy consumption of the system is 374 kJ/mol CO_2, and the model simulation results show that through further optimization, the minimum energy consumption of the system is 164 kJ/mol CO_2. The techno-economic assessment of Breyer et al. points out that this electrochemical process has the characteristic of low energy consumption and does not require any energy input other than electrical energy, making it a competitive alternative path for DAC [156].

On this basis, Xiao et al. integrated the electrolysis regeneration process into the capture device and designed a direct air capture and recovery system using alkaline solution circulation [157]. The capture process is as follows: During the device operation, the carbon dioxide enters a specialized air contactor unit, where it is absorbed by KOH aqueous solution and converted into K_2CO_3. After the electrolytic regeneration using a constant current power supply, the regenerated high concentration alkaline solution is then transported to the lean capture tank for electrolysis. The regenerated KOH is introduced into the storage tank for recycling. After being captured, the air is completely removed from residual

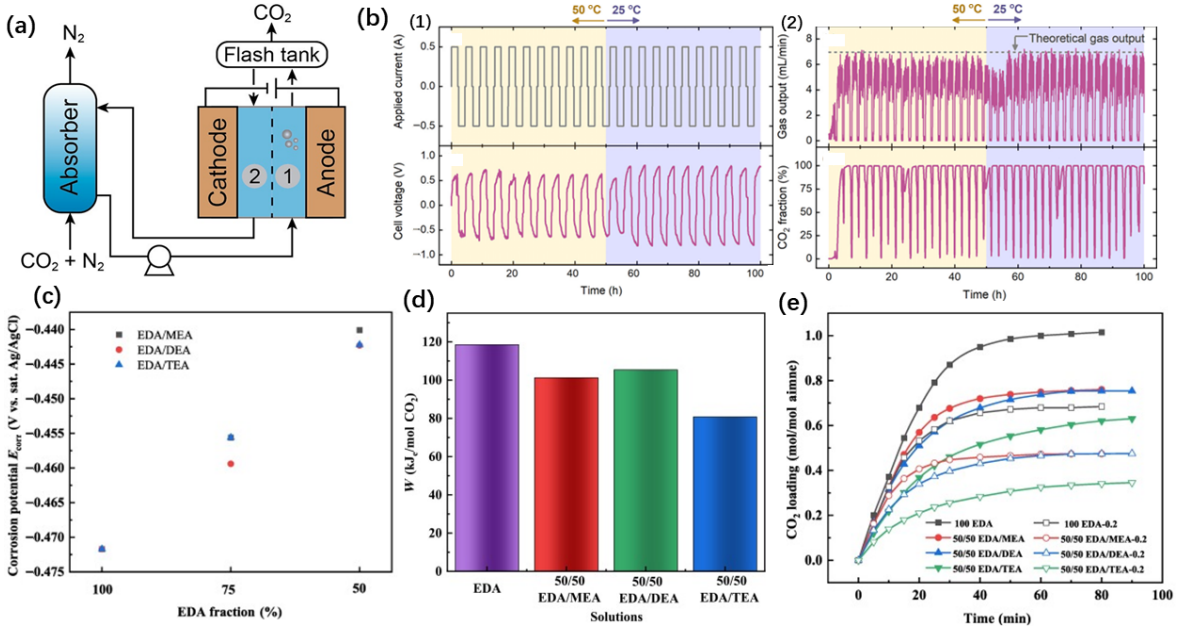

Figure 11 (a) EMAR process schematic diagram. (b) Long-term stability of the 50% EDA mixed amine during continuous operation over 100 h. (1) CO_2 fraction in the output and gas output. (2) Cell voltage and constant current of 0.5 A was applied. Experiment performed at either 50 °C (the first 50 h; highlighted in yellow) or room temperature (the second 50 h; highlighted in blue). Reproduced with permission from Ref. [152], © American Chemical Society 2020. (c) Corrosion potential of different blended solutions. (d) The energetics of the CO_2 desorption process (the total concentration of aqueous amine is 7 mol/kg; the fractions of EDA are 100% and 50%, the concentration of KNO_3 is 0.7 mol/kg (H_2O); and Cu loading is 0.1 mol/mol). (e) CO_2 absorption process under various copper loadings in different blended solvents (the total concentration of amine is 7 mol/kg (H_2O); the fractions of EDA are 100% and 50%, the concentration of aqueous KNO_3 is 0.7 mol/kg; and temperature = 40 °C). Reproduced with permission from Ref. [153], © Elsevier Ltd. 2023.

moisture and solution droplets and then discharged through the air outlet. The system developed by the team has a single-stage CO_2 capture rate range of 10% to 21% and an electrolysis efficiency close to 100%, and no chemical waste is generated during the process [158, 159]

In summary, compared to traditional regeneration technologies, electrochemical regeneration systems provide low-cost opportunities for the deployment of CO_2 capture. But how to achieve high absorbent regeneration rate while maintaining low energy demand, and how to improve carbon dioxide capture capacity are still key issues that need to be solved.

2.4 Other eCCC technologies

2.4.1 Electrochemical voltage capture

Hatton et al. proposed an interesting electrochemical capture method for carbon dioxide, which relies solely on the electrochemical voltage used for CO_2 capture and release. This research group utilized the inherent affinity of the redox active quinone moiety for CO_2 (in liquid phase) to construct a bipolar cell using poly(vinylanthraquinone)-carbon nanotube (PVAQ-CNT) composite cathode and poly(vinylferrocene)-CNT (PVFc CNT) composite anode. They conducted a detailed study on the system characteristics that depend on the operating voltage and successfully demonstrated the passage of CO_2 from (and released to) 400 ppm extremely dilute flow (0.04%) through a mesoscale eight pair bipolar cell. Under optimized conditions, the specific energy consumption per mole of CO_2 is as low as 113 kJ [160, 161].

In summary, the technology proposed by this group is different from existing technologies that typically require temperature and/or pH fluctuations. Electrochemical technology relies entirely on simple voltage modulation, does not require the use of chemical reagents, and solves subsequent waste problems. It has the advantages of simplicity, efficiency, and environmental friendliness. However, this technology still has issues such as high economic costs and relatively low capture efficiency, and further improvement is needed.

2.4.2 Membrane capacitive deionization

Membrane capacitance deionization (MCDI) refers to the ion separation technology that applies battery voltage between two relatively positioned porous electrodes, while placing an ion exchange membrane in front of each electrode [162]. The ions in the water flowing through the transmission channel between the electrodes are removed and stored in the electrical double layer (EDL) in the electrode micropores. This technology is widely used in seawater desalination [159–161]. Hamelers et al. demonstrated through their research that MCDI technology can be used to capture carbon dioxide using HCO_3^- and CO_3^{2-}. The reactions are involved in the capture process as follows (Eq. (19)–(21)) [162, 163]

$$CO_2(g) + H_2O \overset{H^{cc}}{\leftrightarrow} H_2CO_3 \text{ with } H^{cc} = 0.83 \quad (19)$$

$$H_2CO_3^* \overset{K_1}{\leftrightarrow} HCO_3^- + H^+ \text{ with } K_1 = 10^{-6.35}\ \text{M} \quad (20)$$

$$HCO_3^- \overset{K_2}{\leftrightarrow} CO_3^{2-} + H^+ \text{ with } K_2 = 10^{-10.33}\ \text{M} \quad (21)$$

According to the content of CO_2 in the gas, an equilibrium will be formed between CO_2(g) and deionized water. Applying an electric current will cause HCO_3^- and H^+ to adsorb into the porous electrode, breaking the equilibrium and causing CO_2(g) to be absorbed in deionized water. When the current direction reverses, HCO_3^- and CO_3^{2-} ions detach from the carbon electrode, pushing the chemical equilibrium in the opposite direction, i.e., CO_2(g) desorbs into the gas phase. In summary, the control of adsorption and desorption can be achieved by controlling the direction of the current. This research group also verified the feasibility of carbon dioxide capture and reported that this technology requires equivalent or lower energy consumption compared to similar technologies such as swing supercapacitor adsorption. However, the biggest drawback of this technology is its low CO_2 capture rate (6×10^{-9} mol/(s·g) carbon), which is 50 times lower than existing technologies based on adsorption materials such as zeolite for CO_2 capture [162].

Hamelers et al. studied the effectiveness of electrodes and ion exchange membranes in the capture of carbon dioxide by MCDI [163]. The experimental results indicate that anion exchange membranes (AEM) are essential for maintaining high CO_2 absorption efficiency. AEM improves absorption efficiency by ensuring that only bicarbonate and carbonate ions are transported to the anode during charging, as well as by hindering the transfer of co-ions (H^+) discharged from the anode to the spacer solution [163].

Although MCDI technology has advantages such as low energy consumption, no secondary pollution, simplicity, and environmental friendliness, it still has limitations at present [164, 165]. The main challenges faced by carbon dioxide capture using MCDI involve the ion transmembrane migration and electrode adsorption. The migration of ions within the membrane and electrode is typically influenced by the pore size, Donnan effect, and chemical coordination [166].

The mismatch in thermodynamic and kinetic requirements between CO_2 binding and electroreduction. For instance, quinones can reversibly capture CO_2 through one- or two-electron redox reactions, but their reduction potentials (typically –0.4 to –1.0 V vs. Ag/AgCl) are not sufficiently negative to drive multi-electron CO_2 reduction reactions to CO, formate, or hydrocarbons. Applying stronger potential often leads to side reactions or decomposition of the redox carriers.

Additionally, the two processes require incompatible environments: Redox-active molecules operate best in non-aqueous solvents to maintain reversibility, whereas CO_2 electroreduction typically occurs in aqueous or ionic liquid electrolytes using gas diffusion electrodes [46, 90]. This solvent and phase incompatibility hinders effective electron and mass transfer between the redox carrier and catalytic surface. Moreover, when operated together, the redox species and catalyst may compete for electrons, lowering Faradaic efficiency and complicating selectivity control.

Therefore, most current efforts focus on stepwise or indirect coupling, such as using redox mediators for CO_2 release followed by electroreduction. Future progress may depend on developing hybrid systems that immobilize redox-active species on conductive support or catalysts, potentially bridging molecular CO_2 capture with electrochemical conversion in a unified, energy-efficient process.

2.4.3 Molten carbonate systems

The concept of utilizing MCFCs for electrochemical CO_2 concentration was established early in the development of capture technologies. As noted in Section 2, the concept was established early by Huebscher and Babinsky using MCFCs as concentrators,

demonstrating a dual-stack system capable of achieving CO_2 purity of up to 97%–98% [40]. Unlike aqueous pH-swing or redox-carrier systems that typically operate near ambient conditions, MCFCs function as high-temperature electrochemical concentrators (typically 600–700 °C) [167]. This high operating temperature allows for the use of non-precious metal catalysts (typically nickel-based) and facilitates rapid electrode kinetics without the need for expensive platinum group metals. The fundamental capture mechanism relies on a molten carbonate electrolyte, usually a eutectic mixture of lithium and potassium carbonates, held within a porous ceramic matrix. At the cathode, CO_2 from a flue gas stream (e.g., from a natural gas combined cycle or coal boiler) reacts with oxygen and electrons to form carbonate ions (CO_3^{2-}) [168, 169]

$$\text{Cathode}: \ O_2 + 2CO_2 + 4e^- \rightarrow 2CO_3^{2-} \tag{22}$$

Driven by the electrochemical potential gradient, these carbonate ions migrate through the electrolyte to the anode. There, they react with a fuel source, typically hydrogen derived from the internal reforming of methane, to release concentrated CO_2, water, and electrons [170]

$$\text{Anode}: \ CO_3^{2-} + H_2 \rightarrow CO_2 + H_2O + 2e^- \tag{23}$$

A salient attribute of this configuration is its thermodynamically active operation, which enables simultaneous electricity generation and carbon concentration. Unlike amine scrubbing or pressure swing adsorption, which are parasitic processes that consume steam or electricity (imposing an energy penalty), MCFCs generate a net surplus of electricity during the capture process [171]. The electrons generated at the anode travel through an external circuit to the cathode, producing useful power while simultaneously concentrating CO_2 in the anode exhaust for subsequent sequestration. Recent techno-economic assessments have quantified this advantage. Barckholtz et al. reported that although conventional amine systems require SPECCA of approximately 4.91 MJ/kg, MCFC systems can achieve a SPECCA as low as 1.37 MJ/kg [168, 169]. This represents a nearly four-fold reduction in the energy penalty associated with carbon capture. Furthermore, in cogeneration applications, MCFCs have been shown to avoid up to 89.4% of CO_2 emissions, outperforming the 87.6% avoidance typical of amine retrofits. Beyond simple capture, recent innovations have expanded MCFC utility toward the co-production of low-carbon hydrogen. By operating the fuel cell at low fuel utilization (U_f = 30%–45%) rather than the standard high utilization (> 70%), the cell acts as an electrochemical reformer [170–172]. In this mode, excess methane supplied to the anode is reformed into hydrogen, but not all hydrogen is consumed by the oxidation reaction. The anode exhaust thus contains a mix of concentrated CO_2 and surplus H_2. Following separation, this "blue" hydrogen can be exported to decarbonize other industrial heating processes or used as a chemical feedstock, effectively combining post-combustion capture with pre-combustion fuel synthesis [172].

Despite these significant advantages, the widespread deployment faces challenges related to the high capital cost of high-temperature stacks and the corrosive nature of the molten electrolyte, which limit the component durability over long operational lifetimes. Future research is increasingly focused on developing corrosion-resistant materials and optimizing thermal management to extend stack life for industrial-scale CCS applications [171].

2.4.4 *Comparative advantage of electrochemical pathways*

To contextualize the impact of eCCC and eCCU, it is critical to contrast them with conventional thermochemical carbon capture technologies, such as amine scrubbing. As summarized in Table 3, the fundamental distinction lies in the driving force: Thermochemical methods rely on thermal swings (ΔT) driven by phonon transport, which inherently suffer from slow ramping rates and high energy penalties due to the heat capacity of water. In contrast, electrochemical methods are driven by electron potential (ΔE), allowing for isothermal operation, rapid start-up time, and direct compatibility with intermittent renewable electricity [39, 42]. Recent breakthroughs have further widened this performance gap. For instance, advanced catalyst designs have demonstrated significant reductions in the overpotential required for conversion, while novel interface engineering has enhanced product selectivity at industrial current densities [4, 13, 19].

These innovations suggest that electrochemical systems are rapidly approaching the techno-economic tipping point required to displace thermal incumbents.

Table 3 Summary of electrochemical carbon capture units over conventional thermal/amine-based CCS technologies

Feature	Electrochemical carbon capture [13]	Conventional thermal based carbon capture [12]
Technology maturity	Low. Mainly confined to laboratory scale, with limited large-scale experiments, and there is still some distance from industrialization	High. There are already some commercial companies operating in this field
Driving force	Electrical energy (electrons)	Thermal energy (heat/steam)
Regeneration energy	Electricity. Uses electrochemical reactions (e.g., pH swing) to release CO_2	Heat (thermal). Requires large quantities of low-grade steam
Main products	Through the integrated capture-catalysis process, valuable C_1 products such as methane and carbon monoxide can be simultaneously produced along with carbon dioxide, and even C_{2+} products like ethanol [173–176]	Generally, the product is compressed carbon dioxide, with few other byproducts. A small number of companies directly mineralize waste liquids and store them underground.
Modularity and footprint	High modularity. Smaller, stackable units (like batteries/ fuel cells). Potentially smaller footprint	Low modularity: large absorber and stripper columns; requiring extensive piping/heat exchange equipment. Large footprint
Sorbent issues	Uses simpler, less volatile, or metal-based chemistries; generally reduced solvent degradation and less environmental toxicity concern.	Uses amine solvents which are corrosive, degrade over time, and can produce toxic byproducts.
Capital/ operating cost	Currently high due to low maturity, expensive electrode/membrane materials, and novel system design. On the other hand, the cost of catalysts is also a factor that needs to be considered.	Established but high. Operating costs are dominated by the high thermal energy demand for solvent regeneration.

3 Electrochemical CO_2 capture and utilization

eCCU present a transformative alternative to conventional integrated CO_2 capture and conversion (ICCU) systems, which are constrained by the energy-intensive thermal desorption of CO_2 and the inefficiencies associated with operating separate capture and conversion units [30]. In contrast, eCCU merges both functions within a single and electrically driven reactor operating under mild conditions and powered by renewable energy. This integration enables *in-situ* sorbent regeneration and direct electron-driven conversion of captured CO_2 species into value-added products, thereby minimizing thermal energy penalties and improving overall system efficiency [173–176].

Recent developments have demonstrated several electrochemical strategies that exemplify this unified approach. Redox-mediated systems employ redox-active molecules (e.g., quinones, phenazines, or bipyridinium salts) whose CO_2 affinity can be reversibly tuned by applied potential, allowing the capture, release, and conversion to occur in a single cycle without thermal regeneration [143, 177]. pH-swing systems, using bipolar membranes or coupled electrode reactions, generate local acidic and basic zones to simultaneously release CO_2 and electroreduce it into products such as CO or formate [22, 93, 177]. A further approach involves direct electroreduction of captured ionic species (bicarbonate, carbamate, or carbonate) within the capture medium itself, eliminating CO_2 gas desorption and greatly enhancing carbon utilization efficiency. Collectively, these strategies highlight the versatility of eCCU in achieving efficient, selective, and renewable-powered carbon valorization through electrochemical control of potential, catalyst design, and electrolyte composition [178].

To conceptualize varying degrees of integration, as seen in Fig. 12(a), Sullivan et al. classified eCCU systems into three configurations [39]: Type I (independent), Type II (locally coupled), and Type III (fully integrated). In Type I, the CO_2 capture and conversion occur separately, typically involving thermochemical or alkaline regeneration prior to utilization, offering the process flexibility but limited energy synergy [146, 179]. Type II configurations locally couple the two processes: CO_2 is electrochemically released from the capture medium (e.g., via electrochemically mediated amine regeneration, redox-active carriers, or bipolar membrane systems) and directly fed into an electroreduction reactor [150, 180, 181]. These systems require matching capture–conversion fluxes and careful management of side reactions such as oxygen reduction. Type III configurations represent full electrochemical integration, where CO_2-loaded capture agents, such as amines, bicarbonates, ionic liquids, or covalent organic frameworks, serve directly as reactants for electroreduction, enabling simultaneous CO_2 conversion and

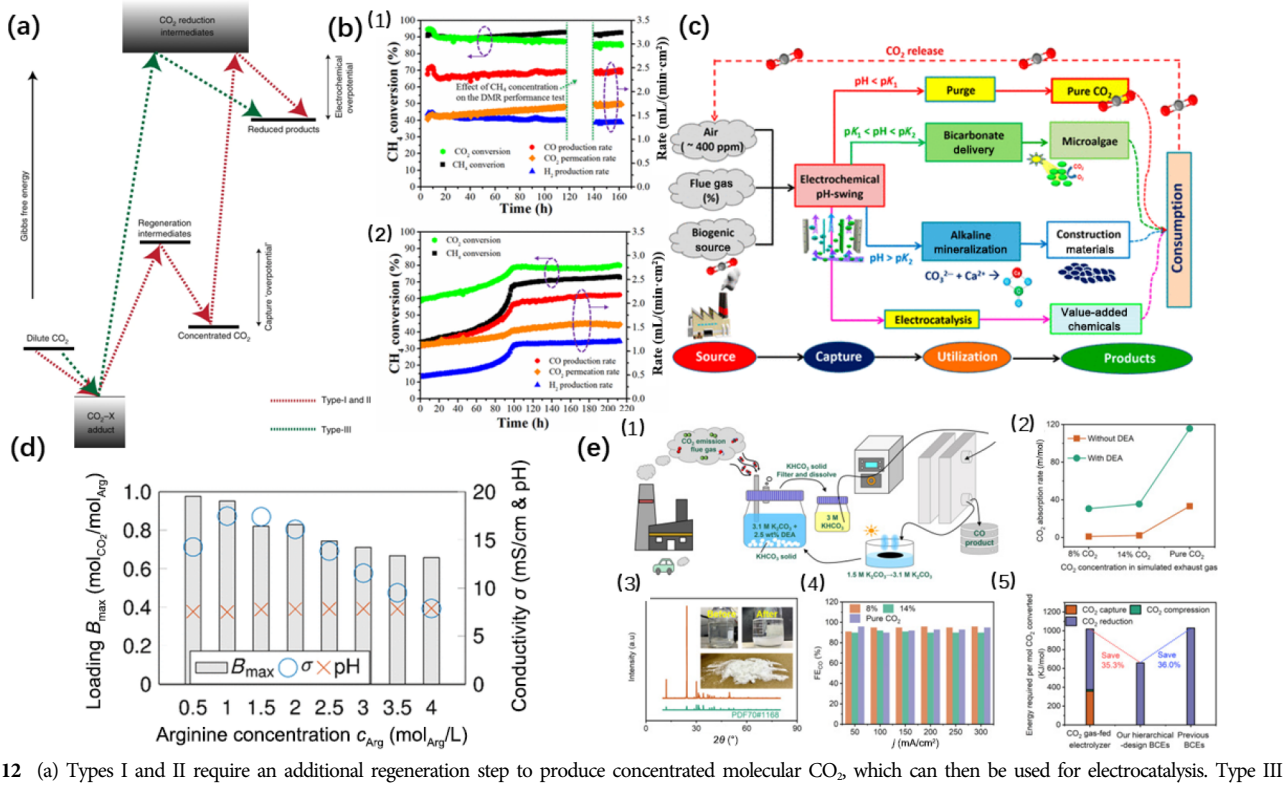

Figure 12 (a) Types I and II require an additional regeneration step to produce concentrated molecular CO_2, which can then be used for electrocatalysis. Type III configuration integrates the capture media regeneration with electrochemical CO_2RR, which results in an improved energy efficiency of the overall capture and conversion system. Reproduced with permission from Ref. [39], © Springer Nature Limited 2021. (b) Effect of temperature on the DMR performance of a GDC-MC membrane reactor with (1) an NMP catalyst and (2) an LNF catalyst. Reproduced with permission from Ref. [194], ©American Chemical Society 2016. (c) Application of EPS processes for CO_2 capture and utilization (CCU) toward a circular carbon economy. Reproduced with permission from Ref. [64], Copyright 2016 American Chemical Society. (d) Maximum specific loading of CO_2 B_{max}, pH, and conductivity as a function of L-arginine concentration. Reproduced with permission from Ref. [192], © Heß, D. et al. 2025. (e) (1) Schematic illustration of CO_2 capture and conversion cycle in BCE system. (2) CO_2 capture rate using K_2CO_3 solution for different simulated exhaust gas compositions. (3) Photograph and X-ray diffraction (XRD) analysis of CO_2 capturesimulatedCO_3 solution. (4) Performance of $KHCO_3$ formed after the capture of CO_2 from different simulated exhaust gas in our hierarchical-design BCEs. (5) Energy consumption comparison between our hierarchical-design BCEs and other reported BCE systems. Energy calculation includes CO_2 capture, compression, and reduction processes. CO_2 conversion efficiency is 50% in CO_2 gas-fed cells and 100% in BCEs. Reproduced with permission from Ref. [195], © Elsevier Inc. 2024.

sorbent regeneration in a single electrochemical cell [182, 183]. Energetically, Type III approach offers the greatest potential for efficiency improvement, as it bypasses the high energy demand of CO_2 desorption and exploits pre-activated CO_2 adducts (e.g., carbamates) that lower electroreduction overpotentials. Compared with Types I and II systems, Type III architectures can reduce overall energy input and capital costs by integrating both capture and conversion into one reactor. Moreover, the local CO_2-rich microenvironment near the electrode enhances mass transfer and reaction selectivity [184, 185].

The eCCU technologies unified the CO_2 capture and electroreduction through an electrified and renewable-compatible framework, achieving higher carbon utilization efficiency and lower energy intensity than thermochemical ICCU. Among its configurations, fully integrated Type III systems hold the most promise for scalable and carbon-neutral chemical manufacturing. The following section presents representative eCCU systems that demonstrate these advantages through redox-mediated, pH-swing, and direct electroreduction strategies [39, 186, 187].

Although the classification into Type I (independent), Type II (locally coupled), and Type III (fully integrated) establishes the theoretical framework for thermodynamic synergy, the practical realization of these architectures is fundamentally constrained by the physicochemical properties of the capture medium [20, 27]. There is no "universal" integration strategy; rather, the technological pathways to Type III systems are inherently dictated by the capture mechanism employed. For instance, achieving full integration in pH-swing systems requires overcoming membrane resistance and managing ion transport across bipolar interfaces, whereas in redox-active carrier systems, the primary barrier lies in matching the thermodynamic redox potential of the organic carrier with the kinetic overpotential of the CO_2 reduction catalyst [19, 48]. Similarly, high-temperature molten carbonate systems face distinct challenges related to thermal management and internal reforming kinetics. Consequently, a monolithic discussion of integration levels would obscure these critical material-specific hurdles. Therefore, the following sections are organized by electrochemical mechanisms to systematically evaluate how specific material classes are being engineered to bridge the gap from independent operation toward fully integrated eCCU systems [78].

3.1 Electrochemical pH-swing (EPS) processes for CO_2 capture and utilization

As discussed in Section 2.1, EPS enables the reversible generation of acidic and basic conditions through bipolar membrane or electrodialysis architectures, facilitating the transformation of diluted CO_2 into dissolved species such as carbonic acid or bicarbonate [90]. Figure 12(c) illustrates several potential product pathways within EPS systems, including the delivery of purified CO_2 gas, bicarbonate solutions for biological applications, carbonate minerals for long-term sequestration, and value-added chemicals produced through coupled electrochemical reactions. One prominent application of EPS lies in microalgae cultivation [64]. Bicarbonate, which predominates in aqueous solutions at pH 6–10, serves as an effective carbon source for microalgae, particularly in systems where direct CO_2 sparging suffers from low mass transfer efficiency. Traditional CO_2 delivery through gas sparging requires significant energy for agitation and aeration, along with high capital expenditure, and is prone to CO_2 losses to the atmosphere [18, 19]. In contrast, EPS generates bicarbonate-rich solutions that can maintain elevated carbon availability within the photobioreactor (PBR), ensuring consistent carbon supply during both light and dark periods. This bicarbonate-based feeding strategy not only enhances the biomass productivity but also reduces operational costs by mitigating CO_2 losses and improving the overall carbon utilization efficiency. Chi et al. highlighted that maintaining stable pH in the bioreactor is critical for optimizing algal growth dynamics, and the inherent pH-buffering capability of EPS aligns naturally with this requirement [187, 188]. Moreover, EPS allows integration with dilute flue gas streams, providing a continuous and renewable-compatible CO_2 source for large-scale microalgae production.

EPS also demonstrates considerable potential in CO_2 mineralization, converting captured CO_2 into stable carbonate minerals such as calcium carbonate and magnesium carbonate. For seawater-based systems, Sharifian et al. achieved 97% total inorganic carbon extraction using a stacked BPMED configuration at pH > 9.6, with energy consumption of 318 ± 29 kJ per mol of $CaCO_3$-significantly lower than conventional alkaline mineralization methods [188], which typically require 640–2880 kJ/mol. Similarly, Chen et al. integrated BPMED with a crystallization chamber to simultaneously capture CO_2 and precipitate sesquioxide ($MgCO_3{\cdot}3H_2O$) from seawater [189]. However, high pH conditions can induce scaling and membrane fouling due to low solubility of hydroxides such as $Mg(OH)_2$, emphasizing the need for careful control of process parameters including CO_2 flow rate, current density, and solution temperature to maintain energy efficiency and system longevity.

Beyond microalgae and mineralization, EPS can be coupled with electrochemical conversion to produce value-added chemicals from bicarbonate or dissolved CO_2. By tuning the pH and local electrolyte environment, EPS facilitates higher CO_2 concentration near the electrode interface, lowering overpotentials for CO_2 reduction and improving selectivity toward simple C_1 products such as formate or CO [39, 106, 190–194]. Recent studies have demonstrated the feasibility of integrating CO_2 capture, electrochemical conversion, and product purification within a single electrochemical platform. Mang et al. developed a coupled system that unites CO_2 capture, electrocatalytic reduction, and gas purification from simulated flue gas. In a lab-scale BPMED cell, CO_2 was first captured by KOH to form carbonate and bicarbonate species, which were then acidified using the BPMED-generated acidic stream to release CO_2 [195]. The released CO_2 was subsequently reduced to CO over a silver gas diffusion electrode (Ag-GDE) in a flow cell. Unreacted CO_2 was reabsorbed by the regenerated alkaline solution, yielding a pure syngas product stream. Operating under mild conditions and powered by renewable electricity, the system achieved a Faradaic efficiency above 90% at 200 mA/cm^2 and remained stable over 15 operation cycles, highlighting its potential for sustainable carbon recycling. Building on this concept, Jiang et al. reported an electrochemical system coupling CO_2 capture and amino acid synthesis. Methionine salt served as both the CO_2 absorbent and reactant, enabling *in-situ* conversion to methionine and CO_2 via a BPMED process [22, 196]. The current efficiency declined with increasing current density, 86.4%, 69.6%, and 50.6% at 1.2, 1.5, and 2.0 A, respectively, demonstrating a tunable trade-off between the energy efficiency and productivity, and suggesting potential for industrial application in organic synthesis from captured CO_2. In Fig. 12(d), under different gas conditions, the methionine productivity all reached more than 95%. The eCCU process also relies heavily on high-

efficiency catalysts [197]. Zou et al. coupled a single-atom catalyst (SAC) with the EPS process, enabling direct electrolysis of the CO_2-captured solution without a separate release step. Operating at 100 mA/cm^2 for 96 h, the system produced syngas with an H_2/CO ratio of ~ 2 while partially regenerating the K_2CO_3 absorbent for reuse. Compared to the conventional two-step CO_2 capture and reduction, the integrated process reduced overall energy consumption by over 40%. Inspired by this strategy, Shen et al. employed a CoPc@CNT SAC with strong CO_2 adsorption capability to suppress CO_2 desorption from the catalyst surface [195], achieving efficient bicarbonate electrolysis to CO with Faradaic efficiencies up to 96.2% across 50–300 mA/cm^2 (Fig. 12(e)).

Expanding beyond simple electroreduction, Peng et al. designed an "all-in-one" reactor combining electrochemical CO_2 capture with catalytic dry methane reforming (DMR) [194]. Using a mixed-conducting membrane comprising an O^{2-} conductor and molten carbonate phase, integrated with Ni-MgO-Pt (NMP) or $LaNi_{0.6}Fe_{0.4}O_{3-\delta}$ (LNF) catalysts, the system achieved a CH_4 conversion of 93.9% and a CO_2 permeation flux of 2.25 mL/(min·cm^2) at 850 °C. The NMP catalyst exhibited higher activity, while LNF provided superior coking resistance and long-term stability over 200 h. With a small addition of steam (3% H_2O), the system produced syngas with a higher H_2/CO ratio suitable for downstream fuel synthesis. Figure 12(b) also demonstrated the stability of this combination process; it achieved a conversion efficiency more than 90% in 160 h of running. Together, these demonstrations underscore the technical viability and flexibility of integrated eCCU systems for scalable and renewable-powered carbon valorization.

3.2 Challenges in coupling redox-active molecules with electrocatalysis

As mentioned in Section 2.2, although redox-active species such as quinones have established themselves as benchmark materials for eCCC process, their transition into fully integrated capture and utilization systems remains limited. This limitation arises from a critical mismatch in the thermodynamic and kinetic requirements between CO_2 binding and electroreduction. In an ideal eCCU system, the potential required to release CO_2 from the capture agent should align with the onset potential of the CO_2RR [46, 47]. However, quinones typically undergo reversible reduction and CO_2 capture at potentials (typically −0.4 to −1.0 V vs. Ag/AgCl) that are insufficiently negative to drive the subsequent multi-electron reduction of CO_2 to valuable products like CO, formate, or hydrocarbons. Attempting to bridge this gap by applying stronger cathodic potentials often leads to irreversible side reactions or the decomposition of the redox carriers themselves. Consequently, current research on quinones is largely restricted to Type I (independent) or Type II (coupled) configurations, where the capture and conversion are spatially or temporally separated. Future progress in achieving Type III (fully integrated) quinone systems will require overcoming both this thermodynamic barrier and the "solvent conflict" between the organic media required for optimal quinone reversibility and the aqueous media typically required for efficient electrocatalysis [31, 46, 47].

Additionally, the two processes require incompatible environments: Redox-active molecules operate best in non-aqueous solvents to maintain reversibility, whereas CO_2 electroreduction typically occurs in aqueous or ionic liquid electrolytes using gas diffusion electrodes. [46, 90]. This solvent and phase incompatibility hinders effective electron and mass transfer between the redox carrier and catalytic surface. Moreover, when operated together, the redox species and catalyst may compete for electrons, lowering Faradaic efficiency and complicating selectivity control.

Therefore, most current efforts focus on stepwise or indirect coupling, such as using redox mediators for CO_2 release followed by electroreduction. Future progress may depend on developing hybrid systems that immobilize redox-active species on conductive support or catalysts, potentially bridging molecular CO_2 capture with electrochemical conversion in a unified and energy-efficient process [195, 196].

3.3 eCCU process with redox-active molecules

Compared with quinones, redox-active amines exhibit physicochemical properties that render them more compatible with integrated eCCU systems. Quinones typically suffer from mismatched CO_2 binding and reduction potentials, as well as poor stability in aqueous electrolytes. In contrast, redox-active amines are highly water-soluble and capable of reversibly binding CO_2 through both chemical and electrochemical pathways under mild potentials [103, 105, 196]. Their intrinsic amine functionalities enable the direct formation of carbamate or bicarbonate species with CO_2, while their redox-active moieties can be electrochemically regenerated without requiring high overpotentials. Moreover, these amines maintain stability and reversibility in aqueous or mixed-solvent environments, overcoming the solvent incompatibility issues that hinder quinone-based systems. Consequently, redox-active amines offer a coherent molecular platform for simultaneous CO_2 capture and conversion, enabling efficient, low-energy, and renewable-driven CO_2 valorization [132].

As discussed in Section 2.3, sp^2/sp^3-hybridized nitrogen structures have been extensively utilized in CO_2 capture due to their strong electron-donating and coordination capabilities. Extending these functionalities to eCCU, Zhang et al. proposed that sp^2/sp^3-N moieties can be incorporated into both metal and nonmetal catalysts to enhance CO_2 adsorption and mass transport [197]. The molecular structure and anchoring configuration of amines exert multiple effects on CO_2RR activity and selectivity. For example, linear amines tend to promote CO_2RR, whereas branched amines often hinder reactivity. Similarly, substituent effects, such as electron-donating alkyl or electron-withdrawing hydroxyl groups, affect CO_2 capture ability, the activation of intermediates, and the suppression of the HER. Overall, the behavior of amines as promoters or inhibitors during CO_2 electrolysis depends strongly on their concentration, p*K*a, and molecular structure.

The integration of sp^2/sp^3-N structures also contributes to co-catalytic effects in gas-phase CO_2 electrolysis. For instance, pyridine-functionalized Ag electrodes (Ag/pyridine) demonstrated a lower onset potential of 200 mV and a tenfold increase in CO partial current density compared with pristine Ag electrodes [198]. Here, the pyridine nitrogen coordinated and stabilized *COOH intermediates, reduced the activation barrier of the rate-determining step, and enhanced charge delocalization, collectively boosting CO_2-to-CO conversion efficiency. Similarly, Sargent's group et al. functionalized Cu electrodes with N-aryl-substituted tetrahydrobipyridine films, achieving an ethylene FE of 72% at −0.83 V, significantly higher than that of bare Cu (< 40%) [199]. The sp^2-N atoms in the pyridine rings enhanced the *CO adsorption, stabilized surface intermediates, and facilitated the CO dimerization, thus promoting the CO_2-to-ethylene conversion.

Inspired by these insights, researchers have explored whether amine molecules can exhibit similar co-catalytic behavior in CO_2 electrolysis [194, 200]. For example, Liu et al. developed amine-functionalized Ag nanoparticles using 4-aminobutylphosphonic acid as a bifunctional ligand [176]. The catalyst achieved a CO FE of 82% in an H-cell, which is 2.6 times higher than pristine Ag nanoparticles. In this system, amino groups facilitated the CO_2 activation and intermediate stabilization, while phosphonic acid groups suppressed the oxygen reduction by dissociating *OOH intermediates and enhanced the local electric field via electrostatic cation trapping. However, small-molecule amines often desorb during electrolysis, leading to unstable catalytic environments. To address this, polyamines with multiple sp^3-N centers offer a more robust configuration. Chen et al. electroplated polyamines on Cu electrodes, achieving enhanced ethylene selectivity and long-term stability [181, 182]. The polyamine layer stabilized intermediates maintained higher CO coverage and surface pH, and modulated surface reactivity even at high current densities. Based on these works, Tao et al. have synthesized redox-active 2-amino-5-mercapto-1,3,4-thiadiazole (AMT) functionalized gold nanoparticles to achieve integrated electrochemical capture and reduction of CO_2 in simulated flue gas (15% CO_2, 4% O_2, balanced with N_2), achieving maximum CO Faradaic efficiency of 80.2% at −0.45 V versus RHE in H-Type cell, and 66.0% at voltage of 2.7 V in a full cell, respectively [201–204]. Recently, several studies have demonstrated the direct electrochemical conversion of amine–CO_2 adducts without a separate desorption step (Fig. 13(a)). As shown in Fig. 13(b), Peng et al. employed piperazine (PZ) in combination with Ni-based single-atom catalysts (SACs) to electrochemically upgrade PZ-carbamate directly to CO, achieving a process energy consumption of approximately 48.8 GJ/t CO [32]. Similarly, Tomas et al. reported the electroreduction of ethylenediaminetetraacetic acid (EDTA) carbamate to CH_4 using Ni-based SACs, effectively coupling CO_2 capture and conversion within a single process (Fig. 13(c)) [205]. Although these studies did not employ fully integrated eCCU systems, their findings provide valuable insight into direct carbamate reduction pathways, which could inspire the future design of more efficient eCCU technologies.

Collectively, sp^2/sp^3-N compounds play distinct yet complementary roles in regulating the mass transfer, proton delivery, and intermediate stabilization in gas-phase CO_2 electroreduction [111, 117, 118, 171]. sp^2-N moieties enhance the electronic conductivity and tune the local electronic structure of active sites, whereas sp^3-N centers promote the CO_2 adsorption due to their strong polarity and localized electronic distribution. This dual functionality enables synergistic enhancement of catalytic efficiency and selectivity. Future research should focus on elucidating how amine molecular structures, substituent effects (alkyl and hydroxyl), and steric factors influence local chemical environments and reaction mechanisms. A deeper understanding of these molecular-scale interactions will guide the rational design of next-generation amine-integrated catalysts for efficient CO_2 electroreduction and eCCU applications.

As Type III system presents the most promising eCCU direction, one of the most concerning points of it is the kinetic balancing and scale-up feasibility [65]. The transition of Type III systems from laboratory H-cells to industrial stacks hinges on resolving the kinetic mismatch between CO_2 capture (gas–liquid mass transfer) and electrochemical reduction (surface charge transfer). In unoptimized systems, the slow release of CO_2 from the capture agent leads to mass transport limitations at the electrode, causing severe parasitic hydrogen evolution [39]. To address this, recent scale-up efforts have focused on "concentration buffering". By utilizing high-concentration electrolytes (e.g., 2 M bicarbonate or

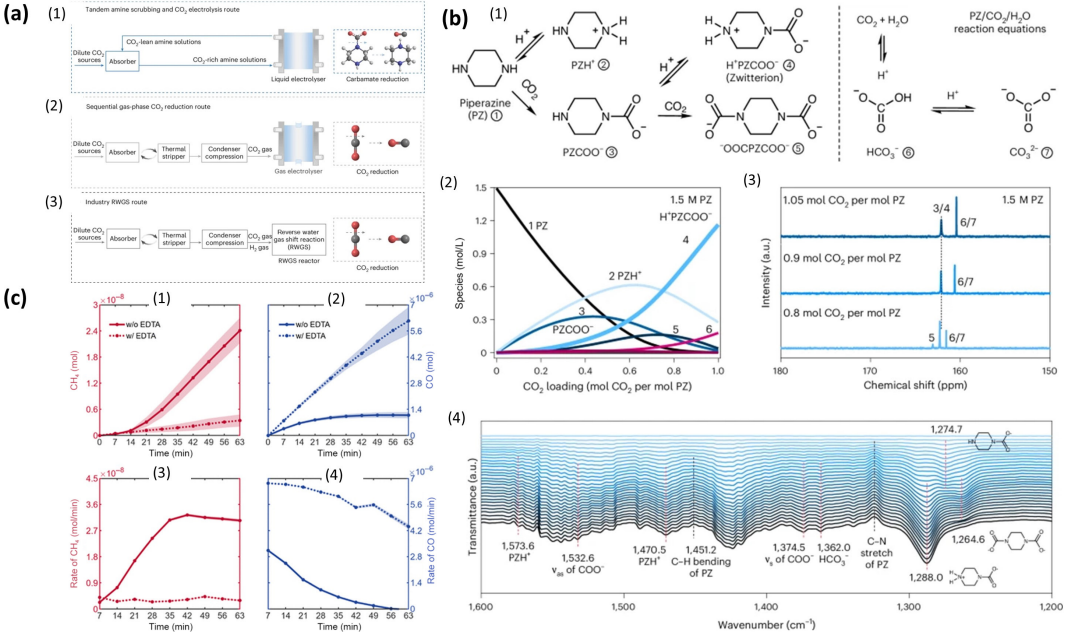

Figure 13 (a) (1) Tandem amine scrubbing and CO_2 electrolysis scheme (also reported as reactive CO_2 capture). (2) Sequential CO_2 capture and gas-phase CO_2 electrolysis scheme. (3) Industrial reverse water gas shift (RWGS) reaction scheme. (b) (1) Elementary reactions and (2) simulated speciation upon CO_2 loading for a 1.5 M PZ aqueous solution. (3) ^{13}C nuclear magnetic resonance (NMR) spectra of 1.5 M PZ solutions at three CO_2 loading capacities (80%, 90%, and 100%). (4) *In-situ* attenuated total reflection-fourier transform infrared (ATR-FTIR) spectra of 1.5 M PZ solution during CO_2 loading until reach saturation condition (~ 1.05 mol CO_2 per mol PZ). Reproduced with permission from Ref. [32], © Li, P. et al. 2025. (c) Reduction of CO_2 capture species on a polycrystalline gold (Au) surface with and without previous treatment with EDTA, yielding (1) CH_4 and (2) CO. To better visualization the data obtained was also plotted as (3) rate of CO production and (4) rate of CH_4 production. Reproduced with permission from Ref. [202], © American Chemical Society 2024.

amine solutions), the solvent itself acts as a dense carbon reservoir, ensuring that the electrocatalytic interface remains saturated even if instantaneous capture rates fluctuate [195]. Preliminary data support the viability of this approach. For instance, Shen et al. demonstrated that a hierarchical electrode design could sustain a current density of 300 mA/cm^2 with a Faradaic efficiency > 90, effectively matching the high reaction rate with sufficient local CO_2 flux [195]. As described in Section 3.3, the piperazine system demonstrated a breakthrough in the direct electrolysis of piperazine carbamates (Type III), achieving an energy consumption of 48.8 GJ/ton CO during whole eCCU process, which is competitive with industrial thermochemical benchmarks [32]. These results indicate that with optimized flow field design and high-capacity solvents, the kinetic barriers to scaling Type III systems are surmountable.

3.4 Catalyst deactivation mechanisms and mitigation strategies

The application of electrocatalysts within integrated capture–conversion systems inevitably leads to degradation over time. Although deactivation is unavoidable in most cases, various measures can be taken to slow down the process or mitigate its effects. Fundamentally, deactivation leads to a reduction in catalytic activity and, in certain cases, a loss of selectivity, which can result in increased energy consumption and secondary emissions. Following the classification adapted from Bartholomew, we categorize the primary deactivation pathways in eCCU into three main mechanisms: chemical, thermal/structural, and mechanical deactivation [203–205].

3.4.1 Chemical deactivation (poisoning and oxidation)

Chemical deactivation existed two main mechanisms including poisoning and oxidation, and it primarily occurs via poisoning by flue gas impurities. Unlike pure CO_2 streams, real-world feeds contain sulfur oxides (SOx), nitrogen oxides (NOx), and particulate matter that irreversibly bind to active sites (particularly on Ag and Cu), drastically reducing catalytic turnover [206]. Additionally, in redox-mediated architectures, reactive oxygen species generated at the anode can chemically degrade organic capture ligands. To counteract these effects, researchers are developing "impurity-tolerant" catalysts with weaker binding affinities for poisons and integrating selective gas-permeable membranes or sacrificial pre-layers that filter toxic species before they reach the electrocatalytic interface [207].

3.4.2 Thermal and structural deactivation (sintering and leaching)

Thermal and structural deactivation mainly refers to sintering and leaching. Although eCCU operates at low temperatures, the "thermal-like" structural degradation occurs due to the high cathodic potentials and local heating effects. This drives the dynamic reconstruction of active sites, such as Ostwald ripening (agglomeration) of copper nanoparticles or the leaching of single atoms from carbon supports in alkaline media. This loss of active surface area shifts the selectivity toward the parasitic HER [208]. To mitigate these irreversible structural changes, spatial nanoconfinement strategies have emerged as a leading solution. By anchoring active sites within the defects of nitrogen-doped carbon or the pores of metal-organic frameworks (MOFs), strong coordination bonds are formed that restrict atomic migration and stabilize the metal center against structural collapse [209, 210].

3.4.3 Mechanical and physical deactivation (fouling and blockage)

Mechanical deactivation in eCCU is dominated by physical blockage and fouling via salt precipitation. In GDEs, the reaction between CO_2 and alkaline electrolytes such as KOH generates carbonate salts that precipitate within the porous gas diffusion layer. This "fouling" mechanically blocks gas transport channels, causing electrode flooding and halting the reaction [211]. Addressing this requires dynamic operation modes, such as pulsed electrolysis (intermittent anodic stripping), which are employed to redissolve precipitated salts and regenerate the electrode surface *in-situ*. Concurrently, the interface engineering, specifically optimizing GDE hydrophobicity and managing local cation concentration, is critical for preventing physical blockage and ensuring continuous mass transport during long-term operation [212].

4 Techno-economic assessment of electrochemical CO_2 capture and utilization

eCCU technologies have emerged as a promising alternative to conventional thermochemical processes, offering the potential for low-temperature operation, modularity, and renewable electricity compatibility. However, the viability of these technologies at industrial scale ultimately depends on their techno-economic feasibility, encompassing energy efficiency, capital expenditure (CAPEX), and operating cost (OPEX). Despite recent breakthroughs in performance metrics at the laboratory scale, the economic competitiveness of eCCU remains a major challenge, particularly in achieving cost targets aligned with large-scale CO_2 mitigation and commodity chemical production [213, 214]

4.1 TEA of eCCC process

eCCC systems primarily focus on separating and releasing CO_2 using redox-active carriers, BPMED, or electro-swing adsorption mechanisms. Compared with the amine-based thermal regeneration, these processes eliminate the need for high-temperature desorption (> 100 °C), potentially reducing the regeneration energy from 3.0–4.0 GJ/t CO_2 to below 1.0 GJ/t CO_2 [3]. Recent techno-economic models estimate that the electricity-driven separation using redox-active quinones or metal-organic frameworks could achieve capture costs between $80–150 every ton of CO_2, assuming renewable electricity prices below $0.03 kW/h [27, 215–217]. Currently, for the technical and economic analysis of eCCC process by using redox-active carriers, there is no system research on their technical and economic performance. In Krish N et al. research, they simulated the redox-active sorbent for CO_2 capture in COMSOL. In COMSOL simulations, they discussed numerous factors such as electrode thickness, reactor length, gas flow rate, current density, and CO_2 inlet concentration that can be optimized for better Electrochemically mediated carbon capture (EMCC) performance [135]. To further compare the energy consumption of the eCCC process with conventional methods, we compiled a table summarizing the energy consumption from various lab-scale experiments below. As shown in Table 4, eCCC achieves a reduction more than 50% in energy consumption compared to traditional thermal-heating methods, highlighting its significant energy efficiency potential.

For BPMED-based systems, the major energy consumption arises from ionic resistance across the bipolar membrane and pH-swing losses. Experimental studies have demonstrated CO_2 recovery efficiencies exceeding 80% at specific energy consumptions of 80–200 kJ/mol CO_2, though system-level analyses suggest that stack

Table 4 The energy consumption comparative of conventional CO_2 capture process and EMCC

Sorbents			Energy consumption	Ref.
Conventional thermal process				
Sodium hydroxide	400 ppm CO_2	Flow absorber	500 to 800 kJ/mol CO_2	[3]
Amine-functionalized solid sorbents	400 ppm CO_2	Flow absorber	238 to 317 kJ/mol CO_2	[3]
eCCC process				
Redox-active isoindigos	1% CO_2/0.3% O_2	Flow cell	224.2 kJ/mol CO_2	[61]
	100% CO_2		157.3 kJ/mol CO_2	[61]
CNT-PAQ	400 ppm CO_2	Fixed bed cell	1192 kJ/mol CO_2	[135]
	15% CO_2		167 kJ/mol CO_2	[135]
	19% CO_2/5% O_2		237 kJ/mol CO_2	[135]
	19% CO_2/5% O_2	Fixed bed cell with gas diffusion layer	192 kJ/mol CO_2	[135]
AzPy	Pure CO_2	EMCC flow cell	16 kJ/mol CO_2 (theoretical)	[61]
	Simulated flue gas		120 kJ/mol CO_2	[61]
Aqueous poly-quinone	15% CO_2/5% O_2	Flow cell (2 cm × 2 cm)	56 kJ/mol CO_2	[113]
NR	400 ppm CO_2	H-cell batch reactor	123 kJ_e/mol CO_2	[104]
	5% CO_2	Flow cell	35 kJ_e/mol CO_2	[104]
	400 ppm CO_2		65 kJ_e/mol CO_2	[104]
Anthraquinone disulfonate solution	15% CO_2/5% O_2	Lab-scale flow cell	49.16 kJ_e/mol CO_2	[217]
	15% CO_2/5% O_2	Pilot-scale flow cell	92.93 kJ_e/mol CO_2	[217]
FMN-Na	15% CO_2/3% O_2	Lab-scale flow cell	0.998 GJ/t CO_2	[218]
BHPC	15% CO_2/3% O_2	Lab-scale flow cell	1.825 GJ/t CO_2	[54]
	15% CO_2 3% O_2	Pilot-scale flow cell	2.264 GJ/t CO_2	[54]

durability and membrane costs remain key barriers. The use of redox-active sorbents, such as quinone-based molecules, can further lower energy requirements by enabling reversible CO_2 binding at mild potentials (−0.5 to −1.0 V vs. Ag/AgCl). However, these systems require expensive electrodes and controlled electrochemical environments, and are often limited by solubility and long-term stability of the redox mediators [219–224]. In some specific cases, such as DAC process and seawater CO_2 capture, their TEAs have been systemically discussed. The first economic analysis of the BPMED process was conducted by Iizuka et al., who demonstrated that improving current efficiency and reducing membrane costs could significantly lower overall costs [221, 225, 226]. Using lab-scale experimental data, they identified optimal operating conditions and calculated a CO_2 recovery cost of \$180/ton CO_2, assuming an electricity cost of \$0.12/kWh. However, the simulation and techno-economic analyses were optimized by extrapolating experimental results, revealing that electricity costs account for about 60% of total costs, while membrane costs make up 30% [95]. Despite these improvements, the minimum cost remains higher than conventional CO_2 recovery processes, such as amine absorption/thermal desorption, which typically costs less than \$100/ton CO_2, particularly when using high-performance amines like KS-1.

A solid techno-economic analysis relies on accurate simulations, and Carbon Engineering's extensive data on the BPMED process and reactor design have been crucial for this. Building on these data, Sabatino et al. analyzed the DAC process using KOH-based BPMED technology [85]. Their sensitivity analysis identified membrane lifetime and electricity cost as the most influential parameters, as the membrane replacement and BPMED power consumption account for the bulk of OPEX and thus many capture costs. The analysis revealed that the KOH-based BPMED process is currently too expensive, with an estimated capture cost of \$773/ton CO_2-significantly higher than conventional amine scrubbing methods [150].

To improve efficiency, Sabatino et al. examined the use of cation-exchange membranes (CEM) and AEM in the DAC process. The BPMED-CEM configuration showed a competitive energy demand of 24 MJ/kg CO_2, like amine scrubbing [85]. However, the BPMED-AEM configuration was less efficient due to membrane selectivity issues. By adding inert salt to enhance conductivity, the energy required for BPMED-CEM was further reduced to 17 MJ/kg CO_2. With the future development of more durable and conductive membranes, costs could potentially drop below \$250/ton CO_2, positioning BPMED-CEM as a viable and fully electrified alternative to gas-dependent processes like Carbon Engineering's [222]. These results suggest that advanced CO_2 sorbents in the BPMED process could significantly lower overall costs [223].

Novel CO_2 sequestration methods coupled with BPMED, such as electrochemical carbon capture from seawater, have demonstrated economic advantages in specific applications. Mehran et al. optimized BPMED for CO_2 capture from seawater, achieving a minimum energy consumption of 1.7 kWh/kg CO_2 at 9 mS/cm conductivity. They observed that increasing feed velocity lowered energy demand but reduced dissolved inorganic carbon (DIC) removal (44% vs. 64% at 1 cm/s). The energy consumption was highly sensitive to operating parameters, with mass transport limitations at high current densities and salt crossover at low current densities affecting the overall efficiency. Although higher

conductivity (above 9 mS/cm) was necessary to drive pH changes, it led to increased energy losses. The study concluded that further optimization of the process and membrane materials is needed to reduce energy consumption, along with investigations using real seawater and assessing long-term operational stability. Building on this, Mark et al. conducted a detailed techno-economic analysis of co-located electrochemical carbon capture and sequestration (hydrates) from oceanwater, specifically in the Gulf of Mexico and their integrated system achieved both CO_2 capture and storage, with the simulation results indicating a levelized cost of \$1131/ton CO_2 for a 1 Mt CO_2/year system. It is notably lower than the estimates for onshore industrial capture (ranging from \$1870/ton CO_2 to \$2050/ton CO_2) due to the elimination of long-distance seawater pumping. Despite this advantage, the cost is still significantly higher than point-source capture or DAC systems, with the cost of CO_2 captured from flue gas and air ranged from \$60 to \$80/ton CO_2 and \$94 to \$232/ton CO_2, respectively [146, 224, 225]. The analysis revealed that CO_2 capture accounted for 87% of the total cost (\$1096/ton CO_2), with the main cost driver being the extensive pre-treatment of seawater, which is more expensive than the electrochemical capture process itself. The total energy requirement for this system was 3.22 kWh/kg CO_2. As for the capital cost assessments, the primary cost driver was seawater pre-treatment (55%), followed by gas striping due to expensive gas separation membranes. The electrochemical capture process consumed 37% of the energy but contributed less than 10% of the total cost, which contrasts with the eCCC process on land.

Opportunities for cost reduction include scaling, renewable electricity, and more durable membranes. To improve economic feasibility, the integration with renewable electricity and process intensification strategies (e.g., electrochemical looping and solid–liquid hybrid cells) are being explored [225, 226]. Lifecycle assessments (LCAs) indicate that eCCC processes powered by solar or wind energy can achieve up to 70% reduction in CO_2-equivalent emissions compared with traditional amine-based systems, if materials and membranes are produced sustainably [87]. Nevertheless, challenges such as scale-up of redox-active materials, stack durability beyond 10,000 h, and efficient product separation must be addressed before large-scale deployment.

4.2 Techno-economic analysis of eCCU process

In eCCU, CO_2 capture and electrochemical conversion occur simultaneously, bypassing the high-energy desorption step. This integrated design not only simplifies the process configuration but also potentially reduces total energy consumption by 30%–50% compared with the conventional capture-plus-electrolysis route [227–231]. For instance, coupling carbonate/bicarbonate capture solutions with SACs has enabled continuous syngas or CO production at current densities above 100 mA/cm^2 with stable operation over tens of hours. Peng et al. reported an energy consumption of ~ 48.8 GJ/ton CO for direct carbamate electroreduction on Ni-based SACs, already competitive with the thermochemical benchmark when powered by renewable electricity [32].

Techno-economic evaluations of eCCU systems highlight several key cost determinants:

(1) electricity price, which contributes over 50% of the total cost;

(2) electrode and catalyst lifetime, particularly for single-atom and molecular catalysts prone to deactivation;

(3) electrolyte management, as solvent evaporation, degradation, and salt precipitation increase maintenance costs;

(4) product value, where high-value products (e.g., formate, ethylene, and ethanol) significantly improve process economics compared to CO or syngas.

Current models estimate that CO production via eCCU could reach \$200–300/ton CO_2 converted under optimized conditions, approaching economic viability when electricity prices drop below \$0.02/kWh and Faradaic efficiencies exceed 90%. Moreover, co-designing catalysts and capture media, such as redox-active amines or sp^2/sp^3-N structures, may further lower cell overpotentials and enhance selectivity, directly improving system-level energy efficiency. The integration with renewable energy storage and flexible grid operation also presents additional economic benefits by enabling load-following carbon utilization during electricity surplus periods.

Nowadays several TEAs have been conducted to evaluate the economic viability of electrochemical CO_2RR systems when coupled with conventional CO_2 capture processes, though no TEA has yet been reported for the eCCU process [32, 192, 230]. Yang et al. compared three CO_2RR systems: (1) conventional MEA CO_2 capture combined with CO_2RR, (2) direct electrolysis of MEA-CO_2 products, and (3) direct electrolysis of KOH-CO_2 products. These systems, named G/CO, B/CO, and M/CO, respectively, produce CO and H_2 through CO_2RR. The M/CO process showed the highest profits, reaching \$99,631/day, the lowest net greenhouse gas (GHG) emissions (−0.763 t CO_2-eq/t CO_2), and the highest net present value (NPV) of \$73.38 million. This system benefited from high CO_2 capture efficiency and avoided energy-intensive pressure swing adsorption. However, the electrolysis process consumed over 90% of the total energy, highlighting the need to improve electrolysis efficiency by reducing cell voltage. A reduction of 1 V in voltage could increase NPV by 43.72%. Despite its advantages, the M/CO process had the highest capital and operational costs, mainly due to substantial electricity costs and the large electrolyzer area required. This analysis underscores the importance of reducing energy consumption in future industrial applications [215]. Yongwook et al. simulated a pilot-scale CO_2RR system coupled with a conventional CO_2 absorption unit, treating 828 tons of CO_2 annually. Their analysis showed a CO breakeven price of \$0.72/kg CO for a system without separations and \$0.94/kg CO with separations. The capital costs for the plant were estimated at approximately \$700,000 without separations and \$1.1 million with separations, demonstrating economic viability. However, the lab-scale system (100 cm^2) showed an unprofitable CO breakeven price of \$5,000/kg CO. This indicates that scaling up CO_2RR systems is crucial for reducing operational costs and improving economics [214]. In a more complex TEA, Theo et al. analyzed the production of ethylene via CO_2RR using a BPM electrolyzer. For an optimal scale of 3150 tons/year, the total annualized cost was estimated at \$3920/ton, with a positive NPV of \$771/ton [34]. This study highlighted the importance of CO_2 purity in optimizing costs, suggesting that integrating eCCC could further reduce ethylene production costs. Jouny et al. explored six different products (n-propanol, formic acid, CO, ethanol, ethylene, and methanol) from CO_2RR [231]. Their analysis showed that only CO and formic acid were economically viable at current electricity prices. For higher-value C_{2+} products, the major operating cost was electricity, and even small changes in electricity prices could significantly impact NPV. Notably, product selectivity and voltage were identified as key performance indicators, with higher selectivity

reducing power requirements and separation costs. For products requiring large electricity inputs, such as ethanol and ethylene, maintaining current densities above 250–300 mA/cm^2 was critical for maximizing NPV. These studies emphasize that renewable energy integration, efficient electrocatalysts, and stable CO_2 capture systems are essential for the economic success of CO_2RR processes. A steady supply of low-cost electricity and high-purity CO_2 is crucial for reducing operational costs and improving the economic feasibility of these systems [232, 233].

Although eCCU is still at an early development stage, its modular, low-temperature, and scalable nature makes it a compelling long-term alternative to thermochemical CO_2 utilization. Future techno-economic optimization should prioritize durable cell architectures, co-optimized capture-conversion kinetics, and life-cycle cost reduction through material innovation. With ongoing advancements in electrochemical reactor design, renewable electricity infrastructure, and redox-active materials, eCCU holds strong potential to evolve into a commercially competitive and carbon-negative pathway for sustainable chemical manufacturing [34, 216, 234].

5 Conclusions and outlook

This review discusses the advancements in eCCC and eCCU technologies published from 2015 to 2025. The development of eCCC and CO_2RR systems date to the 1960s and 1970s, and integrating this process together as eCCU is a newly developed technology, but these technologies have emerged as a promising alternative to traditional thermochemical CO_2 capture methods, offering enhanced energy efficiency, sustainability, and operational flexibility [217–219]. Also, as the cost of electricity continues to decrease, largely driven by breakthroughs in renewable energy technologies, these advancements are expected to accelerate the development and commercialization of eCCC and eCCU systems. However, several obstacles, such as energy consumption, operational stability, and scalability, must be addressed for successful commercialization. Recent studies have introduced strategies to mitigate these issues, including process integration with renewable energy sources, which could significantly reduce operational costs and enhance energy efficiency [235–242]. Moving forward, several key research areas must be prioritized to advance eCCC and eCCU technologies.

5.1 Enhanced reaction pathway understanding and catalyst design

A deeper understanding of reaction pathways, especially for C_{2+} products in CO_2RR systems by using amine carbonate or bicarbonate, is crucial. Advancements in *in-situ* spectroscopy, theoretical calculations, and machine learning will help optimize electrode materials and electrocatalysts for better efficiency [243–247].

5.2 Optimizing CO_2 capture and electrolysis integration

Integrating CO_2 capture and electrolysis systems could maximize mass and energy utilization efficiency. In continuous electrolysis system, optimizing the feed CO_2 steam from captured unit is always neglected, by optimizing the feed gas flow rate, purification, pressure and other properties is important to CO_2RR efficiency [248–253].

5.3 Synergistic coupling with other technologies

Exploring the integration of electrochemistry with other fields such as photochemistry, thermochemistry, and biochemistry could provide additional performance enhancements. For example, combining electrochemical processes with thermal hydrogenation of bicarbonate could improve carbon conversion at room temperature. Additionally, incorporating renewable energy sources from photochemical, thermal, or bioenergy systems could help offset the energy demands of electrochemical CO_2 capture systems, contributing to higher overall efficiency [21, 226].

5.4 Improving energy efficiency and stability for scale up

To scale eCCC systems, improving energy efficiency and long-term stability is crucial. Focus should be on reducing polarization and overpotentials, addressing cost and kinetic challenges to make eCCC systems economically competitive with existing CO_2 capture technologies. Stability is another key issue, particularly for systems like pH swings, redox carriers, and BPMED, which are sensitive to impurities like oxygen and water vapor. Modifications such as pre-separating these impurities and improving CO_2 capture chemistries will be essential for enhancing system durability at scale. Optimizing both energy efficiency and stability will help make eCCC a viable and scalable solution for industrial CO_2 capture [254–268].

5.5 Advanced product separation and downstream processing

Although improving Faradaic efficiency is essential, the energy penalty associated with downstream product separation remains a critical but often overlooked challenge in eCCU systems. For liquid products such as ethanol, formate, or acetate, separating dilute organics from highly conductive electrolyte solutions can consume more energy than the electrochemical conversion itself. Future research must move beyond simple "H-cell" quantification and focus on minimizing crossover and optimizing product concentration [254]. Developing solid-electrolyte reactors and integrating energy-efficient separation technologies (e.g., membrane distillation) will be decisive in determining the economic viability of liquid-product eCCU pathways.

5.6 Dynamic compatibility with intermittent renewables

To truly leverage low-cost renewable electricity, eCCC and eCCU systems must evolve from steady-state baseload operation to dynamic and load-following architectures. Real-world solar and wind profiles are inherently volatile, causing rapid fluctuations in voltage and current density that can accelerate catalyst degradation and destabilize capture kinetics [228]. Future work should prioritize the design of "robust" interfaces capable of tolerating frequent start-stop cycles and ramping rates, ensuring that eCCU technologies can act as flexible grid assets.

5.7 Standardized performance benchmarks and techno-economic targets

To bridge the gap between academic discovery and industrial relevance, the eCCU community must adopt a rigorous set of performance benchmarks derived from LCA and TEA. As summarized in Table 5 below, widespread deployment requires meeting simultaneous targets for activity, selectivity, and durability,

Table 5 Key techno-econ performance metrics and scaling targets for eCCU

Metric	Current lab status (currently)	Pilot scale target (in 5 years)	Industrial scale target (commercial viability)
Current density	1–100 mA/cm^2	> 200 mA/cm^2	500–1000 mA/cm^2
FE	50%–80% (C_1 + C_{2+})	80% (C_{2+})	90% (C_{2+})
Stability/lifetime	10–100 h	> 500 h	> 1000 h
Cell voltage	3.0–4.5 V	< 3.5 V	< 2.5 V
Energy consumption	> 10 GJ/ton CO_2	< 5 GJ/ton CO_2	< 2 GJ/ton CO_2

and this table delineates the critical performance benchmarks required to transition eCCU technologies from current laboratory-scale research to pilot demonstration and final industrial commercialization. Specifically, future flow-cell architectures must demonstrate geometric current densities exceeding 200 mA/cm^2 for high-value products and > 500 mA/cm^2 for commodity fuels while maintaining cell voltages < 3.0 V to minimize capital costs (CAPEX). Furthermore, to compete with thermochemical reforming, systems must achieve single-pass carbon conversion rates > 40%, liquid product concentrations > 10 wt.%, and robust stability against flue gas impurities (SO_x and NO_x) for > 1,000 h at the laboratory scale and > 20,000 h for pilot stacks [229].

In conclusion, although eCCC and eCCU technologies hold substantial promises, significant research and development are required to overcome current limitations in efficiency, stability, and scalability. By addressing these challenges, these technologies could become a key solution for CO_2 capture and conversion, contributing to global carbon mitigation strategies and the transition to sustainable energy systems.

Data availability

Not applicable.

Acknowledgements

This work was financially supported by the National Natural Science Foundation of China (Nos. 52202306 and 22402039), Program from Guangdong Introducing Innovative and Entrepreneurial Teams (Nos. 2019ZT08L101 and RCTDPT-2020-001), Shenzhen Key Laboratory of Eco-materials and Renewable Energy (No. ZDSYS20200922160400001), the Provincial Talent Plan of Guangdong (No. 2023TB0012), The Chinese University of Hong Kong (Shenzhen) Startup Fund, Department of Science and Technology of Guangdong Province (No. 2023QN10L141), the Program for Shenzhen Science and Technology Innovation Committee (No. JSGGKQTD20221101115701006), and the University stability support program of Shenzhen (No. 2023SC0027). The authors acknowledge the financial support from Guangdong Basic Research Center of Excellence for Aggregate Science.

Declaration of competing interest

All the contributing authors report no conflict of interests in this work.

Author contribution statement

M. Q. Z.: Data curation, investigation, visualization, formal analysis, writing manuscript. G. C. L.: Conceptualization, methodology, project administration, visualization, supervision, writing manuscript. X. H. C.: Data curation, investigation, formal analysis, visualization. C. Y. W.: Data curation, investigation, formal analysis. Y. L. Z. and Q. L.: Data curation and investigation. J. B. W.: Project administration, supervision, funding acquisition, writing manuscript. H. G. L.: Conceptualization, project administration, supervision, funding acquisition, writing manuscript. All the authors have approved the final manuscript.

Use of AI statement

None.

References

[1] Lee, S.; Choi, W.; Kim, J. H.; Park, S.; Hwang, Y. J.; Na, J. Techno-economic analysis and life-cycle assessment of the electrochemical conversion process with captured CO_2 in an amine-based solvent. *Green Chem.* **2023**, *25*, 10398–10414.

[2] Raupach, M. R.; Marland, G.; Ciais, P.; Le Quéré, C.; Canadell, J. G.; Klepper, G.; Field, C. B. Global and regional drivers of accelerating CO_2 emissions. *Proc. Natl. Acad. Sci. USA* **2017**, *104*, 10288–10293.

[3] Lu, G. C.; Farrukh, S.; Fan, X. F. Research progress of non-aqueous absorbents for carbon dioxide capture with low energy consumption: A review. *Fuel* **2025**, *391*, 134740.

[4] Lu, G. C.; Wang, Z.; Yue, Z. Y.; Wei, W. J.; Huang, Y.; Zhang, X. L.; Fan, X. F. Development of novel AMP-based absorbents for efficient CO_2 capture with low energy consumption through modifying the electrostatic potential. *Chem. Eng. J.* **2023**, *474*, 145929.

[5] Lu, G. C.; Wang, Z.; Yue, Z. Y.; Yang, L. X.; Zhang, X. L.; Huang, Y.; Qian, J. H.; Fan, X. F. A novel non-aqueous tertiary amine system for low energy CO_2 capture developed via molecular dynamics simulation. *Sep. Purif. Technol.* **2025**, *354*, 128996.

[6] Li, M. X.; He, N. P.; Xu, L.; Peng, C. H.; Chen, H.; Yu, G. R. Eco-CCUS: A cost-effective pathway towards carbon neutrality in China. *Renew. Sustain. Energy Rev.* **2023**, *183*, 113512.

[7] Yan, Y. L.; Borhani, T. N.; Subraveti, S. G.; Pai, K. N.; Prasad, V.; Rajendran, A.; Nkulikiyinka, P.; Asibor, J. O.; Zhang, Z. E.; Shao, D. et al. Harnessing the power of machine learning for carbon capture, utilisation, and storage (CCUS)—A state-of-the-art review. *Energy Environ. Sci.* **2021**, *14*, 6122–6157.

[8] Lu, G. C.; Yue, Z. Y.; Deng, Y. N.; Xue, Y. X.; Huang, Y.; Zhang, X. L.; Chen, X. F.; Fan, X. F. An energy-efficient cyclic amine system developed for carbon capture from both flue gas and air. *Chem. Eng. J.* **2024**, *496*, 154085.

[9] Julio, A. A. V.; Castro-Amoedo, R.; Maréchal, F.; González, A. M.; Escobar Palacio, J. C. Exergy and economic analysis of the trade-off for design of post-combustion CO_2 capture plant by chemical absorption with MEA. *Energy* **2023**, *280*, 128004.

[10] Yang, Y. H.; Du, T.; Li, Y. N.; Yue, Q.; Wang, H. M.; Liu, L. Y.; Che, S.; Wang, Y. S. Techno-economic assessment and exergy

analysis of iron and steel plant coupled MEA-CO_2 capture process. *J. Cleaner Prod.* **2023**, *416*, 137976.

[11] Saeed, I. M.; Alaba, P.; Mazari, S. A.; Basirun, W. J.; Lee, V. S.; Sabzoi, N. Opportunities and challenges in the development of monoethanolamine and its blends for post-combustion CO_2 capture. *Int. J. Greenh. Gas Control.* **2018**, *79*, 212–233.

[12] Lu, G. C.; Wang, Z.; Bhatti, U. H.; Fan, X. Recent progress in carbon dioxide capture technologies: A review. *Clean Energy Sci. Technol.* **2023**, *1*, 32.

[13] Rahimi, M.; Khurram, A.; Hatton, T. A.; Gallant, B. Electrochemical carbon capture processes for mitigation of CO_2 emissions. *Chem. Soc. Rev.* **2022**, *51*, 8676–8695.

[14] Crovetto, R. Evaluation of solubility data of the system CO_2-H_2O from 273 K to the critical point of water. *J. Phys. Chem. Ref. Data.* **1991**, *20*, 575–589.

[15] Li, H. G.; Zick, M. E.; Trisukhon, T.; Signorile, M.; Liu, X. Y.; Eastmond, H.; Sharma, S.; Spreng, T. L.; Taylor, J.; Gittins, J. W. et al. Capturing carbon dioxide from air with charged-sorbents. *Nature* **2024**, *630*, 654–659.

[16] Mori, Y. H. Clathrate hydrate formation at the interface between liquid CO_2 and water phases—A review of rival models characterizing "hydrate films". *Energy Convers. Manage.* **1998**, *39*, 1537–1557.

[17] Lei, Z. G.; Dai, C. N.; Chen, B. H. Gas solubility in ionic liquids. *Chem. Rev.* **2014**, *114*, 1289–1326.

[18] Azdarpour, A.; Asadullah, M.; Mohammadian, E.; Hamidi, H.; Junin, R.; Karaei, M. A. A review on carbon dioxide mineral carbonation through pH-swing process. *Chem. Eng. J.* **2015**, *279*, 615–630.

[19] Jin, S. J.; Wu, M.; Gordon, R. G.; Aziz, M. J.; Kwabi, D. G. pH swing cycle for CO_2 capture electrochemically driven through proton-coupled electron transfer. *Energy Environ. Sci.* **2020**, *13*, 3706–3722.

[20] Khiarak, B. N.; Da Silva, G. T. S. T.; Lai, H. D. T.; Esmaeili, H.; Nguyen, A. N.; Dinh, K. H.; Zhang, Q.; Mascaro, L. H.; Dinh, C. T. Integrated carbon dioxide capture and electrochemical conversion: Chemistry, electrode and electrolyzer design, and economic viability. *Adv. Energy Mater.*, in press, https://doi.org/10.1002/aenm.202502564.

[21] Xiang, K. S.; Shen, F. H.; Fu, Y. X.; Wu, L.; Wang, Z. J.; Yi, H. M.; Liu, X. D.; Wang, P. S.; Liu, M.; Lin, Z. et al. Boosting CO_2 electroreduction towards C_{2+} products via CO* intermediate manipulation on copper-based catalysts. *Environ. Sci.: Nano* **2022**, *9*, 911–953.

[22] Jiang, C. X.; Zhang, Y. L.; Feng, H. Y.; Wang, Q. Y.; Wang, Y. M.; Xu, T. W. Simultaneous CO_2 capture and amino acid production using bipolar membrane electrodialysis (BMED). *J. Membr. Sci.* **2017**, *542*, 264–271.

[23] Kim, S.; Shin, H.; Kang, J. S. Electrochemical reduction of captured CO_2: A route toward the integrated carbon capture and utilization. *Curr. Opin. Electrochem.* **2023**, *40*, 101321.

[24] Mohsin, I.; Al-Attas, T. A.; Sumon, K. Z.; Bergerson, J.; Mccoy, S.; Kibria, M. G. Economic and environmental assessment of integrated carbon capture and utilization. *Cell Rep. Phys. Sci.* **2020**, *1*, 100104.

[25] Pérez-Gallent, E.; Vankani, C.; Sánchez-Martínez, C.; Anastasopol, A.; Goetheer, E. Integrating CO_2 capture with electrochemical conversion using amine-based capture solvents as electrolytes. *Ind. Eng. Chem. Res.* **2021**, *60*, 4269–4278.

[26] Saha, P.; Amanullah, S.; Dey, A. Selectivity in electrochemical CO_2 reduction. *Acc. Chem. Res.* **2022**, *55*, 134–144.

[27] Al Moinee, A.; Rownaghi, A. A.; Rezaei, F. Process development and techno-economic analysis for combined and separated CO_2 capture-electrochemical utilization. *Chem. Eng. J.* **2024**, *499*, 155909.

[28] Zito, A. M.; Clarke, L. E.; Barlow, J. M.; Bím, D.; Zhang, Z. S.; Ripley, K. M.; Li, C. J.; Kummeth, A.; Leonard, M. E.; Alexandrova, A. N. et al. Electrochemical carbon dioxide capture and concentration. *Chem. Rev.* **2023**, *123*, 8069–8098.

[29] Pei, Y. H.; Zhang, B.; Lu, Y. Y. Carbon capture and utilization via electrochemistry, what's next? *Next Nanotechnol* **2023**, *3–4*, 100020.

[30] Zhang, W.; Yang, Y.; Li, Y. X.; Li, F. W.; Luo, M. C. Recent progress on integrated CO_2 capture and electrochemical upgrading. *Mater. Today Catal.* **2023**, *2*, 100006.

[31] Comeau Simpson, T.; Durand, R. R. Reactivity of carbon dioxide with quinones. *Electrochimica. Acta* **1990**, *35*, 1399–1403.

[32] Li, P.; Mao, Y.; Shin, H.; Yang, Q.; Cheng, X.; Li, Y. T.; Li, K. K.; Yu, H.; Mulder, R.; Pang, W. K. et al. Tandem amine scrubbing and CO_2 electrolysis via direct piperazine carbamate reduction. *Nat. Energy* **2025**, *10*, 1262–1273.

[33] Kulkarni, S.; Kaware, J. Regeneration and recovery in adsorption—A review. *Int. J. Innov. Sci. Eng. Technol.* **2014**, *1*, 61–64.

[34] Alerte, T.; Gaona, A.; Edwards, J. P.; Gabardo, C. M.; O'Brien, C. P.; Wicks, J.; Bonnenfant, L.; Rasouli, A. S.; Young, D.; Abed, J. et al. Scale-dependent techno-economic analysis of CO_2 capture and electroreduction to ethylene. *ACS Sustain. Chem. Eng.* **2023**, *11*, 15651–15662.

[35] Page, M. J.; Mckenzie, J. E.; Bossuyt, P. M.; Boutron, I.; Hoffmann, T. C.; Mulrow, C. D.; Shamseer, L.; Tetzlaff, J. M.; Akl, E. A.; Brennan, S. E. et al. The PRISMA 2020 statement: An updated guideline for reporting systematic reviews. *PLoS Med.* **2021**, *18*, e1003583.

[36] Madejski, P.; Chmiel, K.; Subramanian, N.; Kuś, T. Methods and techniques for CO_2 capture: Review of potential solutions and applications in modern energy technologies. *Energies* **2022**, *15*, 887.

[37] Hong, W. Y. A techno-economic review on carbon capture, utilisation and storage systems for achieving a net-zero CO_2 emissions future. *Carbon Capture Sci. Technol.* **2022**, *3*, 100044.

[38] van der Spek, M.; Fout, T.; Garcia, M.; Kuncheekanna, V. N.; Matuszewski, M.; Mccoy, S.; Morgan, J.; Nazir, S. M.; Ramirez, A.; Roussanaly, S. et al. Uncertainty analysis in the techno-economic assessment of CO_2 capture and storage technologies. Critical review and guidelines for use. *Int. J. Greenh. Gas Control.* **2020**, *100*, 103113.

[39] Sullivan, I.; Goryachev, A.; Digdaya, I. A.; Li, X. Q.; Atwater, H. A.; Vermaas, D. A.; Xiang, C. X. Coupling electrochemical CO_2 conversion with CO_2 capture. *Nat. Catal.* **2021**, *4*, 952–958.

[40] Huebscher, R. G.; Babinsky, A. D. Electrochemical concentration and separation of carbon dioxide for advanced life support systems-carbonation cell system. *SAE Transactions* **1969**, 2164–2170.

[41] Li, B. Y.; Duan, Y. H.; Luebke, D.; Morreale, B. Advances in CO_2 capture technology: A patent review. *Appl. Energy* **2013**, *102*, 1439–1447.

[42] Mondal, M. K.; Balsora, H. K.; Varshney, P. Progress and trends in CO_2 capture/separation technologies: A review. *Energy* **2012**, *46*, 431–441.

[43] Hao, S. Y.; Elgazzar, A.; Ravi, N.; Wi, T. U.; Zhu, P.; Feng, Y. G.; Xia, Y.; Chen, F. Y.; Shan, X. N.; Wang, H. T. Improving the operational stability of electrochemical CO_2 reduction reaction via salt precipitation understanding and management. *Nat. Energy* **2025**, *10*, 266–277.

[44] Taniguchi, I.; Ioh, D.; Fujikawa, S.; Watanabe, T.; Matsukuma, Y.; Minemoto, M. An alternative carbon dioxide capture by electrochemical method. *Chem. Lett.* **2014**, *43*, 1601–1603.

[45] Smith, K.; Xiao, G. K.; Mumford, K.; Gouw, J.; Indrawan, I.; Thanumurthy, N.; Quyn, D.; Cuthbertson, R.; Rayer, A.; Nicholas, N. et al. Demonstration of a concentrated potassium carbonate process for CO_2 capture. *Energy Fuels* **2014**, *28*, 299–306.

[46] Abdinejad, M.; Massen-Hane, M.; Seo, H.; Hatton, T. A. Oxygen-stable electrochemical CO_2 capture using redox-active heterocyclic benzodithiophene quinone. *Angew. Chem., Int. Ed.* **2024**, *63*, e202412229.

[47] Simeon, F.; Stern, M. C.; Diederichsen, K. M.; Liu, Y. Y.; Herzog, H. J.; Hatton, T. A. Electrochemical and molecular assessment of quinones as CO_2-binding redox molecules for carbon capture. *J. Phys. Chem. C* **2022**, *126*, 1389–1399.

[48] Zhang, Y. S.; Bai, H. X.; Wang, Y. H. Reactor designs for pH-swing electrochemical CO_2 capture. *Curr. Opin. Electrochem.* **2025**, *53*, 101731.

[49] Bae, H.; Park, J. S.; Senthilkumar, S. T.; Hwang, S. M.; Kim, Y. Hybrid seawater desalination-carbon capture using modified seawater battery system. *J. Power Sources* **2019**, *410–411*, 99–105.

[50] Vallejo Castaño, S.; Shu, Q. D.; Shi, M.; Blauw, R.; Loldrup Fosbøl, P.; Kuntke, P.; Tedesco, M.; Hamelers, H. V. M. Optimizing alkaline solvent regeneration through bipolar membrane electrodialysis for carbon capture. *Chem. Eng. J.* **2024**, *488*, 150870.

[51] Eisaman, M. D.; Alvarado, L.; Larner, D.; Wang, P.; Littau, K. A. CO_2 desorption using high-pressure bipolar membrane electrodialysis. *Energy Environ. Sci.* **2011**, *4*, 4031–4037.

[52] Jin, X. Y.; Jin, S. J.; Li, L.; Gordon, R. G.; Wang, P.; Aziz, M. J.; Ji, Y. L. Direct air capture of CO_2 in a hybrid electrochemical flow cell. *Nat Energy.* **2025**, *10*, 1146–1154.

[53] Ali, F.; Bilger, D.; Patamia, E. D.; Andrew, T. L.; Kwabi, D. G. Towards immobilized proton-coupled electron transfer agents for electrochemical carbon capture from air and seawater. *J. Electrochem. Soc.* **2024**, *171*, 053505.

[54] Jiang, W. C.; Liu, W. R.; Wang, Y. P.; Zhao, Z. Y.; Li, Q.; Wu, Y. F.; Liu, T.; Xie, H. P. Electrochemically regenerated amine for CO_2 capture driven by a proton-coupled electron transfer reaction. *Ind. Eng. Chem. Res.* **2022**, *61*, 13578–13588.

[55] Shu, Q. D.; Sin, C. S.; Tedesco, M.; Hamelers, H. V. M.; Kuntke, P. Optimization of an electrochemical direct air capture process with decreased CO_2 desorption pressure and addition of background electrolyte. *Chem. Eng. J.* **2023**, *470*, 144251.

[56] Shu, Q. D.; Haug, M.; Tedesco, M.; Kuntke, P.; Hamelers, H. V. M. Direct air capture using electrochemically regenerated anion exchange resins. *Environ. Sci. Technol.* **2022**, *56*, 11559–11566.

[57] Ma, P. Q.; Wang, A. M.; Xu, W. C.; Chen, R. H.; Huang, Y. W.; Deng, S. Energy performance evaluation of a liquid electrochemical pH-swing carbon capture system. *Energy Convers. Manage.* **2026**, *348*, 120745.

[58] Lin, M.; Ehret, C.; Hamelers, H. V. M.; Heijne, A. T.; Kuntke, P. Energy efficient carbon capture through electrochemical pH swing regeneration of amine solution. *ACS Sustain. Chem. Eng.* **2024**, *12*, 7309–7317.

[59] Grignon, E.; Su, Z. F.; Liu, J. T.; Lima, A.; Wang, A.; Karimi, P.; Chen, S.; Seferos, D. S. Water-soluble pyridinium redox mediators for pH-swing CO_2 capture. *Chem. Sci.* **2025**, *16*, 19702–19710.

[60] Liu, S. J.; Zhang, J. Q.; Li, F.; Edwards, J. P.; Xiao, Y. C.; Kim, D.; Papangelakis, P.; Kim, J.; Elder, D.; De Luna, P. et al. Direct air capture of CO_2 via cyclic viologen electrocatalysis. *Energy Environ. Sci.* **2024**, *17*, 1266–1278.

[61] Li, X.; Zhao, X. H.; Zhang, L. Y.; Mathur, A.; Xu, Y.; Fang, Z. W.; Gu, L.; Liu, Y. Y.; Liu, Y. Y. Redox-tunable isoindigos for electrochemically mediated carbon capture. *Nat. Commun.* **2024**, *15*, 1175.

[62] Zhao, F.; Deng, Y. M.; Li, M. Y.; Lv, C.; Aminabhavi, T. M.; Orhan, O. Y.; Liu, H. L. Low-energy electrochemical CO_2-amine desorption driven by the proton-coupled electron transfer reaction (PCET). *Chem. Eng. J.* **2024**, *495*, 153217.

[63] Li, X.; Musgrave, C. B.; Liu, A. D.; Meng, J. Y.; Zhang, J. H.; Goddard, W. A.; Liu, Y. Y. Electrifying amine carbon capture with robust redox-tunable acids. *Nat. Commun.* **2025**, *16*, 4339.

[64] Hartley, N. A.; Pugh, S. M.; Xu, Z.; Leong, D. C. Y.; Jaffe, A.; Forse, A. C. Quinone-functionalised carbons as new materials for electrochemical carbon dioxide capture. *J. Mater. Chem. A* **2023**, *11*, 16221–16232.

[65] Li, X. X.; Deng, C.; Chen, R.; Li, X.; Xie, F. R.; Wu, Z. N.; Xie, Y.; Wang, S.; Weng, G. M. Exploiting thiolate/disulfide redox couples toward large-scale electrochemical carbon dioxide capture and release. *Energy Environ. Sci.* **2025**, *18*, 2584–2598.

[66] Wang, M.; Rahimi, M.; Kumar, A.; Hariharan, S.; Choi, W.; Hatton, T. A. Flue gas CO_2 capture via electrochemically mediated amine regeneration: System design and performance. *Appl. Energy* **2019**, *255*, 113879.

[67] Luo, L.; Hou, L. K.; Liu, Y. Y.; Wu, K. J.; Zhu, Y. M.; Lu, H. F.; Liang, B. Regeneration of Na_2Q in an electrochemical CO_2 capture system. *Energy Fuels* **2021**, *35*, 12260–12269.

[68] Fan, H. F.; Mao, Y. H.; Sultan, S.; Yu, Y. S.; Wu, X. M.; Zhang, Z. X. Performance enhancement of desorption reactor in the electrochemically mediated amine regeneration CO_2 capture process: Thru modelling, simulation, and optimization. *Appl. Energy* **2024**, *376*, 124287.

[69] Micari, M.; Hsu, K. J.; Bempeli, S.; Agrawal, K. V. Energy- and cost-efficient CO_2 capture from dilute emissions by pyridinic-graphene membranes. *Nat. Sustain*., in press, https://doi.org/10.1038/s41893-025-01696-5.

[70] Stucki, S.; Schuler, A.; Constantinescu, M. Coupled CO_2 recovery from the atmosphere and water electrolysis: Feasibility of a new process for hydrogen storage. *Int. J. Hydrogen Energy* **1995**, *20*, 653–663.

[71] Sharifian, R.; Wagterveld, R. M.; Digdaya, I. A.; Xiang, C.; Vermaas, D. A. Electrochemical carbon dioxide capture to close the carbon cycle. *Energy Environ. Sci.* **2021**, *14*, 781–814.

[72] Rau, G. H. Electrochemical CO_2 capture and storage with hydrogen generation. *Energy Procedia* **2009**, *1*, 823–828.

[73] Rau, G. H. CO_2 mitigation via capture and chemical conversion in seawater. *Environ. Sci. Technol.* **2011**, *45*, 1088–1092.

[74] Park, H. S.; Lee, J.; Han, J. Y. N.; Park, S.; Park, J.; Min, B. CO_2 fixation by membrane separated NaCl electrolysis. *Energies* **2015**, *8*, 8704–8715.

[75] Taniguchi, I.; Yamada, T. Low energy CO_2 capture by electrodialysis. *Energy Procedia* **2017**, *114*, 1615–1620.

[76] Liu, G. K.; Yang, A. D.; Darton, R. C. Numerical modeling and comparative analysis of electrolysis and electrodialysis systems for direct air capture. *ACS Sustain. Chem. Eng.* **2024**, *12*, 3951–3965.

[77] Datta, S.; Henry, M. P.; Lin, Y. J.; Fracaro, A. T.; Millard, C. S.; Snyder, S. W.; Stiles, R. L.; Shah, J.; Yuan, J. W.; Wesoloski, L. et al. Electrochemical CO_2 capture using resin-wafer electrodeioni zation. *Ind. Eng. Chem. Res.* **2013**, *52*, 15177–15186.

[78] Green, H. J.; Guenther, P. R. Carbon dioxide release from ocean thermal energy conversion (OTEC) cycles. SERI/TP-253–3594; Solar Energy Research Institute: Golden, CO, 1990.

[79] Youn, M. H.; Ki Tae Park, K. T.; Lee, Y. H.; Kang, S. P.; Lee, S. M.; Kim, S. S.; Kim, Y. E.; Ko, Y. N.; Jeong, S. K.; Wonhee Lee, W. Carbon dioxide sequestration process for the cement industry. *J. CO_2 Util.* **2019**, *34*, 325–334.

[80] Gilliam, R. J.; Boggs, B. K.; Decker, V.; Kostowskyj, M. A.; Gorer, S.; Albrecht, T. A.; Way, J. D.; Kirk, D. W.; Bard, A. J. Low voltage electrochemical process for direct carbon dioxide sequestration. *J. Electrochem. Soc.* **2012**, *159*, B627–B628.

[81] Mehmood, A.; Iqbal, M. I.; Lee, J. Y.; Hwang, J.; Jung, K. D.; Ha, H. Y. A novel high performance configuration of electrochemical cell to produce alkali for sequestration of carbon dioxide. *Electrochim. Acta* **2016**, *219*, 655–663.

[82] Wang, C.; Liu, H.; Li, X. Z.; Zheng, L. Z. Importance of ambient O_2 for electrochemical enrichment of atmospheric CO_2. *Ind. Eng. Chem. Res.* **2013**, *52*, 2470–2476.
[83] Pourcelly, G. Electrodialysis with bipolar membranes: Principles, optimization, and applications. *Russ. J. Electrochem.* **2002**, *38*, 919–926.
[84] Eisaman, M. D.; Alvarado, L.; Larner, D.; Wang, P.; Garga, B.; Littau, K. A. CO_2 separation using bipolar membrane electrodialysis. *Energy Environ. Sci.* **2011**, *4*, 1319–1328.
[85] Sabatino, F.; Gazzani, M.; Gallucci, F.; van Sint Annaland, M. Modeling, optimization, and techno-economic analysis of bipolar membrane electrodialysis for direct air capture processes. *Ind. Eng. Chem. Res.* **2022**, *61*, 12668–12679.
[86] Ozden, A. CO_2 capture via electrochemical pH-mediated systems. *ACS Energy Lett.* **2025**, *10*, 1550–1576.
[87] Bouaboula, H.; Belmabkhout, Y.; Zaabout, A. Life cycle assessment of electrochemical pH-swing direct air capture. *Energy Convers. Manage.* **2025**, *342*, 120134.
[88] Wang, Q. Y.; Jiang, C. X.; Wang, Y. M.; Yang, Z. J.; Xu, T. W. Reclamation of aniline wastewater and CO_2 capture using bipolar membrane electrodialysis. *ACS Sustain. Chem. Eng.* **2016**, *4*, 5743–5751.
[89] Zhou, J. Y.; Guan, X. F. Closed-loop and precipitation-free CO_2 capture process enabled by electrochemical pH gradient. *ChemSusChem* **2025**, *18*, e202401533.
[90] Cao, T. N. D.; Snyder, S. W.; Lin, Y. I.; Lin, Y. J.; Negi, S.; Pan, S. Y. Unraveling the potential of electrochemical pH-swing processes for carbon dioxide capture and utilization. *Ind. Eng. Chem. Res.* **2023**, *62*, 20979–20995.
[91] Chen, T. Y.; Shen, R. C.; Sun, H. S.; Bi, J. T.; Sun, M. M.; Wang, S. Z.; Guo, X. F.; Li, W. H.; Liu, J. L.; Zhao, Y. Y. Saline water treatment coupled with carbon dioxide capture by bipolar membrane electrodialysis in a continuous feed-bleed mode: The effect of proton leakage. *Chem. Eng. J.* **2024**, *498*, 155092.
[92] Lai, W. C.; Qiao, Y.; Wang, Y. N.; Huang, H. W. Stability issues in electrochemical CO_2 reduction: Recent advances in fundamental understanding and design strategies. *Adv. Mater.* **2023**, *35*, 2306288.
[93] Bi, J. T.; Chen, T. Y.; Xie, Y.; Shen, R. C.; Li, B.; Sun, M. M.; Guo, X. F.; Zhao, Y. Y. Bipolar membrane electrodialysis integrated with *in-situ* CO_2 absorption for simulated seawater concentrate utilization, carbon storage and production of sodium carbonate. *J. Environ. Sci.* **2024**, *142*, 21–32.
[94] Bang, J. H.; Chae, S. C.; Lee, S. W.; Kim, J. W.; Song, K.; Kim, J.; Kim, W. Sequential carbonate mineralization of desalination brine for CO_2 emission reduction. *J. CO_2 Util.* **2019**, *33*, 427–433.
[95] Aliaskari, M.; Wezstein, J.; Saravia, F.; Horn, H. A systematic analysis of operating parameters for CO_2 capture from seawater by bipolar membrane electrodialysis (BPMED). *Sep. Purif. Technol.* **2024**, *339*, 126679.
[96] Song, H.; Fernández, C. A.; Choi, H.; Huang, P. W.; Oh, J.; Hatzell, M. C. Integrated carbon capture and CO production from bicarbonates through bipolar membrane electrolysis. *Energy Environ. Sci.* **2024**, *17*, 3570–3579.
[97] Chen, Z.; Zhang, Y. S.; Deng, H. Y.; Wang, Y. H. The impact of CO_2 regeneration positions on electrochemical CO_2 reduction. *ChemElectroChem* **2025**, *12*, e202500200.
[98] Xu, T. W.; Huang, C. H. Electrodialysis-based separation technologies: A critical review. *AIChE J.* **2008**, *54*, 3147–3159.
[99] Koytsoumpa, E. I.; Bergins, C.; Kakaras, E. The CO_2 economy: Review of CO_2 capture and reuse technologies. *J. Supercrit. Fluids* **2018**, *132*, 3–16.
[100] Gentry, E. C.; Knowles, R. R. Synthetic applications of proton-coupled electron transfer. *Acc. Chem. Res.* **2016**, *49*, 1546–1556.
[101] Mizen, M. B.; Wrighton, M. S. Reductive addition of CO_2 to 9,10 - phenanthrenequinone. *J. Electrochem. Soc.* **1989**, *136*, 941–946.
[102] Bui, A. T.; Hartley, N. A.; Thom, A. J. W.; Forse, A. C. Trade-off between redox potential and the strength of electrochemical CO_2 capture in quinones. *J. Phys. Chem. C* **2022**, *126*, 14163–14172.
[103] Iijima, G.; Naruse, J.; Shingai, H.; Usami, K.; Kajino, T.; Yoto, H.; Morimoto, Y.; Nakajima, R.; Inomata, T.; Masuda, H. Mechanism of CO_2 capture and release on redox-active organic electrodes. *Energy Fuels* **2023**, *37*, 2164–2177.
[104] Seo, H.; Hatton, T. A. Electrochemical direct air capture of CO_2 using neutral red as reversible redox-active material. *Nat. Commun.* **2023**, *14*, 313.
[105] Liu, A. D.; Musgrave, C. B.; Li, X.; Goddard, W. A.; Liu, Y. Y. Non-aqueous alkoxide-mediated electrochemical carbon capture. *Nat. Energy* **2024**, *9*, 1415–1426.
[106] Renfrew, S. E.; Starr, D. E.; Strasser, P. Electrochemical approaches toward CO_2 capture and concentration. *ACS Catal.* **2020**, *10*, 13058–13074.
[107] Moss, G. P.; Smith, P. A. S.; Tavernier, D. Glossary of class names of organic compounds and reactivity intermediates based on structure (IUPAC recommendations 1995). *Pure Appl. Chem.* **1995**, *67*, 1307–1375.
[108] Clarke, L. E.; Leonard, M. E.; Brushett, F. R. Thermodynamic modeling of CO_2 separation systems with soluble, redox-active capture species. *ECS Meet. Abstr.* **2022**, *61*, 10531–10546.
[109] Scovazzo, P.; Poshusta, J.; DuBois, D.; Koval, C.; Noble, R. Electrochemical separation and concentration of < 1% carbon dioxide from nitrogen. *J. Electrochem. Soc.* **2003**, *150*, D91.
[110] Barlow, J. M.; Yang, J. Y. Oxygen-stable electrochemical CO_2 capture and concentration with quinones using alcohol additives. *J. Am. Chem. Soc.* **2022**, *144*, 14161–14169.
[111] Tam, S. M.; Tessensohn, M. E.; Tan, J. Y.; Subrata, A.; Webster, R. D. Competition between reversible capture of CO_2 and release of CO_2^- using electrochemically reduced quinones in acetonitrile solutions. *J. Phys. Chem. C* **2021**, *125*, 11916–11927.
[112] Gurkan, B.; Simeon, F.; Hatton, T. A. Quinone reduction in ionic liquids for electrochemical CO_2 separation. *ACS Sustain. Chem. Eng.* **2015**, *3*, 1394–1405.
[113] Liu, Y. Y.; Ye, H. Z.; Diederichsen, K. M.; Van Voorhis, T.; Hatton, T. A. Electrochemically mediated carbon dioxide separation with quinone chemistry in salt-concentrated aqueous media. *Nat. Commun.* **2020**, *11*, 2278.
[114] Barlow, J. M.; Clarke, L. E.; Zhang, Z. S.; Bím, D.; Ripley, K. M.; Zito, A.; Brushett, R.; Alexandrova, A. N.; Yang, J. Y. Molecular design of redox carriers for electrochemical CO_2 capture and concentration. *Chem. Soc. Rev.* **2022**, *51*, 8415–8433.
[115] Diederichsen, K. M.; Liu, Y. Y.; Ozbek, N.; Seo, H.; Hatton, T. A. Toward solvent-free continuous-flow electrochemically mediated carbon capture with high-concentration liquid quinone chemistry. *Joule* **2022**, *6*, 221–239.
[116] Wang, J.; Krishna, R.; Yang, J. F.; Deng, S. G. Hydroquinone and quinone-grafted porous carbons for highly selective CO_2 capture from flue gases and natural gas upgrading. *Environ. Sci. Technol.* **2015**, *49*, 9364–9373.
[117] Wielend, D.; Apaydin, D. H.; Sariciftci, N. S. Anthraquinone thin-film electrodes for reversible CO_2 capture and release. *J. Mater. Chem. A* **2018**, *6*, 15095–15101.
[118] Guo, Y. H.; Massen-Hane, M.; Endy, G.; Hatton, T. A. Porous polymeric electrodes for electrochemical carbon dioxide capture. *Adv. Mater.* **2024**, *36*, 2407567.
[119] Kullapere, M.; Seinberg, J. M.; Mäeorg, U.; Maia, G.; Schiffrin, D. J.; Tammeveski, K. Electroreduction of oxygen on glassy carbon electrodes modified with *in situ* generated anthraquinone diazonium cations. *Electrochim. Acta* **2009**, *54*, 1961–1969.
[120] Apaydin, D. H.; Głowacki, E. D.; Portenkirchner, E.; Sariciftci, N. S.

Direct electrochemical capture and release of carbon dioxide using an industrial organic pigment: Quinacridone. *Angew. Chem., Int. Ed.* **2014**, *53*, 6819–6822.

[121] Hoffman, M. Z.; Hayon, E. One-electron reduction of the disulfide linkage in aqueous solution. Formation, protonation, and decay kinetics of the RSSR-radical. *J. Am. Chem. Soc.* **1972**, *94*, 7950–7957.

[122] Singh, P.; Rheinhardt, J. H.; Olson, J. Z.; Tarakeshwar, P.; Mujica, V.; Buttry, D. A. Electrochemical capture and release of carbon dioxide using a disulfide-thiocarbonate redox cycle. *J. Am. Chem. Soc.* **2017**, *139*, 1033–1036.

[123] Harris, D.; Bushnell, E. Density functional theory study of the capture and release of carbon dioxide by benzyl-disulfide, -diselenide, and -ditelluride. *J. Phys. Chem. A* **2019**, *123*, 3383–3388.

[124] Kheirabadi, R.; Vakili, M.; Morad, R.; Maaza, M. Computational modeling of the catalytic cycle of the di-chalcogenide compounds in the capture and release of carbon dioxide: Effect of temperature and substitution on the catalytic activity. *J. Iran. Chem. Soc.* **2022**, *19*, 3963–3979.

[125] Wan, M. Y.; Yang, Z. Y.; Morgan, H.; Shi, J. Q.; Shi, F.; Liu, M. X.; Wong, H. W.; Gu, Z. Y.; Che, F. L. Enhanced CO_2 reactive capture and conversion using aminothiolate ligand–metal interface. *J. Am. Chem. Soc.* **2023**, *145*, 26038–26051.

[126] Wu, J. K.; Niu, J. P.; Hou, L.; Cheng, S. L.; Xie, R. J.; Zhu, N. Highly efficient thiolate-based ionic liquid catalysts for reduction of CO_2: Selective N-functionalization of amines to form N-formamides and N-methylamines. *Chem.—Eur. J.* **2024**, *30*, e202304315.

[127] Kaes, C.; Katz, A.; Hosseini, M. W. Bipyridine: The most widely used ligand. A review of molecules comprising at least two 2,2′-bipyridine units. *Chem. Rev.* **2000**, *100*, 3553–3590.

[128] Ishida, H.; Ohba, T.; Yamaguchi, T.; Ohkubo, K. Interaction between CO_2 and electrochemically reduced species of N-propyl-4,4′-bipyridinium cation. *Chem. Lett.* **1994**, *23*, 905–908.

[129] Singh, P.; Tarakeshwar, P.; Buttry, D. A. Experimental, simulation, and computational study of the interaction of reduced forms of *N*-methyl-4,4′-bipyridinium with CO_2. *ChemElectroChem* **2020**, *7*, 469–475.

[130] Ranjan, R.; Olson, J.; Singh, P.; Lorance, E. D.; Buttry, D. A.; Gould, I. R. Reversible electrochemical trapping of carbon dioxide using 4,4′-bipyridine that does not require thermal activation. *J. Phys. Chem. Lett.* **2015**, *6*, 4943–4946.

[131] Rayer, A. V.; Sumon, K. Z.; Jaffari, L.; Henni, A. Dissociation constants (pK_a) of tertiary and cyclic amines: Structural and temperature dependences. *J. Chem. Eng. Data* **2014**, *59*, 3805–3813.

[132] Zhang, Z. F.; Li, Y. T.; Zhong, Y. W.; Li, P.; Zhu, L. F.; Zheng, Z.; Jia, B. H.; David, M.; Fu, Y.; Yu, H. et al. sp^2/sp^3-Hybridized nitrogen-mediated electrochemical CO_2 capture and utilization. *Sci. Adv.* **2025**, *11*, eadw6592.

[133] Lai, W. C.; Qiao, Y.; Zhang, J. W.; Lin, Z. Q.; Huang, H. W. Design strategies for markedly enhancing energy efficiency in the electrocatalytic CO_2 reduction reaction. *Energy Environ. Sci.* **2022**, *15*, 3603–3629.

[134] Jin, S. J.; Wu, M.; Jing, Y.; Gordon, R. G.; Aziz, M. J. Low energy carbon capture via electrochemically induced pH swing with electrochemical rebalancing. *Nat. Commun.* **2022**, *13*, 2140.

[135] Jayarapu, K. N.; Mathur, A.; Li, X.; Liu, A. D.; Zhang, L. Y.; Kim, J.; Kim, H.; Kuk, S. K.; Liu, Y. Y. Indigo as a low-cost redox-active sorbent for electrochemically mediated carbon capture. *Adv. Funct. Mater.* **2024**, *34*, 2402355.

[136] Li, X.; Zhao, X. H.; Liu, Y. Y.; Hatton, T. A.; Liu, Y. Y. Redox-tunable Lewis bases for electrochemical carbon dioxide capture. *Nat. Energy* **2022**, *7*, 1065–1075.

[137] Seo, H.; Rahimi, M.; Hatton, T. A. Electrochemical carbon dioxide capture and release with a redox-active amine. *J. Am. Chem. Soc.* **2022**, *144*, 2164–2170.

[138] Kang, J. S.; Kim, S.; Hatton, T. A. Redox-responsive sorbents and mediators for electrochemically based CO_2 capture. *Curr. Opin. Green Sustain. Chem.* **2021**, *31*, 100504.

[139] Luo, J. F.; Preciado, S.; Xie, P.; Larrosa, I. Carboxylation of phenols with CO_2 at atmospheric pressure. *Chem.—Eur. J.* **2016**, *22*, 6798–6802.

[140] Xie, H. P.; Wu, Y. F.; Liu, T.; Wang, F. H.; Chen, B.; Liang, B. Low-energy-consumption electrochemical CO_2 capture driven by biomimetic phenazine derivatives redox medium. *Appl. Energy* **2020**, *259*, 114119.

[141] Pang, S.; Jin, S. J.; Yang, F. C.; Alberts, M.; Li, L.; Xi, D. W.; Gordon, R. G.; Wang, P.; Aziz, M. J.; Ji, Y. L. A phenazine-based high-capacity and high-stability electrochemical CO_2 capture cell with coupled electricity storage. *Nat. Energy* **2023**, *8*, 1126–1136.

[142] de Lannoy, C. F.; Eisaman, M. D.; Jose, A.; Karnitz, S. D.; Devaul, R. W.; Hannun, K.; Rivest, J. L. B. Indirect ocean capture of atmospheric CO_2: Part I. Prototype of a negative emissions technology. *Int. J. Greenh. Gas Control.* **2018**, *70*, 243–253.

[143] Schimanofsky, C.; Wielend, D.; Kröll, S.; Lerch, S.; Werner, D.; Gallmetzer, J. M.; Mayr, F.; Neugebauer, H.; Irimia-Vladu, M.; Portenkirchner, E. et al. Direct electrochemical CO_2 capture using substituted anthraquinones in homogeneous solutions: A joint experimental and theoretical study. *J. Phys. Chem. C* **2022**, *126*, 14138–14154.

[144] Wang, C. G.; Zhang, Z. L.; Wang, Y. Quinacridone-based π-conjugated electronic materials. *J. Mater. Chem. C* **2016**, *4*, 9918–9936.

[145] Xie, H. P.; Jiang, W. C.; Liu, T.; Wu, Y. F.; Wang, Y. F.; Chen, B.; Niu, D. W.; Liang, B. Low-energy electrochemical carbon dioxide capture based on a biological redox proton carrier. *Cell Rep. Phys. Sci.* **2020**, *1*, 100046.

[146] Keith, D. W.; Holmes, G.; St. Angelo, D. *; Heidel, K. A process for capturing CO_2 from the atmosphere. Joule* **2018**, *2*, 1573–1594.

[147] Yasri, N. G.; Roberts, E. P. L. Electrochemical regeneration of adsorbents: An Electrochemist's perspective. *Curr. Opin. Electrochem.* **2024**, *46*, 101504.

[148] Li, K. K.; Leigh, W.; Feron, P.; Yu, H.; Tade, M. Systematic study of aqueous monoethanolamine (MEA)-based CO_2 capture process: Techno-economic assessment of the MEA process and its improvements. *Appl. Energy* **2016**, *165*, 648–659.

[149] Meng, F. Z.; Meng, Y.; Ju, T. Y.; Han, S. Y.; Lin, L.; Jiang, J. G. Research progress of aqueous amine solution for CO_2 capture: A review. *Renew. Sustain. Energy Rev.* **2022**, *168*, 112902.

[150] Stern, M. C.; Simeon, F.; Herzog, H.; Hatton, T. A. Post-combustion carbon dioxide capture using electrochemically mediated amine regeneration. *Energy Environ. Sci.* **2013**, *6*, 2505–2517.

[151] Wang, M.; Hariharan, S.; Shaw, R. A.; Hatton, T. A. Energetics of electrochemically mediated amine regeneration process for flue gas CO_2 capture. *Int. J. Greenh. Gas Control.* **2019**, *82*, 48–58.

[152] Rahimi, M.; Diederichsen, K. M.; Ozbek, N.; Wang, M.; Choi, W.; Hatton, T. A. An electrochemically mediated amine regeneration process with a mixed absorbent for postcombustion CO_2 capture. *Environ. Sci. Technol.* **2020**, *54*, 8999–9007.

[153] Wu, X. M.; Mao, Y. H.; Fan, H. F.; Sultan, S.; Yu, Y. S.; Zhang, Z. X. Investigation on the performance of EDA-based blended solvents for electrochemically mediated CO_2 capture. *Appl. Energy* **2023**, *349*, 121656.

[154] Ebewele, E. O.; Al-Marzouqi, M. H. Regeneration of solvent for CO_2 capture: A reviewRegeneration of solvent for CO_2 capture: A review. In *2021 6th International Conference on Renewable Energy: Generation and Applications (ICREGA)* Al Ain, United Arab Emirates, **2021**, *54*, 163–167.

[155] Shu, Q. D.; Legrand, L.; Kuntke, P.; Tedesco, M.; Hamelers, H. V. M. Electrochemical regeneration of spent alkaline absorbent from direct air capture. *Environ. Sci. Technol.* **2020**, *54*, 8990–8998.
[156] Fasihi, M.; Efimova, O.; Breyer, C. Techno-economic assessment of CO_2 direct air capture plants. *J. Cleaner Prod.* **2019**, *224*, 957–980.
[157] Liu, L. S.; Gong, F.; Xiao, R. Direct air carbon capture and recovery utilizing alkaline solution circulation. *Energy Fuels* **2023**, *37*, 9339–9346.
[158] Hemmatifar, A.; Kang, J. S.; Ozbek, N.; Tan, K. J.; Hatton, T. A. Electrochemically mediated direct CO_2 capture by a stackable bipolar cell. *ChemSusChem* **2022**, *15*, e202102533.
[159] Porada, S.; Zhao, R.; van der Wal, A.; Presser, V.; Biesheuvel, P. M. Review on the science and technology of water desalination by capacitive deionization. *Prog. Mater. Sci.* **2013**, *58*, 1388–1442.
[160] Suss, M. E.; Porada, S.; Sun, X.; Biesheuvel, P. M.; Yoon, J.; Presser, V. Water desalination via capacitive deionization: What is it and what can we expect from it. *Energy Environ. Sci.* **2015**, *8*, 2296–2319.
[161] Zhao, R.; Biesheuvel, P. M.; van der Wal, A. Energy consumption and constant current operation in membrane capacitive deionization. *Energy Environ. Sci.* **2012**, *5*, 9520–9527.
[162] Legrand, L.; Schaetzle, O.; de Kler, R. C. F.; Hamelers, H. V. M. Solvent-free CO_2 capture using membrane capacitive deionization. *Environ. Sci. Technol.* **2018**, *52*, 9478–9485.
[163] Legrand, L.; Shu, Q.; Tedesco, M.; Dykstra, J. E.; Hamelers, H. V. M. Role of ion exchange membranes and capacitive electrodes in membrane capacitive deionization (MCDI) for CO_2 capture. *J. Colloid Interface Sci.* **2020**, *564*, 478–490.
[164] Xiao, Q.; Ma, J. X.; Xu, L. Q.; Zuo, K. C.; Guo, H.; Tang, C. Y. Membrane capacitive deionization (MCDI) for selective ion separation and recovery: Fundamentals, challenges, and opportunities. *J. Membr. Sci.* **2024**, *699*, 122650.
[165] Wu, Q. H.; Liang, D. W.; Lu, S. F.; Wang, H. N.; Xiang, Y.; Aurbach, D.; Avraham, E.; Cohen, I. Advances and perspectives in integrated membrane capacitive deionization for water desalination. *Desalination* **2022**, *542*, 116043.
[166] Długołęcki, P.; Ogonowski, P.; Metz, S. J.; Saakes, M.; Nijmeijer, K.; Wessling, M. On the resistances of membrane, diffusion boundary layer and double layer in ion exchange membrane transport. *J. Membr. Sci.* **2010**, *349*, 369–379.
[167] Wang, C. H.; Jiang, K. Q.; Yu, H.; Li, S.; Zhao, Y.; Zheng, Z.; Liu, H. M.; Xia, X. B.; Zhao, P. F.; Li, Y. B. et al. Review of electrochemical carbon dioxide capture towards practical application. *Next Mater.* **2025**, *8*, 100660.
[168] Barckholtz, T. A.; Taylor, K. M.; Narayanan, S.; Jolly, S.; Ghezel-Ayagh, H. Molten carbonate fuel cells for simultaneous CO_2 capture, power generation, and H_2 generation. *Appl. Energy* **2022**, *313*, 118553.
[169] Campanari, S.; Chiesa, P.; Manzolini, G.; Bedogni, S. Economic analysis of CO_2 capture from natural gas combined cycles using molten carbonate fuel cells. *Appl. Energy* **2014**, *130*, 562–573.
[170] Jiang, R.; Gao, M. X.; Mao, X. H.; Wang, D. H. Advancements and potentials of molten salt CO_2 capture and electrochemical transformation (MSCC-ET) process. *Curr. Opin. Electrochem.* **2019**, *17*, 38–46.
[171] Spinelli, M.; Di Bona, D.; Gatti, M.; Martelli, E.; Viganò, F.; Consonni, S. Assessing the potential of molten carbonate fuel cell-based schemes for carbon capture in natural gas-fired combined cycle power plants. *J. Power Sources* **2020**, *448*, 227223.
[172] Duan, L. Q.; Yue, L.; Qu, W. J.; Yang, Y. P. Study on CO_2 capture from molten carbonate fuel cell hybrid system integrated with oxygen ion transfer membrane. *Energy* **2015**, *93*, 20–30.
[173] Bai, W. T.; Zeng, H. Y.; Chen, F. J.; Wu, S. S.; Wang, S. C.; Du, Y. P.; Liu, S. L.; Wang, D. S.; Dai, Z. H. Emerging atomistic modeling catalysts for C-N electrocatalysis. *Adv. Mater.*, in press, https://doi.org/10.1002/adma.202510907.
[174] Zhang, M. Y.; Zhu, W.; Liu, Z. Y.; Chen, S. R.; Zhou, D. Y.; Mu, X. Q.; Zhuang, Z. C.; Wang, S. C.; Yang, J. R.; Du, Y. P. et al. Selective sieving effect of multi-atomic bismuth interfaces for efficient formate electrosynthesis and evolution at industrial current density. *Angew. Chem., Int. Ed.* **2025**, *64*, e202510206.
[175] Zhang, M. Y.; Zhou, D. Y.; Mu, X. Q.; Wang, D. S.; Liu, S. L.; Dai, Z. H. Regulating the critical intermediates of dual-atom catalysts for CO_2 electroreduction. *Small* **2024**, *20*, 2402050.
[176] Liu, Z. K.; Yan, T.; Shi, H.; Pan, H.; Kang, P. Grafting amine-functionalized ligand layer on catalyst for electrochemical CO_2 capture and utilization. *Appl. Catal. B: Environ.* **2024**, *343*, 123456.
[177] Zhang, J. F.; Zhang, J. T.; Wei, B.; Chen, Z. Diminishing C–C coupling capacity by synergistic interaction between Sn and the Cu/Cu_2O interfaces for high-performance CO_2 reduction to CO. *Renew. Energy* **2026**, *256*, 124477.
[178] Digdaya, I. A.; Sullivan, I.; Lin, M.; Han, L. H.; Cheng, W. H.; Atwater, H. A.; Xiang, C. X. A direct coupled electrochemical system for capture and conversion of CO_2 from oceanwater. *Nat. Commun.* **2020**, *11*, 4412.
[179] Dutcher, B.; Fan, M. H.; Russell, A. G. Amine-based CO_2 capture technology development from the beginning of 2013—A review. *ACS Appl. Mater. Interfaces* **2015**, *7*, 2137–2148.
[180] Xia, W.; Xie, Y. J.; Jia, S. Q.; Han, S. T.; Qi, R. J.; Chen, T.; Xing, X. Q.; Yao, T.; Zhou, D. W.; Dong, X. et al. Adjacent copper single atoms promote C–C coupling in electrochemical CO_2 reduction for the efficient conversion of ethanol. *J. Am. Chem. Soc.* **2023**, *145*, 17253–17264.
[181] Stern, M. C.; Hatton, T. A. Bench-scale demonstration of CO_2 capture with electrochemically-mediated amine regeneration. *RSC Adv.* **2014**, *4*, 5906–5914.
[182] Chen, L.; Li, F. W.; Zhang, Y.; Bentley, C. L.; Horne, M.; Bond, A. M.; Zhang, J. Electrochemical reduction of carbon dioxide in a monoethanolamine capture medium. *ChemSusChem* **2017**, *10*, 4109–4118.
[183] Khurram, A.; Yan, L. F.; Yin, Y. M.; Zhao, L. L.; Gallant, B. M. Promoting amine-activated electrochemical CO_2 conversion with alkali salts. *J. Phys. Chem. C* **2019**, *123*, 18222–18231.
[184] Filotás, D.; Nagy, T.; Nagy, L.; Mizsey, P.; Nagy, G. Extended investigation of electrochemical CO_2 reduction in ethanolamine solutions by SECM. *Electroanalysis* **2018**, *30*, 690–697.
[185] Li, Y. C.; Lee, G.; Yuan, T. G.; Wang, Y.; Nam, D. H.; Wang, Z. Y.; García De Arquer, F. P.; Lum, Y.; Dinh, C. T.; Voznyy, O. et al. CO_2 electroreduction from carbonate electrolyte. *ACS Energy Lett.* **2019**, *4*, 1427–1431.
[186] Li, T. F.; Lees, E. W.; Goldman, M.; Salvatore, D. A.; Weekes, D. M.; Berlinguette, C. P. Electrolytic conversion of bicarbonate into CO in a flow cell. *Joule* **2019**, *3*, 1487–1497.
[187] Chi, Z. Y.; Elloy, F.; Xie, Y. X.; Hu, Y. C.; Chen, S. L. Selection of microalgae and cyanobacteria strains for bicarbonate-based integrated carbon capture and algae production system. *Appl. Biochem. Biotechnol.* **2014**, *172*, 447–457.
[188] Sharifian, R.; Boer, L.; Wagterveld, R. M.; Vermaas, D. A. Oceanic carbon capture through electrochemically induced *in situ* carbonate mineralization using bipolar membrane. *Chem. Eng. J.* **2022**, *438*, 135326.
[189] Chen, T. Y.; Bi, J. T.; Zhao, Y. Y.; Du, Z. T.; Guo, X. F.; Yuan, J. S.; Ji, Z. Y.; Liu, J.; Wang, S. Z.; Li, F. et al. Carbon dioxide capture coupled with magnesium utilization from seawater by bipolar membrane electrodialysis. *Sci. Total Environ.* **2022**, *820*, 153272.
[190] Tang, C.; Gong, P.; Xiao, T. S.; Sun, Z. Z. Direct electrosynthesis of 52% concentrated CO on silver's twin boundary. *Nat. Commun.* **2021**, *12*, 2139.

[191] Wang, M.; Luo, J. S. A coupled electrochemical system for CO_2 capture, conversion and product purification. *eScience* **2023**, *3*, 100155.
[192] Heß, D.; Rubin, M.; Dittmeyer, R. A novel approach to electrochemical direct air capture using aqueous L-arginine amino acid solutions as an absorption solvent: Proof-of-concept and technoeconomics. *Ind. Eng. Chem. Res.* **2025**, *64*, 14973–14985.
[193] Zou, Y. B.; Zheng, A. C.; Feng, L. H.; Du, L.; Daasbjerg, K.; Hu, X. M. Integrated capture and electrochemical conversion of CO_2 from flue gas mediated by carbonate/bicarbonate cycle. *J. Mater. Chem. A* **2025**, *13*, 36191–36201.
[194] Zhang, P.; Tong, J. J.; Huang, K. Combining electrochemical CO_2 capture with catalytic dry methane reforming in a single reactor for low-cost syngas production. *ACS Sustain. Chem. Eng.* **2016**, *4*, 7056–7065.
[195] Shen, M. X.; Ji, L. Y.; Cheng, D. F.; Wang, Z. W.; Xue, Q. W.; Feng, S. J.; Luo, Y.; Chen, S. Y.; Wang, J. H.; Zheng, H. Z. et al. Hierarchical design enables sufficient activated CO_2 for efficient electrolysis of bicarbonate to CO. *Joule* **2024**, *8*, 1999–2015.
[196] Hollas, A.; Wei, X. L.; Murugesan, V.; Nie, Z. M.; Li, B.; Reed, D.; Liu, J.; Sprenkle, V.; Wang, W. A biomimetic high-capacity phenazine-based anolyte for aqueous organic redox flow batteries. *Nat. Energy* **2018**, *3*, 508–514.
[197] Zhang, Z. F.; Su, M. D. Mechanistic insights into the reactivity and activation barrier origins for CO_2 capture by heavy group-14 imine analogues. *Inorg. Chem.* **2024**, *63*, 19687–19700.
[198] Abdinejad, M.; Irtem, E.; Farzi, A.; Sassenburg, M.; Subramanian, S.; Iglesias Van Montfort, H. P.; Ripepi, D.; Li, M. R.; Middelkoop, J.; Seifitokaldani, A. et al. CO_2 electrolysis via surface-engineering electrografted pyridines on silver catalysts. *ACS Catal.* **2022**, *12*, 7862–7876.
[199] Li, F. W.; Thevenon, A.; Rosas-Hernández, A.; Wang, Z. Y.; Li, Y. L.; Gabardo, C. M.; Ozden, A.; Dinh, C. T.; Li, J.; Wang, Y. H. et al. Molecular tuning of CO_2-to-ethylene conversion. *Nature* **2020**, *577*, 509–513.
[200] Schmitt, K. G.; Gewirth, A. A. *In situ* surface-enhanced Raman spectroscopy of the electrochemical reduction of carbon dioxide on silver with 3,5-diamino-1,2,4-triazole. *J. Phys. Chem. C* **2014**, *118*, 17567–17576.
[201] Yan, T.; Liu, S.; Liu, Z. K.; Sun, J.; Kang, P. Integrated electrochemical carbon capture and utilization by redox-active amine grafted gold nanoparticles. *Adv. Funct. Mater.* **2024**, *34*, 2311733.
[202] Neves-Garcia, T.; Hasan, M.; Zhu, Q. S.; Li, J.; Jiang, Z.; Liang, Y. Y.; Wang, H. L.; Rossi, L. M.; Warburton, R. E.; Baker, L. R. Integrated carbon dioxide capture by amines and conversion to methane on single-atom nickel catalysts. *J. Am. Chem. Soc.* **2024**, *146*, 31633–31646.
[203] Aguilar-Romero, M.; Camposeco, R.; Castillo, S.; Marín, J.; Rodríguez-González, V.; García-Serrano, L. A.; Mejía-Centeno, I. Acidity, surface species, and catalytic activity study on V_2O_5-WO_3/TiO_2 nanotube catalysts for selective NO reduction by NH_3. *Fuel* **2017**, *198*, 123–133.
[204] Wu, H. M.; Li, J. L.; Gao, M. J.; Chen, Y. F.; Ren, S.; Yang, J.; Liu, Q. C. Deactivation mechanisms and strategies to mitigate deactivation of iron-based catalysts in NH_3-SCR for NO_x reduction: A comprehensive review. *Sep. Purif. Technol.* **2025**, *358*, 130268.
[205] Xu, J. Q.; Chen, G. R.; Guo, F.; Xie, J. Q. Development of wide-temperature vanadium-based catalysts for selective catalytic reducing of NO_x with ammonia: Review. *Chem. Eng. J.* **2018**, *353*, 507–518.
[206] Nian, J. N.; Chen, S. A.; Tsai, C. C.; Teng, H. Structural feature and catalytic performance of Cu species distributed over TiO_2 nanotubes. *J. Phys. Chem. B* **2006**, *110*, 25817–25824.
[207] Busca, G.; Lietti, L.; Ramis, G.; Berti, F. Chemical and mechanistic aspects of the selective catalytic reduction of NO_x by ammonia over oxide catalysts: A review. *Appl. Catal. B: Environ.* **1998**, *18*, 1–36.
[208] Antoniak-Jurak, K.; Kowalik, P.; Franczyk, E.; Michalska, K.; Bicki, R.; Próchniak, W. The effect of controlled catalyst hydrothermal deactivation on morphology, structural and activity of K-decorated $ZnO/ZnAl_2O_4$ catalysts for HT-WGS. *Fuel* **2024**, *357*, 129758.
[209] Anekwe, I. M. S.; Isa, Y. M. Unlocking catalytic longevity: A critical review of catalyst deactivation pathways and regeneration technologies. *Energy Adv.* **2025**, *4*, 1075–1113.
[210] Yeh, T.; Linic, S.; Savage, P. E. Deactivation of Pt catalysts during hydrothermal decarboxylation of butyric acid. *ACS Sustain. Chem. Eng.* **2014**, *2*, 2399–2406.
[211] Alzaid, A.; Wiens, J.; Adjaye, J.; Smith, K. J. Catalyst deactivation and reactor fouling during hydrogenation of conjugated cyclic olefins over a commercial Ni-Mo-S/γ-Al_2O_3 catalyst. *Energy Fuels* **2018**, *32*, 6213–6223.
[212] Liu, J. J.; Yang, J. R.; Dou, Y. H.; Liu, X. W.; Chen, S. H.; Wang, D. S. Deactivation mechanism and mitigation strategies of single-atom site electrocatalysts. *Adv. Mater.* **2025**, *37*, 2420383.
[213] Gowd, S. C.; Ganeshan, P.; Vigneswaran, V. S.; Hossain, M. S.; Kumar, D.; Rajendran, K.; Ngo, H. H.; Pugazhendhi, A. Economic perspectives and policy insights on carbon capture, storage, and utilization for sustainable development. *Sci. Total Environ.* **2023**, *883*, 163656.
[214] Kim, Y.; Namdari, M.; Jewlal, A. M. L.; Chen, Y. F.; Pimlott, D. J. D.; Stolar, M.; Berlinguette, C. P. Economic viability of integrated CO_2 capture and conversion. *ACS Energy Lett.* **2025**, *10*, 403–409.
[215] Wang, Y.; Gong, L.; Yue, P. T.; Ma, L.; Li, J.; Zhang, L.; Zhu, X.; Fu, Q.; Liao, Q. CO_2 capture and electrochemical upgrade of MEA-based solution: Life cycle assessment and techno-economic analysis. *Appl. Energy* **2025**, *384*, 125400.
[216] Hamalian, M.; Bhati, A.; Maynor, K.; Bahadur, V. Techno-economic analysis of electrochemical carbon capture from oceanwater integrated with hydrates-based sequestration. *Appl. Energy* **2025**, *392*, 125960.
[217] Liu, T.; Wang, Y. P.; Wu, Y. F.; Jiang, W. C.; Deng, Y. C.; Li, Q.; Lan, C.; Zhao, Z. Y.; Zhu, L. Y.; Yang, D. S. et al. Continuous decoupled redox electrochemical CO_2 capture. *Nat. Commun.* **2024**, *15*, 10920.
[218] Jiang, W. C.; Tang, L.; Wang, Y. P.; Song, X. C.; Zhao, Z. Y.; Lan, C.; Wu, Y. F.; Liu, T.; Xie, H. P. Electrochemical proton-coupled electron transfer driven amine regeneration for CO_2 capture. *Chem. Eng. J.* **2025**, *520*, 166315.
[219] Mostafa, M.; Varela, C.; Zondervan, E. Optimization of electrolysis and carbon capture processes for sustainable production of chemicals through Power-to-X. *Phys. Sci. Rev.* **2023**, *8*, 4805–4819.
[220] Hadi, A. I.; Yan, A.; Hu, Y. P.; Lin, B.; Zhou, T. G.; Ouyang, D. H.; Tang, J. L. A comprehensive review of carbon capture: From conventional to emerging electrochemical technologies. *Next Energy* **2025**, *9*, 100415.
[221] Iizuka, A.; Hashimoto, K.; Nagasawa, H.; Kumagai, K.; Yanagisawa, Y.; Yamasaki, A. Carbon dioxide recovery from carbonate solutions using bipolar membrane electrodialysis. *Sep. Purif. Technol.* **2012**, *101*, 49–59.
[222] Sabatino, F.; Mehta, M.; Grimm, A.; Gazzani, M.; Gallucci, F.; Kramer, G. J.; Van Sint Annaland, M. Evaluation of a direct air capture process combining wet scrubbing and bipolar membrane electrodialysis. *Ind. Eng. Chem. Res.* **2020**, *59*, 7007–7020.
[223] Ran, J.; Wu, L.; He, Y. B.; Yang, Z. J.; Wang, Y. M.; Jiang, C. X.; Ge, L.; Bakangura, E.; Xu, T. W. Ion exchange membranes: New developments and applications. *J. Membr. Sci.* **2017**, *522*, 267–291.
[224] Rubin, E. S.; Davison, J. E.; Herzog, H. J. The cost of CO_2 capture and storage. *Int. J. Greenh. Gas Control.* **2015**, *40*, 378–400.
[225] Goeppert, A.; Czaun, M.; Jones, J. P.; Prakash, G. K. S.; Olah, G. A. Recycling of carbon dioxide to methanol and derived products-closing the loop. *Chem. Soc. Rev.* **2014**, *43*, 7995–8048.
[226] Manuale, D. L.; Torres, G. C.; Vera, C. R.; Yori, J. C. Study of an energy-integrated biodiesel production process using supercritical

methanol and a low-cost feedstock. *Fuel Process. Technol.* **2015**, *140*, 252–261.

[227] Pimlott, D. J. D.; Kim, Y.; Berlinguette, C. P. Reactive carbon capture enables CO_2 electrolysis with liquid feedstocks. *Acc. Chem. Res.* **2024**, *57*, 1007–1018.

[228] Banerjee, A.; Morales-Guio, C. G. Integrated CO_2 capture and electrochemical conversion: Coupled effects of transport, kinetics and thermodynamics in the direct reduction of captured-CO_2 adducts. *EES Catal.* **2025**, *3*, 205–234.

[229] Liu, M. J.; Zhan, L. S.; Wang, Y. C.; Zhao, X.; Wu, J.; Deng, D. N.; Jiang, J. B.; Zheng, X. R.; Lei, Y. P. Achieving integrated capture and reduction of CO_2: A promising electrocatalyst. *J. Mater. Sci. Technol.* **2023**, *165*, 235–243.

[230] Lees, E. W.; Goldman, M.; Fink, A. G.; Dvorak, D. J.; Salvatore, D. A.; Zhang, Z. S.; Loo, N. W. X.; Berlinguette, C. P. Electrodes designed for converting bicarbonate into CO. *ACS Energy Lett.* **2020**, *7*, 2165–2173.

[231] Jouny, M.; Luc, W.; Jiao, F. General techno-economic analysis of CO_2 electrolysis systems. *Ind. Eng. Chem. Res.* **2018**, *57*, 2165–2177.

[232] Hung, S. F. Electrochemical flow systems enable renewable energy industrial chain of CO_2 reduction. *Pure Appl. Chem.* **2020**, *92*, 1937–1951.

[233] Kauffman, D. R.; Thakkar, J.; Siva, R.; Matranga, C.; Ohodnicki, P. R.; Zeng, C. J.; Jin, R. C. Efficient electrochemical CO_2 conversion powered by renewable energy. *ACS Appl. Mater. Interfaces* **2015**, *7*, 15626–15632.

[234] Wang, X. Y.; Wei, W. J.; Zhou, S. Y.; Pan, Y. Z.; Yang, J. R.; Gan, T.; Zhuang, Z. C.; Li, W. H.; Zhang, X.; Pan, Y. M. et al. Phosphorus-doped single atom copper catalyst as a redox mediator in the cathodic reduction of quinazolinones. *Angew. Chem.* **2025**, *137*, e202505085.

[235] Amal, R.; Chou, S. L.; Zhao, M.; Wang, D. W.; Li, J. B.; Yang, H. Y. Carbon neutralization: The exploration of clean energy and ecological environment to achieve low carbon emission. *Carbon Neutralization* **2022**, *1*, 4–5.

[236] Ma, R. Z.; Zhang, J.; Gong, J. X.; Lin, Y. X.; Zhang, J. L.; Huang, Z. Q.; Chang, C. R.; Liu, S. J.; Zhu, W.; Wang, Y. X. et al. The cooperative effects of the Rh–M dual-metal atomic pairs in formic acid oxidation. *Angew. Chem., Int. Ed.* **2025**, *64*, e202503095.

[237] Liu, G. Q.; Zhang, H.; Wang, P. F.; Gao, C.; Zhuang, Z. C.; Wang, D. S.; Zhan, S. H. Atomic-level design of acid-base pairs in oxides for selective catalytic reduction of nitrogen oxides with ammonia. *Angew. Chem., Int. Ed.* **2025**, *64*, e202509362.

[238] Yang, Y.; Zhang, W. J.; Wu, G. C.; Huang, Q.; Wen, J. H.; Wang, D. S.; Liu, M. Y. Electronic structure tuning in Cu–Co dual single atom catalysts for enhanced COOH* spillover and electrocalytic CO_2 reduction activity. *Angew. Chem.* **2025**, *137*, e202504423.

[239] Tang, B.; Ji, Q. Q.; Zhang, X. L.; Shi, R. C.; Ma, J.; Zhuang, Z. C.; Sun, M.; Wang, H. J.; Liu, R. Q.; Liu, H. J. et al. Symmetry breaking of FeN_4 moiety via edge defects for acidic oxygen reduction reaction. *Angew. Chem.* **2025**, *137*, e202424135.

[240] Zhao, J.; Gao, G.; Li, T.; Deng, Y. T.; Wang, B.; Dai, P. H.; Li, H. S.; Zhuang, Z. C.; Yang, J. R.; Wang, J. Z. et al. Single atom-substituted chalcogenides with anion vacancy bonded on graphene nanotubes for achieving "1 + 1 + 1 > 3" synergistic enhanced sodium storage. *Angew. Chem.* **2025**, *137*, e202512028.

[241] Sun, M.; Wang, X. K.; Gao, F.; Xu, M. M.; Fan, W. D.; Xu, B.; Sun, D. F. Synthesis strategies of metal-organic frameworks for CO_2 capture. *Microstructures* **2023**, *3*, 2023032.

[242] Ni, J. R.; Zhao, R. F.; Shi, C. D.; Ji, Y. Y.; Hao, A. Z.; Xie, A. T.; Yu, H. J.; Boong, S. K.; Lee, H. K.; Zhou, C. Q. et al. Structure-tailored superlattice $Bi_7Ti_4NbO_{21}$: Coupling octahedral tilting and rotation induced high ferroelectric polarization for efficient piezo-photocatalytic CO_2 reduction. *Adv. Mater.* **2025**, *4*, 100265.

[243] Todorova, T. K.; Schreiber, M. W.; Fontecave, M. Mechanistic understanding of CO_2 reduction reaction (CO_2RR) toward multicarbon products by heterogeneous copper-based catalysts. *ACS Catal.* **2020**, *10*, 1754–1768.

[244] Shen, J.; Tang, M. H.; Shi, Z. H.; Guan, S. Y.; Shi, Y. J.; Zhuang, Z. C.; Li, R. Z.; Yang, J. R.; He, D. P.; Liu, B. Z. et al. Efficient generation of negative hydrogen with bimetallic-ternary-structured catalysts for nitrobenzene hydrogenation. *Angew. Chem.* **2025**, *137*, e202423626.

[245] Zhang, M. Y.; Zhu, W.; Liu, Z. Y.; Chen, S. R.; Zhou, D. Y.; Mu, X. Q.; Zhuang, Z. C.; Wang, S. C.; Yang, J. R.; Du, Y. P. et al. Selective sieving effect of multi-atomic bismuth interfaces for efficient formate electrosynthesis and evolution at industrial current density. *Angew. Chem.* **2025**, *137*, e202510206.

[246] Chen, Y. X.; Meng, Z. H.; Wei, X. L.; Wu, M. J.; Xiong, Y. F.; Tang, H. B.; Wang, R.; Tian, T.; Wang, D. S.; Tang, H. L. Tellurium-nitrogen-carbon support boosting platinum catalysis in high-efficiency proton exchange membrane fuel cells. *Angew. Chem.* **2025**, *137*, e202512315.

[247] Wang, S. Y.; Jiang, J. C.; Wang, D. S.; Wang, K. Unlocking the free radical evolution for directed conversion of furoic acid to 2,5-furandicarboxylic acid over lattice-distorted MnO_x. *Angew. Chem.* **2025**, *137*, e202515012.

[248] Guan, S. Y.; Liu, Y. Y.; Liu, S. L.; Zhuang, Z. C.; Shen, R. F.; Zhang, H. H.; Liang, E. J.; Fan, Y. P.; Jiang, J. C.; Liu, B. Z. et al. MXene-supported Ru-Ni: A common active site for hydrolysis, hydrogen oxidation, and hydrogenation. *Angew. Chem., Int. Ed.* **2025**, *64*, e202506869.

[249] Zhang, K.; Zhang, D.; Wang, Y.; Li, Y. H.; Ren, C.; Ding, M. Y.; Liu, T. Promoting catalysis activity with optimizable self-generated Co-Fe alloy nanoparticles for efficient CO_2 electrolysis performance upgrade. *Nano Res.* **2023**, *16*, 10992–10999.

[250] Guan, M. L.; Lu, N.; Zhang, X.; Wang, Q. W.; Bao, J.; Chen, G. Y.; Yu, H.; Li, H. M.; Xia, J. X.; Gong, X. Z. Engineering of oxygen vacancy and bismuth cluster assisted ultrathin $Bi_{12}O_{17}Cl_2$ nanosheets with efficient and selective photoreduction of CO_2 to CO. *Carbon Energy* **2024**, *6*, e420.

[251] Liu, Z. H.; Shi, S. B.; Ji, Y. C.; Wang, K.; Tan, T. W.; Nielsen, J. Opportunities of CO_2-based biorefineries for production of fuels and chemicals. *Green Carbon* **2023**, *1*, 75–84.

[252] Guo, H. W.; Wang, Y. J.; Liu, H.; Zeng, Y. N.; Wang, W. J.; Liu, T. J.; Kang, L. L.; Ji, R.; Wang, Y. T.; Li, J. G. et al. Metallurgical slag used for efficient growth of Chlorella pyrenoidosa to achieve CO_2 conversion to biodiesel. *Carbon Neutralization* **2024**, *3*, 471–487.

[253] Ji, G. R.; Ji, L.; Wu, S. W.; Meng, L. X.; Jia, Y. T.; Liu, Z. N.; Dong, S. H.; Tian, J.; Li, Y. Z. *In-situ* exsolved ultrafine Ni nanoparticles from $CeZrNiO_2$ solid solution for efficient photothermal catalytic CO_2 reduction by CH_4. *Adv. Powder Mater.* **2024**, *3*, 100188.

[254] Nguyen, D. L. T.; Kim, Y.; Hwang, Y. J.; Won, D. H. Progress in development of electrocatalyst for CO_2 conversion to selective CO production. *Carbon Energy* **2020**, *2*, 72–98.

[255] Zhang, J.; Gao, M. T.; Wang, R. Y.; Li, X. C.; Huang, T. F.; Wang, J.; Wang, Y. W.; Zheng, Z. F. Switching of CO_2 hydrogenation selectivity via chlorine poisoning over Ru/TiO_2 catalyst. *Nano Res.* **2023**, *16*, 4786–4792.

[256] Zhao, Y.; Liu, J.; Han, M. L.; Yang, G. P.; Ma, L. F.; Wang, Y. Y. Two comparable Ba-MOFs with similar linkers for enhanced CO_2 capture and separation by introducing N-rich groups. *Rare Met.* **2021**, *40*, 499–504.

[257] Yan, T. X.; Chen, X. Y.; Kumari, L.; Lin, J. L.; Li, M. L.; Fan, Q.; Chi, H. Y.; Meyer, T. J.; Zhang, S.; Ma, X. B. Multiscale CO_2 electrocatalysis to C_{2+} products: Reaction mechanisms, catalyst design, and device fabrication. *Chem. Rev.* **2023**, *123*, 10530–10583.

[258] Song, D.; Lin, Y.; Fang, S. W.; Li, Y.; Zhao, K.; Chen, X. F.; Huang, Z.; He, F.; Zhao, Z. L.; Huang, H. Y. et al. Unraveling the atomic interdiffusion mechanism of $NiFe_2O_4$ oxygen carriers during chemical looping CO_2 conversion. *Carbon Energy* **2024**, *6*, e493.

[259] Yang, J. R.; Zhu, C. X.; Wang, D. S. A simple organo-electrocatalysis system for the chlor-related industry. *Angew. Chem., Int. Ed.* **2024**, *63*, e202406883.

[260] Yang, J. R.; Zhu, C. X.; Li, W. H.; Zheng, X. S.; Wang, D. S. Organocatalyst supported by a single-atom support accelerates both electrodes used in the chlor-alkali industry via modification of non-covalent interactions. *Angew. Chem., Int. Ed.* **2024**, *63*, e202314382.

[261] Tang, M. H.; Shen, J.; Zhang, F. T.; Zhao, Y. F.; Gan, T.; Zeng, W.; Li, R. X.; Wang, D. S.; Han, B. X.; Liu, Z. M. Upcycling of polyamide wastes to tertiary amines using Mo single atoms and Rh nanoparticles. *Angew. Chem.* **2025**, *137*, e202416436.

[262] Gao, Y.; Yang, C. D.; Sun, F. L.; He, D. P.; Wang, X. Q.; Chen, J.; Zheng, X. B.; Liu, R. C.; Pan, H. G.; Wang, D. S. Ligand-tuning metallic sites in molecular complexes for efficient water oxidation. *Angew. Chem., Int. Ed.* **2025**, *64*, e202415755.

[263] Xu, Y.; Li, E. S.; Hu, C. G.; Zhang, F. C.; Meng, X. G. Recycling of iron and steel slag for carbon reduction and low-environment load application. *Carbon Neutralization* **2024**, *3*, 606–628.

[264] Li, J.; Luo, M. Z.; Wang, K.; Li, G. M.; Zhang, G. Q. Review of carbon dioxide mineralization of magnesium-containing materials. *Carbon Neutralization* **2023**, *2*, 574–584.

[265] Ye, B. C.; Li, W. H.; Zhang, X.; Chen, J.; Gao, Y.; Wang, D. S.; Pan, H. G. Advancing heterogeneous organic synthesis with coordination chemistry-empowered single-atom catalysts. *Adv. Mater.* **2024**, *36*, 2402747.

[266] Yang, H. C.; Duan, P. F.; Zhuang, Z. C.; Luo, Y. W.; Shen, J.; Xiong, Y. L.; Liu, X. W.; Wang, D. S. Understanding the dynamic evolution of active sites among single atoms, clusters, and nanoparticles. *Adv. Mater.* **2025**, *37*, 2415265.

[267] Burdyny, T.; Smith, W. A. CO_2 reduction on gas-diffusion electrodes and why catalytic performance must be assessed at commercially-relevant conditions. *Energy Environ. Sci.* **2019**, *12*, 1442–1453.

[268] De Luna, P.; Hahn, C.; Higgins, D.; Jaffer, S. A.; Jaramillo, T. F.; Sargent, E. H. What would it take for renewably powered electrosynthesis to displace petrochemical processes. *Science* **2019**, *364*, eaav3506.